Oxidative Damage and Selective Neuronal Vulnerability in Alzheimer's Disease

by

Jacqueline Starr Welty

Bachelor of Science, University of New Mexico, 2013

Submitted to the Graduate Faculty of

The School of Medicine in partial fulfillment

of the requirements for the degree of

Doctor of Philosophy

University of Pittsburgh

2019

UNIVERSITY OF PITTSBURGH

SCHOOL OF MEDICINE

This dissertation was presented

by

Jacqueline Starr Welty

It was defended on

January 10, 2019

and approved by

Judith Yanowitz, Associate Professor, Microbiology & Molecular Genetics

Amantha Thathiah, Assistant Professor, Neurobiology

Gary Thomas, Professor, Microbiology & Molecular Genetics

Jian Yu, Professor, Pathology

Kathy Shair, Assistant Professor, Microbiology & Molecular Genetics

Dissertation Director: Michael Tsang, Associate Professor, Developmental Biology

Oxidative Damage and Selective Neuronal Vulnerability in Alzheimer's Disease

Jacqueline Starr Welty, PhD

University of Pittsburgh, 2019

Human cells are constantly under assault by damaging agents that arise from endogenous and exogenous sources. Damage to DNA is especially harmful because it encodes essential RNA molecules and proteins necessary for cellular functions. Failure to carry out sufficient DNA repair may compromise the genome and lead to the development of mutations and potential disease. Specifically, oxidative damage in the form of reactive oxygen species (ROS) and resulting DNA double strand breaks (DSBs) have been implicated in neurodegenerative diseases such as Alzheimer's Disease (AD). Many cells, such as epithelial cells, are constantly replaced and do not need robust systems of repair. However, terminally differentiated and post-mitotic cells such as neurons must survive a lifetime and maintain genomic stability. How they manage to do so is still under investigation.

For error-free repair of DSBs, homologous recombination (HR) can occur during the S/G_2 phases of the cell cycle utilizing a sister chromatid template. However, for post-mitotic cells such as neurons that cannot utilize a sister chromatid template, only the error-prone non-homologous end joining (NHEJ) pathway has been proposed. Recent studies in my lab have elucidated a novel RNA-templated recombination based repair pathway that occurs in the G_0/G_1 phase of the cell cycle. How post-mitotic terminally differentiated neuronal cells utilize these pathways has yet to be understood.

The goal of my thesis is to understand how post-mitotic neurons maintain genomic integrity in repairing DSBs when faced with excessive oxidative damage. My preliminary studies have shown recruitment of transcription coupled homologous recombination (TC-HR) factor RAD52 to sites of DSB induced by laser microirradiation in primary post-mitotic rat cortical

neuronal cells. This recruitment is largely dependent upon active transcription. How neurons utilize TC-HR proteins in DSB repair has yet to be elucidated. **My main hypothesis is that terminally differentiated post-mitotic neurons utilize the TC-HR pathway to repair DSBs and maintain genomic integrity.** To test this hypothesis, I investigated the roles of TC-HR associated proteins in post-mitotic neurons and how toxic soluble amyloid beta ($A\beta_{1-42}$) oligomers compromise this pathway, which may lead to neurodegenerative pathologies seen in AD.

Table of Contents

List of Tables

List of Figures

List of Abbreviations

a.a.	Amino acid
Aβ	Amyloid beta
AD	Alzheimer's Disease
APP	Amyloid precursor protein
bp	Base pair
BER	Base excision repair
CRISPR	Clustered regularly interspaced short palindromic repeats
CSB	Cockayne syndrome B
DIV	Days in vitro
DNA	Deoxyribonucleic acid
DDR	DNA damage response
DMT	Disease modifying therapies
DSB	Double strand break
DSBR	Double strand break repair
dsDNA	Double stranded DNA
dsRNA	Double stranded RNA
EMSA	Electrophoresis mobility shift assay
es	Embryonic stem cell
FAD	Familial Alzheimer's Disease
HR	Homologous recombination
KR	KillerRed
MMEJ	Microhomology mediated end joining

MMR	Mismatch repair
mRNA	Messenger RNA
NER	Nucleotide excision repair
NHEJ	Non-homologous end joining
RNA	Ribonucleic acid
ROS	Reactive oxygen species
SDSA	Synthesis dependent strand annealing
SSA	Single strand annealing
SSB	Single strand break
SSBR	Single strand break repair
ssDNA	Single stranded DNA
TA	Transcription activation
TC-HR	Transcription coupled homologous recombination
TC-NER	Transcription coupled nucleotide excision repair
TCR	Transcription coupled repair
tetR	Tetracycline repressor
TRE	Tet Response Element
UV	Ultraviolet radiation
wt	Wild type

Acknowledgements

I'd first like to thank Dr. Arthur Samuel Levine, without whom this project would have never taken place. He has provided me with valuable insight and inspiration throughout my doctorate program. I am looking forward to continuing my career under his guidance and support. Thank you, also, to Dr. Li Lan who has been my esteemed mentor throughout my graduate career, and who has been essential in my education on structuring experiments, publications, and presentations. Thank you to all former members of the Lan lab who helped with my project, and to all of the collaborators who worked with me to optimize my experiments and interpret data in the best manner possible.

Special thanks is needed for Dr. Amantha Thathiah for welcoming me into her lab during the last portion of my thesis development. Despite many hurdles, her support, wisdom, and guidance enabled me to finish my research and begin new inspired studies so that I can continue progress in the much needed field of Alzheimer's Disease research. Her lab has been a new home, and I would like to thank all of the other lab members for welcoming me there.

I'd also like to thank the other members of my thesis committee: Dr. Judith Yanowitz, Dr. Gary Thomas, Dr. Kathy Shair, and Dr. Jian Yu, for providing me with constructive criticism when I most needed it, and for offering suggestions to further my research in order to draw the best conclusions. You have helped shape me into a stronger scientist with better perspective on how questions should be approached.

This work was primarily funded by the NIH grant NIHGM11833 (L. Lan).

Last, but not at all least, I would like to thank my beloved husband, Tarl Earnshaw, my parents, Donald and Virginia Welty, my sister, Melanie Welty, and my dear best friend, Shannon Thompson, for their unwavering belief in me. Their support during the hardest of times kept me

standing when I thought I couldn’t, and their encouragement kept me plowing ahead when resistance felt strong. Thank you all so much.

1.0 Introduction

1.1 Alzheimer's Disease

1.1.1 Alzheimer's Disease statistics and characteristics

Alzheimer's Disease (AD) is an irreversible neurodegenerative disorder that afflicts millions of people worldwide. It is the leading cause of dementia among the elderly, comprising approximately 60-80 percent of dementia cases. It currently has no cure. By 2025, it is estimated that the number of individuals over 65 with Alzheimer's dementia will reach 50 million worldwide, a 35% increase from 2017. More women than men are affected by AD, but the reason for this remains unknown [1].

In its early stages, AD is characterized by difficulty remembering recent conversations, names or events, along with apathy and depression. Late stage symptoms include impaired communication, disorientation, confusion, poor judgment, behavior changes and finally difficulties with motor movements such as coordination, walking, and swallowing. Later stage AD can lead to death due to immobility, swallowing disorders, malnutrition, and pneumonia [1, 2]. Characteristics of AD are typically analyzed post-mortem and consist of extracellular amyloid beta (Aβ) plaques and intracellular hyper-phosphorylated tau tangles in the brain. AD progresses throughout the basal forebrain, frontal lobe, cerebral cortex and hippocampal regions of the brain, leading to neuronal loss and synaptic dysfunction as the disease progresses [3-5]. Studies now indicate that AD can begin up to 20 years prior to the manifestation of symptoms [6-9].

Currently, diagnosis of AD requires a comprehensive medical evaluation as there is no single test. The National Institute on Aging-Alzheimer's Association has established updated criteria to assess AD in the elderly which now includes a pre-clinical stage and degrees of amyloid

accumulation, tau tangle-bearing neurons, and neuritic plaques [10]. These criteria help to distinguish AD from other neurologic diseases such as Parkinson's and Lewy body disease.

Tests for biomarkers such as Aβ have been recently developed and are currently being used in AD diagnosis. Structural imaging of the brain utilizing magnetic resonance imaging (MRI) or computed tomography (CT) scans can be used to identify brain atrophy associated with later stage neurodegeneration [11]. Imaging compounds such as Pittsburgh compound B, which selectively binds Aβ deposits and can be visualized using PET scans, can be used to detect earlier stages of AD [12]. Although there is no current cure or efficient treatment for AD, these diagnostic screens can assist with tracking and staging of the disease process, differential diagnosis, and identification of prodromal stages of neurodegeneration. They can also be helpful to establish clinical trials of treatments involving early stage AD patients in the hope of preventing the progression of the disease into irreparable neuronal degeneration.

Studies have shown the accumulation of aggregated Aβ plaques found in AD patients has been associated with increased amounts of oxidative damage and consequent DSBs in the human brain [13, 14]. These Aβ aggregates primarily consist of the longer form of Aβ precursory product, $A\beta_{1\text{-}42,}$ as compared to the shorter, more commonly found $A\beta_{1\text{-}40}$ [15]. DSBs are the most deleterious forms of DNA damage, and can lead to mutations, cellular senescence, and apoptosis. How $A\beta_{1\text{-}42}$ is associated with DSB repair in post-mitotic neurons is generally unknown, such as whether this toxic precursory form of Aβ aggregates directly or indirectly affects repair processes, or affects the DNA itself through the production of ROS. Understanding the direct role of $A\beta_{1\text{-}42}$ in DNA damage and repair will increase our understanding of other neurodegenerative diseases such as Parkinson's disease which are also characterized by protein aggregates.

1.1.2 Alzheimer's Disease associated mutations

Only a small subset of AD cases is a result of identified inherited genetic mutations. Named early-onset familial AD (FAD), these constitute about 1% or less of all AD cases. They are the result of mutations in three genes: APP (amyloid precursor protein), PSEN1, and PSEN2 (presenilin 1 and 2). Presenilin 1 and 2 are subunits of the γ-secretase complex, one of the secretase enzymes responsible for processing APP into soluble $A\beta_{1-42}$ oligomers. Individuals with mutations in APP or PSEN1 are guaranteed to develop AD. Those with mutations in PSEN2 have a 95% chance of developing AD. Individuals with these specific mutations tend to develop AD well before age 65, typically around age 30, while the remaining population tends to develop late-stage AD after age 65 [1]. Importantly, mice and rats do not produce Aβ that aggregates in the same manner as human Aβ found in AD pathology. Mouse and human APP differ by 17 amino acids, 3 of which are located in the Aβ region, thus affecting its cleavage and aggregation [16]. Therefore, in order to more accurately investigate AD pathology in a rodent model, transgenic mice and rats are engineered using these FAD mutations to create more accurate models for essential research. Individuals with trisomy 21, or an extra copy of chromosome 21, are also prone develop AD due to overexpression of the APP gene. Reports indicate that nearly all individuals with trisomy 21, or Down's Syndrome, display AD neuropathology after age 40 due to higher amyloid plaque load and neurofibrillary tangles[17].

Risk factors known to increase the likelihood of developing late-stage AD include type II diabetes, obesity, cardiovascular disease, smoking, lack of physical and mental activity, and hypertension [1, 18-20]. Individuals may also carry genetic risk factors such as specific isoforms of the apolipoprotein gene (APOE). Unlike the APP and PSEN1 and PSEN2 mutations, however, having specific APOE isoforms does not guarantee the development of late-stage AD. The APOE gene codes for a protein that redistributes lipids (e.g.- cholesterol) in the central nervous system (CNS), and is normally synthesized and secreted by astrocytes[21]. There are three isoforms of

APOE which differ in single amino acid substitutions: ε2, ε3, or ε4, one of which is inherited from each parent. The most common isoform is ε3, with ε2 being the least common. Having the ε2 isoform may decrease one's risk of developing AD, while having one allele of the ε4 isoform increases one's risk by threefold compared to having two alleles of the ε4 isoform, which increases one's risk by eight to twelve fold. *In vitro* studies associated apoε3 and apoε2 with the production of long neurites, while apoε4 was associated with an inhibition of neurite outgrowth [22-24]. This association was specific to microtubule assembly in that apoε3 would stimulate the polymerization of β-tubulin and stabilize the formation of microtubules, and apoε4 would destabilize their formation. It was hypothesized that since apoε3 preferentially interacts with tau, it may protect tau from hyper-phosphorylation, one of the hallmarks of AD pathology [24, 25]. Another hypothesis states that low levels of apoε as seen in apoε4 carriers would lead to impaired clearance of soluble $A\beta_{1-42}$. This is a pathology reported in the cortex and hippocampus of apoε4/AD patients, and is based upon research findings postulating that apoε lipoprotein complexes bind to the lipophilic portion of soluble Aβ (localized in the amino acid 18–42 portion of the peptide) and clear it from the extracellular space [26].

In FAD mutations which lead to early onset AD, many contribute to increased $A\beta_{1-42}$ levels due to mutations in APP or its cleavage. However, these mutations are not present in late-stage AD. Aβ deposits have been associated with elevated levels of $A\beta_{1-42}$ in transgenic rodent models expressing human APP [27]. The accumulation of extracellular $A\beta_{1-42}$ has also been associated with both the seeding and further deposition of long and short forms of Aβ [28, 29]. Therefore, not only is the production of Aβ and its precursors relevant in understanding the development and pathology of AD as seen in the FAD associated mutations, but as illustrated in the case of apoε, clearing mechanisms of Aβ and its precursors before aggregation products develop is also essential to our understanding in order to develop strategies to prevent this devastating disease.

1.2 Tau pathology

Tau is a microtubule–associated protein (MAP) that stimulates tubulin assembly into microtubules in the brain. The single tau gene encodes six isoforms as a result of alternative splicing, all of which are expressed in the adult human brain [30]. Its reported beneficial effect is to stabilize microtubules, promoting neuritic extension and stabilization. A negative effect of tau is its competition with the motor protein kinesin, which could lead to decreased axonal transport [31-33].

Tau can be post-translationally modified in numerous ways including phosphorylation, glycosylation, ubiquitination, polyamination, nitration, truncation, and aggregation. However, the hyper-phosphorylation of tau has most strongly been implicated in the pathology of AD [34]. Phosphorylation sites implicated in AD include Ser199/Ser202/Thr205, Thr212, Thr231/Ser235, Ser262/Ser356, and Ser422 which have been found to convert tau to an inhibitory molecule that sequesters normal microtubule-associated proteins from microtubules [35]. Phosphorylation at Thr231, Ser396, and Ser422 promotes the self-aggregation of tau into filaments, impacting its activity and disrupting microtubules [36]. How abnormal tau leads to toxicity isn't fully understood. Some studies have shown a gain in toxic ability of abnormal hyper-phosphorylated tau to sequester normal tau and other microtubule associated proteins, leading to microtubule disassembly [37-39]. More recent studies have even begun probing correlations between amyloid beta protein (Aβ) and tau hyper-phosphorylation, and whether one may contribute to the other. For example, a study found aggregated Aβ peptides induced tau phosphorylation in primary rat neuronal cultures [40]. For the purposes and simplicity of this thesis, however, we focused on Aβ's role in AD pathology.

1.3 The amyloid beta hypothesis

1.3.1 Amyloid beta processing

The amyloid precursor protein (APP), a transmembrane protein consisting of 695-770 amino acids involved in neurodevelopment, synaptogenesis, and cell adhesion, is proteolytically processed along two separate pathways: 1) the amyloidogenic, which leads to amyloid beta (Aβ) production, and 2) the non-amyloidogenic pathway [41-44]. As illustrated in **Fig. 1-1**, in the non-amyloidogenic pathway, APP cleavage is mediated by α-secretases (ADAM9, ADAM10, or ADAM17), releasing: the larger soluble ectodomain sAPPα. The membrane-anchored carboxy-terminal domain of C83 can undergo further cleavage by γ- secretase to produce p3 [45, 46], an innocuous fragment. In the amyloidogenic pathway, β- secretase (BACE1) first cleaves APP to release an ectodomain (sAPPβ), leaving 99 amino acids of APP within the membrane (C99). C99 is then cleaved by γ- secretase 38-43 amino acids from the N-terminus to produce Aβ [43, 44, 47]. The final cleavage of Aβ produces fragments which vary in length from 37-43 amino acids. The longer Aβ peptides, including $A\beta_{1-42,}$ are more hydrophobic and more prone to aggregate in the brains of AD patients. Low concentrations (pM) of $A\beta_{1-42}$ have been confirmed in the interstitial fluid of normal brains by microdialysis, but higher concentrations in the nM-μM range lead to neurotoxicity and neuronal death [48, 49].

It is only partially known what triggers the amyloidogenic vs the non-amyloidogenic pathway in neurons: the α-secretases, which cleave APP along the non-amyloidogenic pathway, are more abundant than the β-secretases, which cleave APP in the amyloidogenic pathway [50-52]. However, what function $A\beta_{1-42}$ serves is not clear.

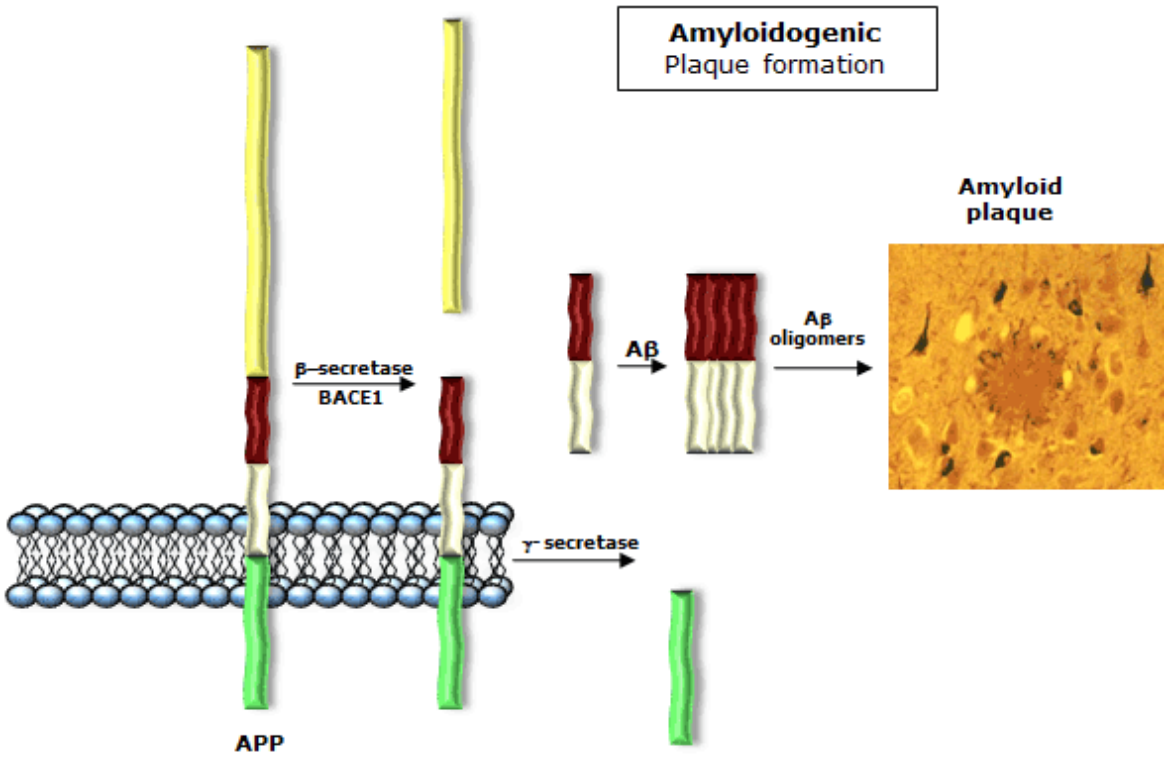

Figure 1-1 The amyloidogenic pathway of Aß production.

In the amyloidogenic pathway, amyloid precursor protein (APP) is cleaved by β-secretase (BACE1) and γ-secretase to generate amyloid-beta fragments ranging in size from 38-43aa. These aggregate outside the cells into oligomers, and further aggregate into fibrils and plaques.

1.3.2 Amyloid beta as a metallo-protein

Free metals such as Fe, Cu, and Zn are essential for numerous functions in the brain such as neuronal transmission, oxygen transport, and electron transfer. Maintaining homeostasis of these metals and their reduced/oxidized forms is critical. Aβ has been implicated in numerous interactions with Fe, Cu, and Zn, both in beneficial and detrimental ways. For example, prior research has found that Fe^{2+} concentrations are higher in advanced AD brains than in normal patients [53]. Iron plays an extensive role in the production of oxidative stress by the formation of

a hydroxyl radical via the Fenton reaction. Here, Fe^{2+} is reduced to Fe^{3+} by O_2, producing O_2^-. O_2^- then reacts with H^+ and produces H_2O_2, which reacts with Fe^{2+} and produces hydroxyl radicals [54]. These chemically reactive hydroxyl radicals in turn generate lipid peroxidation products, protein carbonyl modifications, and nucleic acid adducts such as 8-hydroxyguanosine (8-OHG) which have all been implicated as characteristic of AD neuropathology [55, 56]. In vitro studies have also showed that Fe induces Aβ aggregation and tau hyper-phosphorylation [57, 58].

Cu can be distributed differently throughout each brain region. However, overall levels of Cu are found to be lower in the cerebral cortex of AD patients compared to healthy patients, hypothetically due to the association of Cu to aggregated Aβ plaques and its depletion from the surrounding tissue and cells [59, 60]. Cu is known to directly bind Aβ. This Cu- Aβ peptide then produces H_2O_2 through the reduction of Cu^{2+} to Cu^{3+} and the production of hydroxyl radicals [61]. The redox activity of Aβ is greatest for $Aβ_{1-42}$, largely mediated by the Cu- Aβ interaction. This then leads to the oxidative stress toxicity observed in neuronal cell culture and the evidence presented prior that oxidative injury contributes to the pathology of AD [62, 63]. An opposing effect, however, is that Cu^{2+} has also been shown to prevent the amyloid fibril formation of Aβ by binding with Aβ, thus inhibiting the production of Aβ aggregates [64].

Brain tissue contains the highest levels of Zn in the human body where it is substantially enriched in the glutamatergic nerve terminals [65, 66]. Upon neuronal activation it is released into the synaptic cleft and interacts with neuronal receptors, ion channels, and transmitters to regulate neuronal transmission [67-69]. It has been established that Zn is highly enriched in AD in Aβ plaques, potentially mislocalizing functional Zn from the rest of the brain [60, 70-72]. Zn can also bind Aβ via its histidine residues. This binding alters Aβ's conformation and prevents its binding to Cu, inhibiting the H_2O_2 production that would result from Cu^{2+} reduction[62, 73]. High Zn concentrations are neurotoxic, however, so it is only in lower competitive concentrations that Zn binding protects against Aβ toxicity [74].

These studies indicate both protective and detrimental roles of Aβ, leading to questions about when and under what specific conditions it would serve these contradictory functions.

1.3.3 APP cleavage products are necessary for normal function

The “Amyloid hypothesis” focuses on the imbalance of production and clearance of $A\beta_{1-42}$ and its related peptides as the neurotoxic factors that contribute to gradual impaired neuronal function and cell death as seen in the progressive pathology of AD [75]. Numerous therapies and studies have focused on understanding both the physiological roles of APP and its cleavage products. They also focus on how the imbalance of these products may contribute to neurodegeneration in order to provide treatments that do not exacerbate the effects of depleting what could be a necessary and functioning protein. For example, APP knockout mice initially appear normal in early development, but eventually show reductions in body weight, grip strength, locomotor activity and synaptic transmission as well as sensitivity to epileptic seizures, forebrain defects, and a reduction in cerebral blood flow as a response to ischemia (restriction in blood supply) or hypoxia (oxygen deprivation) [76, 77]. Both APP and $A\beta_{1-42}$ expression were found to be increased in hypoxic and ischemic conditions in the wild type, indicating a role for APP and its cleavage fragments in cerebral blood flow under specific conditions [77]. Experiments with mice over-expressing human APP show they have increased basal levels of DSBs and retain them longer after exploring novel environments, implicating a reduced capacity for repair [78]. A specific β-secretase (BACE-1) knockout mouse model shows no consistent phenotypic difference from wild type littermates, despite BACE being the primary β-secretase of APP and its knockout resulting in significantly less $A\beta_{1-40}$ and $A\beta_{1-42}$ production overall [79].

γ-secretase knockouts, however, are not conducive to AD studies as this enzyme is not specific to a single pathway. The γ-secretase complex cleaves numerous substrates including

APP and Notch. Specifically, the γ-secretase subunit PSEN1 is a key regulator of Notch and Wnt, and is essential for the developmental maturation of glia and neurons. Notch signaling itself is responsible for neuronal differentiation during embryogenesis and is also involved in neuronal plasticity [80, 81]. PSEN1 knockout mouse models exhibit perinatal lethality, skeletal deformations, intracranial hemorrhaging, and CNS abnormalities resembling Notch knockout phenotypes [82, 83]. PSEN2 knockout mice, however, only show a mild pulmonary phenotype, indicating the γ-secretase subunits PSEN1 and PSEN2 have non-identical functions in mice [84, 85]. Numerous γ-secretase inhibitors have been tested that successfully reduce the amount of Aβ produced in mouse models and patients. These inhibitors specifically target the PSEN1 and PSEN2 subunits of γ-secretase. Due to off target effects and side effects, however, including those affecting Notch signaling, these γ-secretase inhibitors are not currently able to be used in clinical trials for use as AD therapeutics [86]. What these and future studies do provide is insight into the targets of the secretases, maintenance of homeostasis of Aβ, and how to modify treatments to target specific proteins in order to prevent the pathology of AD from developing.

1.4 Oxidative stress in AD

Oxidative stress is characterized by an imbalance in the production of ROS and manifests in high levels of oxidized proteins, advanced glycation end products, lipid peroxidation end products, and the formation of toxic species such as peroxides, alcohols, aldehydes, free carbonyls, ketones, cholestenone and oxidative modifications in nuclear and mitochondrial DNA. ROS are generated endogenously by cellular metabolism and by a variety of exogenous agents such as ionizing radiation. Metabolically-generated ROS can generate ~10,000 oxidative lesions in DNA per day [87]. Neurons also carry a large number of mitochondria which are the main

sources of ROS during glutamate excitotoxicity [88].

Oxidative DNA lesions resulting from ROS can consist of single and double strand DNA breaks and oxidized base adducts such as 8-hydroxyguanosine (8-OHG). Studies have found both increased levels of 8-OHG in mitochondrial and nuclear DNA in the cortex of AD patients and increased levels of γ-H2AX, a modified histone and marker for DSBs, in the hippocampal region of AD patients [13, 89].

Other markers for oxidation have been used to indicate oxidative stress in AD studies, including methionine, an essential amino acid [90]. In the case of $A\beta_{1-42}$, which contains a methionine at residue 35, it is suggested that the interaction of the sulfur atom of Met-35 with Ile-31 leads to an intermediate that can be oxidized by free oxygen to produce a sulfuramyl radical [91]. When introduced to rat embryonic primary hippocampal neurons, it induces oxidative damage evidenced by protein carbonyls and neurotoxicity. Vitamin E, a chain breaking antioxidant, modulates these effects [90]. When the sulfur in methionine is substituted with a methylene moiety to lead to a norleucine derivative (Aβ(1-42M35NLE), these peptide led to no oxidative damage, no neurotoxicity, and no free radical formation in 9-11 day murine primary hippocampal neurons [92]. *In vivo* studies utilizing transgenic *Caenorhabditis elegans* modified to produce human Aβ in their muscle wall further confirmed the importance of methionine in the oxidative and neurotoxic properties of $A\beta_{1-42}$ as experimental organisms with Met^{35} substitutions displayed reduced Aβ aggregates and did not show progressive paralysis or slow growth observed in the wt Aβ strains [93]. These studies support that $A\beta_{1-42}$ itself induces oxidative stress and that antioxidant therapies may modulate its neurotoxic effects.

More evidence of free radical induced oxidative stress in AD has been found in lipid peroxidation, protein oxidation, and DNA/RNA oxidation in AD patient brain samples. Altered indices of lipid peroxidation in AD brains include thiobarbituric acid reactive substances (TBARS), phospholipid composition, enzyme activity to clear lipid peroxidation products, isoprostane

concentrations, and concentrations of α- and β- unsaturated aldehydes [94, 95]. Thiobarbituric acid reacts with lipid peroxidation products, providing a means to measure oxidative stress. Levels of TBARS were found to be significantly increased in the hippocampal and pyriform cortex regions of AD patients compared to controls, indicating increased oxidative stress in AD patients [94]. Polyunsaturated fatty acids such as arachidonic acid and docosohexenoic acid are abundant in the brain and have been shown to be highly oxidizable. Studies on membrane phospholipids have indicated a decrease in levels of these specific phospholipids in AD, indicating high levels of oxidation activity [96].

As mentioned in Chapter 1.3 redox recycling of Aβ produces hydrogen peroxide. This has been found to occur in the presence of biological reducing reagents with cholesterol and long-chain fatty acids as the most likely reductants due to Aβ toxicity mostly associated with the membrane [97-99]. One β- unsaturated aldehyde, HNE (4-hydroxy-2-trans-noneal), is a major product of lipid peroxidation in the membrane, and concentrations of HNE have been shown to be increased in multiple brain regions, including the hippocampus, and in the ventricular cerebrospinal fluid (CSF) of AD patients [100]. HNE has also been implicated in Fe-induced oxidative damage in cholinergic neurons [100, 101]. These are the neurons primarily affected in the basal forebrain of advanced AD patients with a reduction in number of cholinergic neurons and decrease in choline acetyltransferase (ChAT) activity correlating with cognitive decline [102-104].

Studies have shown that oxidative stress induces the γ-secretase mediated expression of β-secretase, contributing to an increase in amyloidogenic Aβ production in AD pathology. In response to oxidative stress [e.g.-production of lipid peroxidation product 4-hydroxy-2,3 noneal (HNE)], γ-secretase cleavage of APP produces the ACID cleavage product which translocates to the nucleus and mediates transcriptional upregulation of BACE1 expression [105-107]. Some studies have found an increase in Aβ oligomers associated with an increase in DSBs in human

brain tissue, while others have found higher levels of oxidative damage associated with an increase in Aβ oligomers in human AD patients despite research claiming an anti-oxidative role of Aβ [13, 14, 105].

The oxidative modification of amino acid side chains and protein cross-linking can alter protein function and prevent malfunctioning proteins from being degraded by proteinases [108-110]. Direct attacks on amino acid side chains by free radicals or the products of lipid peroxidation (e.g.-HNE) acting upon proteins can produce protein carbonyl groups which can be used as biomarkers of oxidative stress [111]. These can be detected via numerous fluorescent or immunochemical assays [108, 112]. Studies have consequently shown that protein carbonyl levels are increased in the frontal pole, hippocampus, and superior middle temporal gyrus in AD brains, correlating with AD histopathology [113-117].

Together, these studies that utilize markers for evidence of oxidative stress including increased levels of 8-OHG, γ-H2AX, lipid peroxidation, DNA/RNA oxidation, and protein carbonyl groups imply a strong correlation between oxidative damage, Aβ, and AD neuropathology.

1.5 DNA repair and genomic stability

1.5.1 DNA repair mechanisms

Many different types of DNA lesions can occur due to damage from endogenous and exogenous sources. The main pathways to repair DNA lesions are nucleotide excision repair (NER), base excision repair (BER), mismatch repair (MMR), single strand break repair (SSBR), and double strand break repair (DSBR) (**Fig. 1-2**). UV light and polycyclic aromatic hydrocarbons can directly damage DNA, leading to 6-4 photoproducts, bulky adducts, or cyclobutane pyrimidine dimers. The DNA strand containing the lesion is excised via NER. X-rays, ROS from oxidative

damage, and alkylating agents can cause abasic sites, oxidized, deaminated, and alkylated bases, and DNA single strand breaks (SSBs) which can be removed via BER or single strand annealing (SSA). In the BER pathway, specific glycosylases recognize and remove damaged nucleotide bases [118]. Ionizing radiation, UV light, and chemotherapy agents such as hydroxyurea can all lead to DSBs in the backbone of DNA. They can also occur due to SSBs in close proximity, or replication past previously existing lesions. DSBs are repaired via DSBR, either through single strand annealing (SSA), microhomology-mediated end joining (MMEJ), homologous recombination (HR), or non-homologous end joining (NHEJ). In SSA, homologous repeats are used to bridge DSB ends with RAD52 promoting the annealing of complementary ssDNA [119-121]. MMEJ promotes the use of 5-25 bp microhomologous sequences as broken DNA ends are aligned before ligation and does not rely on the NHEJ associated Ku70/80 complex proteins. This pathway often leads to significant deletions, insertions, translocations, inversions and rearrangements [122]. In NHEJ, the broken DNA ends are processed/digested and then directly ligated, potentially leading to nucleotide deletions and consequent frameshift mutations. Thus, NHEJ is considered error-prone [123]. HR utilizes undamaged templates in order to direct repair of the damaged strands. Replication and recombination errors can result in base mismatches, insertions and deletions. These erroneous nucleotides are excised via MMR independently of any specific glycosylases, unlike the BER pathway [124, 125].

Maintaining the stability of the genome is essential for survival and overall health. Failure to efficiently and completely repair DNA lesions can lead to deleterious mutations, insertions and deletions, premature stop codons, and interrupted essential coding genes, the consequences of which can lead to cellular apoptosis or senescence and disease pathologies such as cancer or neurodegeneration [126-132]. Numerous studies have shown that deficiencies in BER, which is utilized primarily for the repair of DNA base modifications, play a large role in neurodegeneration. For example, the expression of DNA polymerase β, the polymerase that conducts gap-filling DNA synthesis, was reduced in AD patients [133]. Also, numerous mutations in BER proteins have

resulted in an increase in genomic mutation rates, implying that the reduction in efficient repair could lead to genomic instability, cancer, and neurodegenerative pathologies [134]. Mutations in genes required for efficient repair of SSBs or DSBs can also lead to numerous neurodegenerative diseases such as Cockayne syndrome (CS), Xeroderma pigmentosum (XP), and Ataxia telangiectasia (A-T) [135]. Studies have also found high levels of oxidized DNA bases such as 8-oxoG in nuclear and mitochondrial DNA in the brains of Mild Cognitive Impairment (MCI) patients who are in the phase between normal aging and early dementia [136].

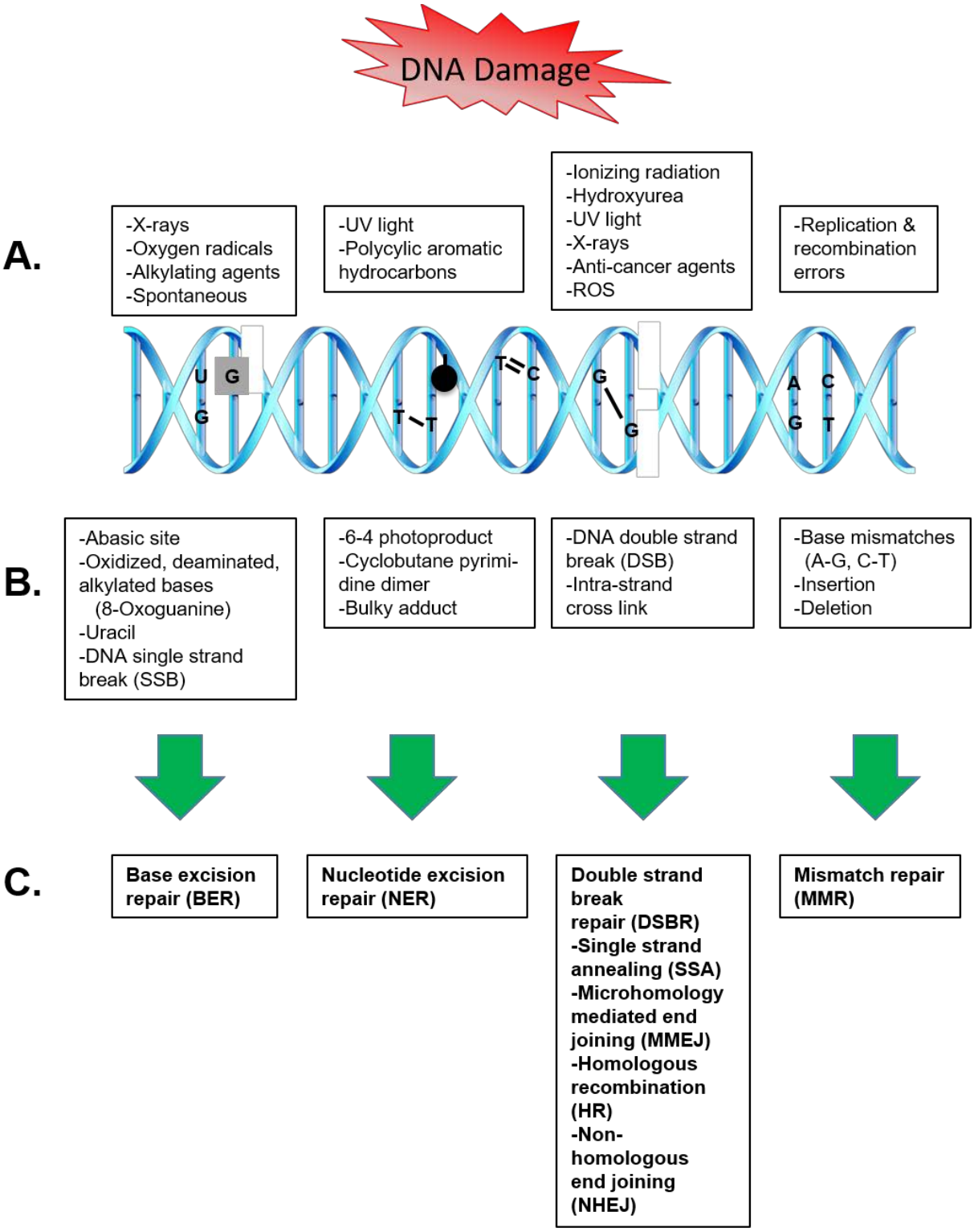

Figure 1-2 Representation of DNA repair pathways.

A. Endogenous and exogenous sources of DNA damage. B. Types of DNA lesions resulting from damage.

C. DNA repair pathways utilized for repair of specific DNA lesions.

1.5.2 Homologous Recombination (HR)

DSB are the most deleterious forms of DNA damage. While NHEJ tends to be more error prone and HR more error free, there are numerous factors that influence DSB repair pathway choice. These factors include the cell cycle phase and the initial resectioning process [137]. The result after damage is the initiation of cell cycle arrest and repair either via HR or NHEJ followed by the re-initiation of the cell cycle or, failing sufficient repair, apoptosis or senescence.

For more error-free repair of DSBs, canonical HR can occur during the late S & G_2/M phases of the cell cycle when an intact sister chromatid is present and in close proximity of the break & can be utilized as a template (**Fig. 1-3**) [138]. This pathway first involves resection, or degradation of the broken DNA ends, into single stranded DNA tails with 3' overhangs by the MRN complex of nucleases (MRE11, RAD50, NBS1) and its co-factor Sae2. Once the MRN complex binds to the DSB ends, the endonuclease CtIP interacts with the complex and initiates resectioning in the 5' to 3' direction, generating 3'-OH single-stranded DNA (ssDNA) overhangs. The ssDNA generated is immediately coated by the ssDNA binding protein replication protein A (RPA) to prevent degradation or direct ligation [139].

RAD51 filament formation, which is essential for HR recombination, occurs following RPA coating. However, RPA directly blocks RAD51 binding to ssDNA. In human cells, BRCA1 recruits PALB2 (Partner and Localizer of BRCA2) and BRCA2 to assist in loading RAD51 onto the DNA [140]. This is another step where pathway choice can be mediated. Here, ubiquitylation of key residues of PALB2 by the E3 ligase complex CRL3-KEAP1 in the G_1 phase of the cell cycle prevents BRCA1 binding, thus favoring NHEJ instead in the G_1 phase. CRL3-KEAP1 is downregulated in the S phase when the deubiquitinase USP11 is upregulated, thus favoring HR in the S phase [141]. ATR activation at the resected DSB also leads to the phosphorylation of S59 in PALB2, enhancing its complex formation with BRCA1 and further favoring HR [142].

After BRCA1 recruits PALB2 and BRCA2, BRCA2 assists in loading RAD51 recombinase onto the 3' DNA overhangs to form nucleoprotein filaments, displacing RPA. In yeast cells, Rad52 is essential for Rad51 filament formation *in vivo*. This is not the case in human cells as RAD52's role in canonical HR is not clearly defined [143, 144]. However, in BRCA2 deficient cells, RAD52 becomes essential for RAD51 filament formation [145]. In vertebrates, there are five different RAD51 paralogs (RAD51B, RAD51C, RAD51D, XRCC2, XRCC3), each necessary for RAD51 foci formation after damage, and each playing different roles in filament formation that are still being investigated [146]. These RAD51 paralogs each load into the RAD51 filament in a varying arrangement, the purpose of which isn't entirely known. It is speculated, however, that their arrangement helps protect the ssDNA from nuclease activity as Rad55 and Rad57 in yeast form a heterodimer that blocks Srs2 helicase activity intended to prevent hyper-recombination [147].

These RAD51 filaments then search for a homologous DNA template on the sister chromatid and form a joint heteroduplex molecule between the damaged DNA and undamaged template. RAD54 associates with the RAD51-ssDNA filaments and stabilizes them independently of its ATPase activity [148]. The 3' end of the invading DNA strand must then intertwine with the donor complement strand to form a primer-template junction competent for DNA synthesis. This is known as the D-loop. Minimally, only the 3' end is required to form a primer-template junction, however it can be hundreds of base pairs long. As evidenced by studies using substrates with terminal heterologies, the junction forming sequence need not be directly located at the 3' end [149].

DNA synthesis begins at the D-loop, involving Pol δ, PCNA, and its loader RFC1-5, followed by disengagement of the invading strand [150]. The resulting ssDNA strands are then immediately bound by RPA. The DNA ends can now anneal within the region of homology created within the D-loop. However, how this annealing process occurs is largely unknown. In yeast, Rad52 fulfills this role [151]. In humans, RAD52 is capable of annealing homologous RPA-coated

ssDNA strands such as in the SSA pathway [119, 121]. However, there are no studies that currently clearly define its role in HR.

If annealing does not occur, the formation of double Holliday junctions (dHJ) may proceed. In forming the dHJ, the second resected DSB end may anneal to the D-loop, or both DSB ends instead invade the donor and proceed onto DNA synthesis. When the dHJ is processed, it will result in either non-crossover or crossover products. Due to crossover products (as high as 50%), somatic cells largely avoid the formation of dHJ, and prefer resolution of HR via annealing, also known as synthesis-dependent strand annealing (SDSA) [152].

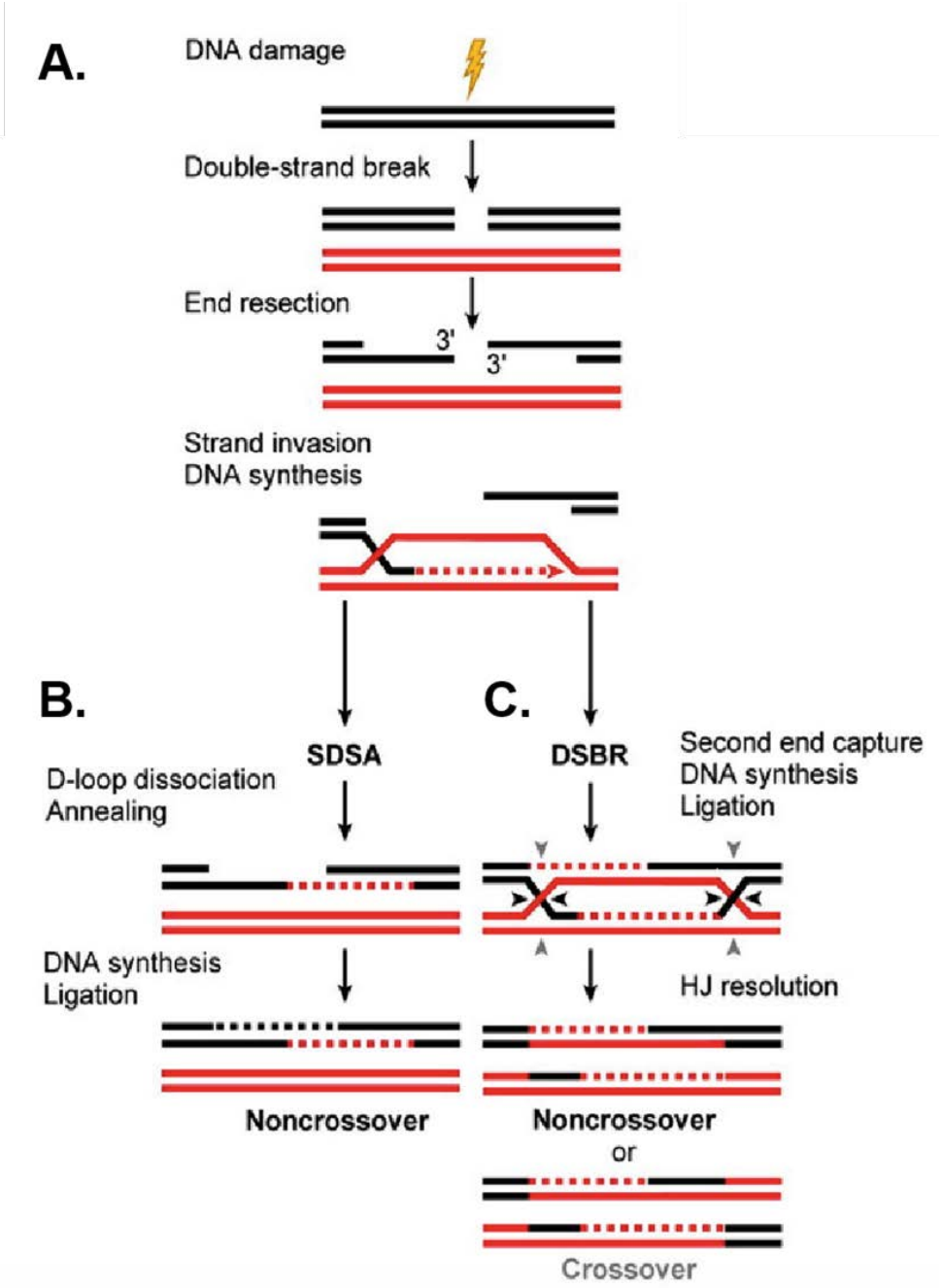

Figure 1-3 Simplified representation of Homologous Recombination (HR) repair pathway.

A. After DSB formation, resection occurs to form 3' ssDNA overhangs. After successful homology search, strand invasion occurs to form a D-loop structure, followed by DNA synthesis. **B.** In SDSA, only non-crossover products are formed after the D-loop unwinds and the freed ssDNA anneals with the complementary ssDNA on the other end. **C.** Alternately, the second DSB end can be captured to form an

intermediate, resulting in noncrossover or crossover products after resolution of two Holliday junctions (HJ)s.

1.5.3 Non-homologous end joining (NHEJ)

For more error-prone resolution of DSBs, the NHEJ pathway can be used throughout the cell cycle (**Fig 1-4**) [153]. In studies using human fibroblasts, NHEJ was found to repair nearly all DSBs outside of the G_2/S cell cycle phases, as well as almost 80% of DSBs within the G_2/S phases not proximal to replication forks [154]. It has been proposed that preference for NHEJ repair is largely due to a high abundance of Ku protein, one of the first proteins recruited to broken DNA ends, which promotes NHEJ and also inhibits the DNA resectioning event that leads to HR [155, 156]. 53BP1 has also been identified as a negative regulator of HR, promoting NHEJ instead. It limits the resection process by binding to specific histone modifications around the break site. The Tudor domain of 53BP1 binds to H4K20Me_2, a histone modification present throughout the genome, while its "Ubiquitin-Dependent Recruitment" region binds to H2AK15ub, a histone modification induced by RNF168 after DNA damage signaling at the DSB [157, 158]. This negative regulation of HR by 53BP1 is counteracted by BRCA1, which allows resection to continue in the presence of 53BP1. 53BP1 binding is also influenced by multiple factors, thus affecting its ability to direct DSB repair pathway choice. These factors include proteins that compete for H4K20Me_2 binding sites such as JMJD2A and L3MBTL1, or the histone acetyltransferase complex TIP60 [159, 160]. TIP60 also creates a chromatin environment more favorable to BRCA1 binding than 53BP1 by acetylating H4K16 to H4K16ac, interfering with the binding between 53BP1's Tudor domain and histone H4 [161, 162]. 53BP1 also has reduced binding during S phase due to a lessening of H4K20Me_2 modifications during DNA replication, driving DSB repair towards HR [163].

Nuclease activity occurs first at the two incompatible broken DNA ends involved in a DSB. The resectioning process in NHEJ occurs by the recruitment of DNA-PKcs with the endonuclease Artemis. In NHEJ, the Ku heterodimer consisting of Ku70 and Ku80 is first recruited to the damage site. This complex acts as a scaffold for DNA-PKcs as DNA-PKcs interact with the C-terminus of Ku80. Although the last 12 amino acids of Ku80 are sufficient for this interaction, Ku80 must be bound to a DNA end in order to form a strong complex with DNA-PKcs [164-166]. Following binding to DNA, the DNA-PKcs autophosphorylate and activate Artemis. This is accomplished by the phosphorylated DNA-PKcs phosphorylating the C-terminal inhibitory region of Artemis, dissociating it from the N-terminal catalytic domain [167]. When in complex with DNA-PKcs, activated Artemis has endonuclease activity on the 5' and 3' overhangs [168, 169]. Numerous members of the polymerase X family of polymerases then participate in DSB repair by NHEJ. These polymerases, such as Pol μ and Pol λ have an N-terminal BRCA1 C terminus (BRCT) domain that allows them to interact with the Ku complex [167]. These polymerases incorporate nucleotides during NHEJ, but in a template independent manner [170, 171]. In a complex with X-ray repair cross-complementing 4 (XRCC4) protein, DNA ligase IV (Lig4) then ligates the two DNA ends together [172]. The result of NHEJ is not a perfect joining of the two broken DNA ends as Artemis activity can lead to nucleotide loss and polymerase activity can lead to nucleotide gain [173]. These final results can promote frameshift mutations, interrupted essential genes, and premature stop codons, all of which compromise genomic fidelity.

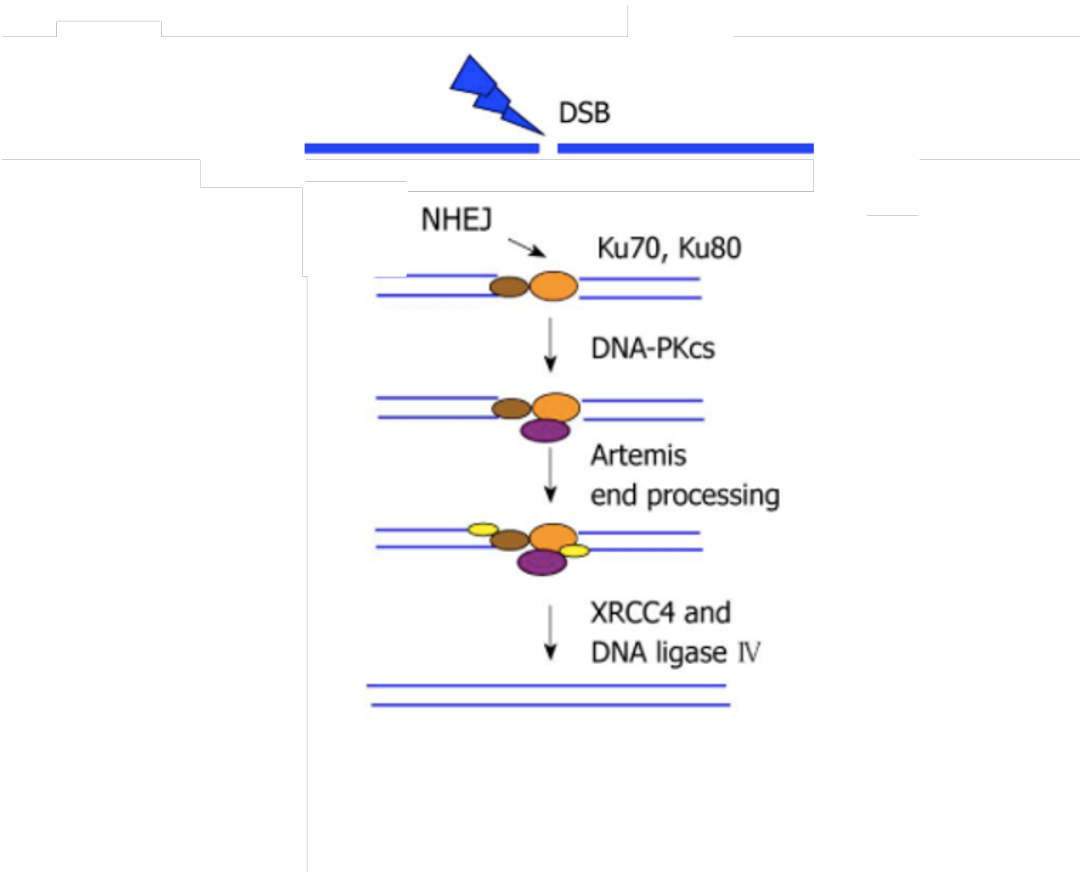

Figure 1-4 Simplified representation of Non-homologous end joining (NHEJ) repair pathway.

The broken DNA ends are processed and directly ligated by actions of the end-binding Ku70/80 complex and DNA-PKcs, followed by Artemis end processing and XRCC4 and DNA ligase IV.

1.5.4 Transcription-coupled homologous recombination (TC-HR)

It has long been assumed that HR can only take place during the late S/G_2 phases of the cell cycle where sister chromatids are present as templates [174]. Except for in the hippocampus and striatum, most neurons in the adult human brain are terminally differentiated and non-dividing, and therefore are assumed to be incapable of utilizing HR for DSB repair [175, 176]. For post-mitotic cells such as terminally differentiated neurons that cannot utilize a sister chromatid template, only the error-prone NHEJ pathway has been proposed [123]. However, recent studies in the Lan lab have elucidated an RNA-templated HR repair mechanism of DSBs at active

transcription sites during the G_0/G_1 phase called transcription-coupled homologous recombination (TC-HR) [177].

Cockayne syndrome B (CSB) protein is involved in the transcription-coupled NER (TC-NER) pathway. After DNA damage induced by UV light, RNA polymerase II (RNA POLII) stalls at bulky lesions and CSB is recruited to facilitate NER directed repair of the transcribed DNA strand [178, 179]. Due to the fact that patients with CSB deficiencies also manifest neurodegenerative pathologies and CSB-defective cells are sensitive to IR, it was hypothesized that CSB must play a larger role in maintaining genomic stability against other forms of DNA damage, specifically DSBs, the more deleterious form of damage [180-183]. The Lan lab therefore investigated the role of CSB in DSB repair using the DNA damage at active transcription sites (DART) system (**Fig. 1-5A-D**), which enables the study of molecular responses to light-induced DNA damage at single genomic loci with controllable transcription [184, 185]. In the DART system, when activated by visible light (550-580 nm), the modified red fluorescent protein chromophore KillerRed (KR) emits site-specific ROS [186, 187] (**Fig. 1-5A**). When positioned directly onto DNA, KR can induce oxidative damage and DNA strand breaks after white fluorescent light excitation. In order to localize KR, a tandem tetracycline repressive element (TRE) array cassette of approximately 200 copies of 96 random TRE repeats was integrated at a defined genomic locus in U2OS TRE cells. This specific locus has been determined as adjacent to the centromere of the X chromosome in a heterochromatinized region, or region with condensed chromatin. A CMV promoter is located after the TRE repeats to allow the activation of transcription upon transient expression of TRE-fusion proteins, specifically those fused to the transcription activator VP16 (TA) (**Fig. 1-5B**). U2OS TRE cells are exposed to white light for 15 min, and the tet-repressor (tetR)- or tet-transcription activator (TA)-tagged KR proteins (tetR-KR or TA-KR) induce similar amounts of ROS-induced DSBs at transcriptionally inactive or active sites, respectively in real time [184] (**Fig. 1-5C&D**).

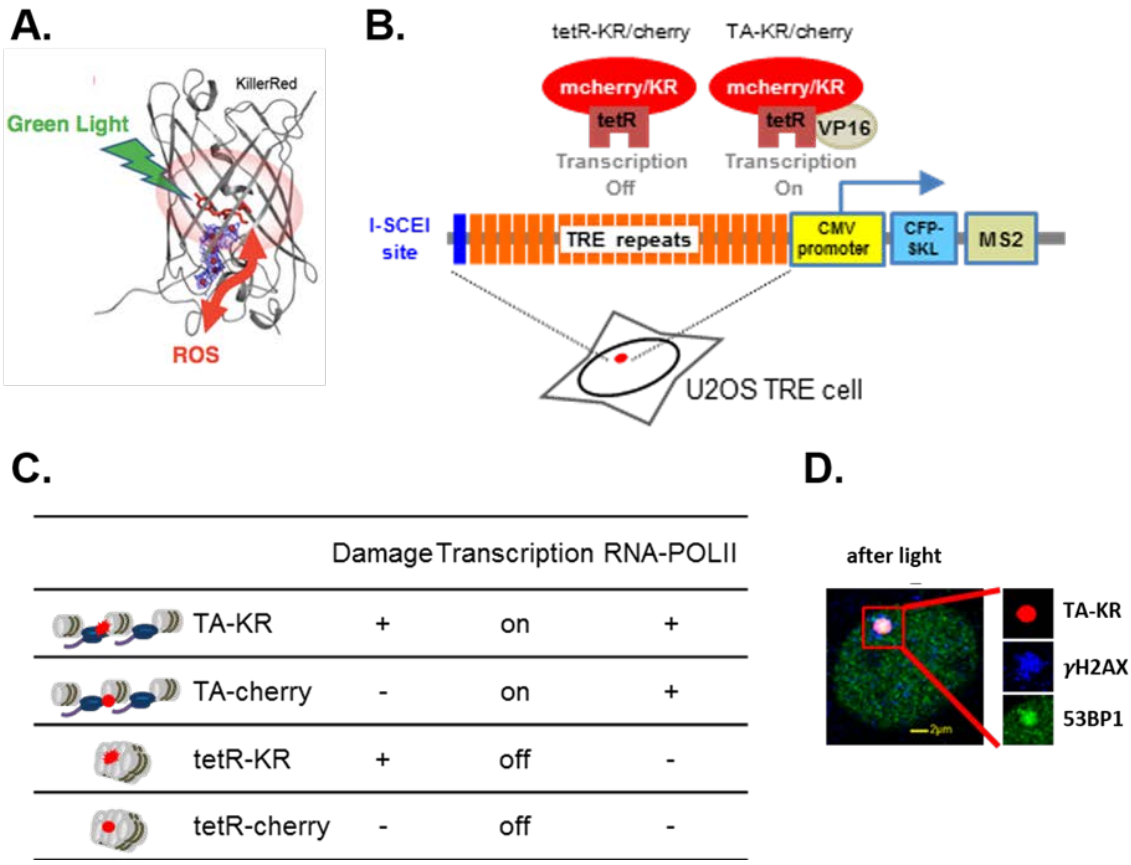

Figure 1-5. Schematic for the DNA damage at active transcription sites (DART) system for targeted single cell nuclei DNA damage.

A. KillerRed (KR) induced by white or green light (550-580nm) produces ROS. **B.** A tandem tetracycline repressive element (TRE) array cassette integrated at a defined genomic locus in U2OS-TRE cells allows fusion proteins to translocate to a specific location for DNA damage induction. A CMV promoter is located after the TRE repeats to allow the activation of transcription upon transient expression of transcription activator (VP16) containing proteins. **C.** Scheme of the experimental system and senerios of TA-KR/cherry and tetR-KR/cherry in U2OS TRE cells where cherry is the non-ROS producing control. **D.** Confocal image of single U2OS-TRE nucleus with TA-KR (red), DSB marker γ-H2AX (blue), and DSB repair protein 53BP1 (green) after light induction to illustrate DNA damage. Adapted from [177] with permission from the publisher.

Using the DART system, the Lan lab demonstrated that HR proteins RAD52, RAD51, RAD51C, and RPA1 are enriched at transcriptionally active DNA damage sites in cells synchronized in the G_0/G_1 phase. This recruitment is dependent upon CSB repair protein (**Fig. 1-6**). They also found that RAD52 and RAD51C interact with CSB independently of DNA after damage, but this interaction is abolished with transcription inhibition. The C-terminus of RAD52 co-localizes to actively transcribed DNA damage sites [177]. These data imply that RAD52 foci at actively transcribed DNA damage sites require the presence of an RNA template. This messenger RNA (mRNA) may be utilized as a bridge or template for the recombination process for error-free break repair in TC-HR [188-190]. Finally, inhibition of transcription sensitizes wild type cells to IR, but not CSB-deficient cells. This indicates that CSB facilitates transcription-coupled recombination to enable cell survival [177].

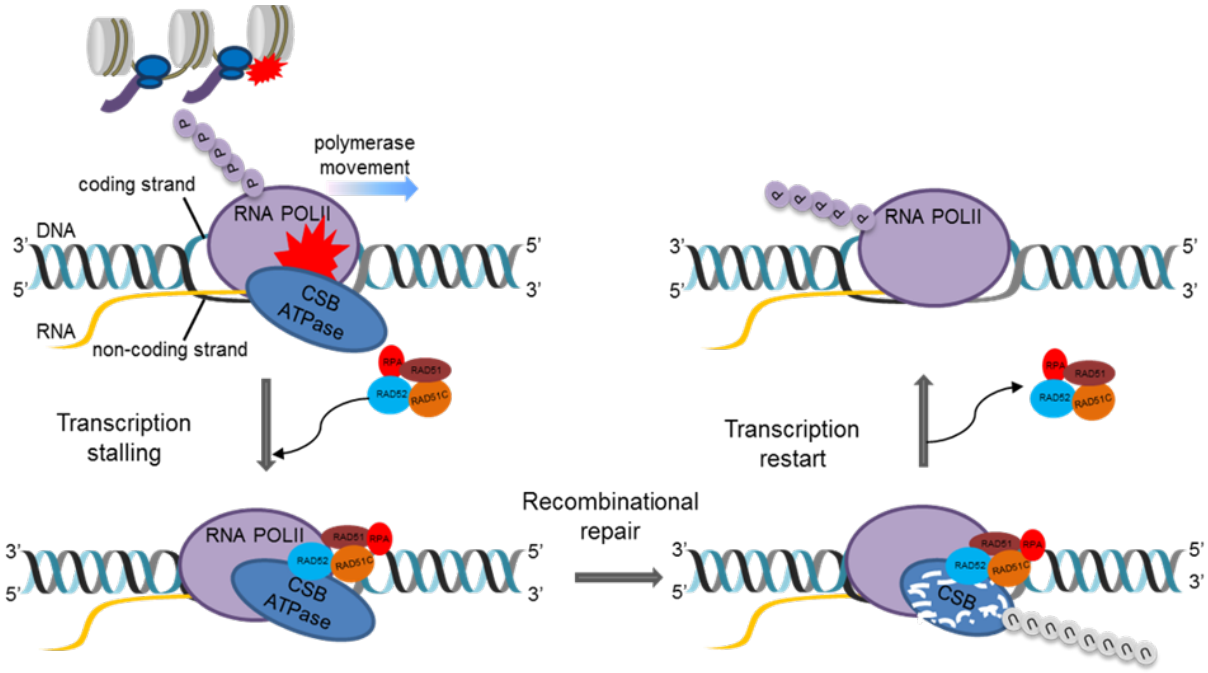

Figure 1-6. Model of CSB dependent RNA templated repair at transcriptionally activated DNA damage sites.

RNA polymerase II stalls at actively transcribed DNA damage sites containing DSBs, followed by recruitment of CSB, RAD52 and RAD51C, RAD51 and RPA. After repair, CSB is polyubiquitinated, followed by the release of remaining repair factors and RNA polymerase II phosphorylation to resume transcription.

An RNA-templated, RAD52 directed mechanism of HR has also been reported in yeast [191]. Prior to my research, however, it was not known whether this transcription dependent HR pathway existed in neurons or other post-mitotic cells.

R-loops are three stranded nucleic acid structures formed during the transcription process. They are composed of a nascent RNA strand hybridized with the DNA template and the single stranded non-template DNA strand. They are formed by RNA polymerase II transcribing a C-rich template so that a G-rich transcript is generated and depend on three main features: high G density, negative supercoiling, and DNA nicks [192-194]. It's been hypothesized that the formation of R-loops can lead to genomic instability. The precise mechanisms for this are still under investigation, but models have been proposed showing that the exposure of ssDNA during the

RNA/DNA hybrid formation would leave the ssDNA strand susceptible to DNA lesions [195]. Also, the unpaired strand may be susceptible to DNA damage from deamination of dC to dU, leading to DSBs [196-198]. Unpublished research in the Lan lab using the DART system and antibodies for anti-S9.6, which is an antibody specific for RNA/DNA hybrids, has also shown that oxidative stress induces the formation of R-loops. TC-HR repair factors RAD52 and RAD51 have been shown to co-localize with R-loops at actively transcribed damage sites as compared to I-SceI endonuclease cleavage sites. (Of note, the I-SceI endonuclease recognizes a specific 18bp sequence and leaves a 4bp 5' overhang, but does not induce or require transcriptional activity [199].)

1.6 Therapies and treatments

Current treatments for AD cannot slow or stop the neuronal death or synaptic loss seen in AD pathology, nor have they been able to sufficiently prevent toxic $A\beta_{1-42}$ oligomers from incurring AD associated damage to neurons. Many therapies focus instead on alleviating symptoms through increasing neurotransmitter levels. There are five such treatments currently available, which are rivastigmine, galantamine, donepezil, memantine, and memantine combined with donepezil. Rivastigmine, galantamine, and donepezil are acetylcholinesterase inhibitors. Synthesis of the neurotransmitter acetylcholine (ACh) takes place in the cytoplasm of cholinergic neurons via synthesis from choline and acetyl-coenzyme-A by the enzyme choline acetyltransferase (ChAT) [200]. During neurotransmission, ACh is released from a nerve into the synaptic cleft where it binds to ACh receptors on the post-synaptic membrane and relays a signal from the nerve. Acetylcholinesterase terminates this signal by hydrolyzing ACh [201]. Cholinergic neurons innervate almost all regions of the human brain. They are involved in critical processes such as waking and sleep, memory formation, learning, stress response, and sensory information

[202]. In AD, one notable change in the human brain is a significant reduction in cholinergic neurons. Cholinergic neuronal loss and consequent deficits in cholinergic transmission have been shown to impair cortical and hippocampal information processing, decision-making processes, and changes in hippocampal synaptic transmission which correlate with memory loss [203-208]. The use of acetylcholinesterase inhibitors has been shown to temporarily improve symptoms in AD patients by increasing availability of the neurotransmitter ACh, but the effectiveness of the drugs is patient specific and limited in duration [1].

There are over 112 agents being tested for use as treatment for AD in 2018. These include 26 agents in 35 trials in phase III, 63 agents in 75 trials in phase II, and 23 agents in 25 trials in phase I. 63% of these are disease modifying therapies (DMTs) intended to prevent or delay the onset of AD or slow its progression, 22% are symptomatic cognitive enhancers, 12% are symptomatic agents addressing neuropsychiatric and behavioral changes, and 3% have undisclosed methods of action (MOAs). The majority of individuals involved in these studies include cognitively normal patients with evidence of amyloid pathology (analyzed by cerebrospinal fluid-CSF measures or amyloid positron emission tomography-PET) or individuals with genetic profiles placing them at high risk for developing AD, patients with prodromal AD/mild cognitive impairment (MCI), and patients with mild-moderate AD [209].

There are very few agents currently being tested that target the moderate to advanced stages of AD. The reason for this is the lack of surrogate markers, or measures of disease that can be used for a clinical endpoint. There are also very few biomarkers in AD. The most common ones used in the 2018 clinical trials were CSF amyloid, CSF tau, volumetric magnetic resonance imaging (MRI), and amyloid PET [209]. This dearth of biomarkers has led to a misdiagnosis rate of upwards of 20% in previous AD clinical trials. This can contribute significantly to trial failures [210]. What is important to consider is that these trials are increasingly using preclinical and prodromal populations, reflecting current research findings that indicate AD pathology develops much earlier than when patients manifest the disease symptoms.

1.7 Summary

Although a great amount of research has been conducted on AD, little progress has been made on the actual treatment of the disease. This is mainly due to the elusive nature of the disease's causal factors. Although the amyloid hypothesis can explain the pathology and progression of AD, it does not explain what leads to the initial events that trigger overproduction and accumulation of toxic Aβ, nor how it affects distinct cellular processes.

The data acquired in this thesis implies that although the TC-HR pathway provides the means for post-mitotic cells (and cells in the G_0/G_1 phase of the cell cycle) to maintain genomic stability over the more error-prone NHEJ DSB repair pathway, the process of active transcription and R-loop formation itself can predispose these neuronal cells to detrimental DNA damage when exposed to endogenous cellular products like $A\beta_{1-42}$. This thesis also provides insight into how Aβ contributes to the downregulation of essential repair proteins and their DNA damage response in the TC-HR pathway, pointing to a mechanism of Aβ and the dysregulation of DNA damage repair in the development of AD.

2.0 Materials and Methods

Cell cultures and transfection

U2OS osteocarcinoma cells and U2OS-TRE osteocarcinoma stable cells containing a tandem tetracycline repressive element (TRE) array cassette were cultured in high-glucose Dulbecco's modified Eagle's medium (DMEM) with 10% (vol/vol) fetal bovine serum (FBS) at 37°C, 5% CO_2. U2OS-TRE cell line for the DART system has been described in previous literature [177]. DR-GFP and Ej5-GFP stable cells were cultured in Dulbecco's modified Eagle's medium with 4.5 g/L glucose and L-glutamine without sodium pyruvate with 10% (vol/vol) FBS and 0.1X GlutaMAX (Gibco) at 37°C, 5% CO_2. Primary neuronal cultures were prepared as previously described [211] with minor modifications. Rat cortical tissues were dissected from E17 Sprague Dawley rat brains. For the first 48 hr, brain cultures were maintained in MEM (Life Technologies) containing 2% heat-inactivated fetal bovine serum (Cellgro), 2% heat-inactivated horse serum (Life Technologies), 1 g/L glucose (Sigma), 2 mM Glutamax (Life Technologies), 1 mM sodium pyruvate (Cellgro), 100 μM non-essential amino acids (Cellgro), 50 U/mL penicillin and 50 μg/mL streptomycin (Corning). The culture medium was then changed to 0.5 mL/well of fresh serum-free Neurobasal medium containing 2% B27 supplement (Life Technologies), 2 mM Glutamax I (Life Technologies), 0.5 mg/mL albumax I (Life Technologies) and penicillin-streptomycin (Corning). Primary neurons were plated at 1.0×10^5 on 3.5 cm glass bottom culture PDL (0.1 mg/mL) coated dishes (MatTek) or on 12mm glass coverslips coated with poly-D-lysine (Millipore) in 6-well plates.

Neuronal cells were treated or transfected at DIV12-14. For transfection, Neurobasal media was removed and saved in 37°C, 5% CO_2, and 1 mL pre-warmed transfection media was added (1XMEM w/o bicarb [11430-030, Invitrogen], 2XGlutamax [35050-061, Invitrogen], 0.02 M

Hepes [H30237.01, Thermo Fisher], 1 mM NaPyruvate [11360-070, Invitrogen], and 0.033 M filter sterilized glucose [G5400, Sigma]). Transfected neurons were incubated at 37°C, 0% CO_2 for 1.5 hr, then transfection media was removed and replaced with warmed saved Neurobasal media.

All U2OS cells were transfected using Lipofectamine 2000 (Invitrogen) and Opti-MEM (Gibco). All neurons were transfected using 1 mL transfection media, 500 μL OptiMEM, 5 μL Lipofectamine2000, and 4 μg total DNA per 3.5 cm MatTek glass-bottom dish

Plasmids

pBROAD3/TA-KR, tetR-KR, TA-Cherry, tetR-Cherry, pCMV-NLS-I-SceI, pEGFP-RAD52 [177], pEGFP-Ku70, pEGFP-XRCC1, and pEGFP-BRCA1 [212] are described in previous literature.

Polymerase II inhibitors

RNA polymerase II inhibitors 5,6-Dichlorobenzimidazole 1-β-d-ribofuranoside (DRB; D1916, Sigma) was added with a final concentration of 40 μM for 24 hr, or α-amanitin (A2263, Sigma) at 100 μg/mL for 15 min before laser microirradiation.

The error bars in all figures represent standard error of the mean (SEM) and the P value was calculated by student's unpaired *t* test. *p<0.05, **p<0.01, ***p<<0.01.

RNase H treatment

Previously transfected 80% confluent U2OS cells and neurons in 3.5cm glass bottom dishes (MatTek) were rinsed once with 1XPBS and incubated with 1xRNase H buffer with/without RNase H (EN0201, Thermo Scientific) at room temperature (RT) for 15 min. Cells were treated with 0.1 mM 8-MOP and incubated for 10 min at 37°C followed by confocal microscopy and laser microirradiation.

The error bars in all figures represent standard error of the mean (SEM) and the P value was calculated by student's unpaired *t* test. *p<0.05, **p<0.01, ***p<<0.01.

Immunofluorescent staining (IF)

For staining, 80-100% confluent neurons and U2OS cells in a 3.5 cm dish were washed with 1XPBS three times and fixed with 3.7% paraformaldehyde (Affymetrix, 19943 1 LT) for 15 min at RT. The fixed cells were rinsed three times with 1XPBS, then permeabilized with 0.2% Triton X-100 for 10 min at room temperature, then rinsed three times with 1XPBS. They were optionally blocked by 5% BSA (SIGMA, A-7030) in 0.1% PBS-Tween (PBST) for 1 hr at room temperature. Primary antibodies were diluted in 0.1% PBST and 5% BSA and incubated with cells overnight in 4°C. Cells were then washed three times with 0.05% PBST and incubated with secondary antibody Alexa Fluor 488 goat anti-mouse immunoglobulin G and Alexa Fluor 594 goat anti-rabbit immunoglobulin G conjugate; or Alexa Fluor 488 goat anti-rabbit immunoglobulin G conjugate, Alexa Fluor 594 goat anti-mouse immunoglobulin G conjugate, and Alexa Fluor 405 goat anti-mouse immunoglobulin G conjugate (Invitrogen) for 1 hr at room temperature. Cells were washed three times with 0.05% PBST and once with 1XPBS. For optional DAPI staining of the nuclei, cells were treated with 1:1000 DAPI for 5 min, washed three times in 1XPBS. Cells were then washed once with DI water, dried, then kept in 1XPBS and imaged using an Olympus FV1000 confocal microscopy system (Cat. F10PRDMYR-1, Olympus). Primary antibodies used in this research were anti-γH2AX ser139 (1:2000, JBW301, Millipore), anti-MAP2 (1:1000, MAB378, Millipore), anti-BrdU (IIB5) (I1212, Santa Cruz), anti-phospho-histone H3 (Ser10) (1:100, PA5-17869, Invitrogen),

FV1000 software was used for acquisition of images. For quantification of relative foci intensity at KR sites, the intensity of foci and background was acquired by ImageJ 1.50i software, and the fold increase of foci is calculated as the foci intensity divided by background intensity (n=10). For quantification of the percentage of foci positive cells, 100 cells were counted in every

experiment (n=3), and representative data are shown. For quantification of γ-H2AX foci frequency after IR, the cells with more than 20 γ-H2AX foci were counted and divided by the total cell number.

The error bars in all figures represent standard error of the mean (SEM) and the P value was calculated by student's unpaired *t* test or two-way ANOVA and Tukey's multiple comparisons test. *p<0.05, **p<0.01, ***p<<0.01.

Immunostaining of R-loops (anti-S9.6 antibody)

For S9.6 staining, U2OS-TRE cells were fixed and permeabilized in a 3.5 cm glass-bottom dish using standard protocol with 4% paraformaldahyde, then incubated in TE buffer (10 mM Tris-HCl, 2 mM EDTA, pH=9) and steamed on a 95°C heating block for 20 min to expose the antigen. Then the dish was allowed to cool and washed 3 times with 1XPBS. The cells were then blocked using 5% BSA in 0.1% PBST for 0.5 h at room temperature. The first antibody S9.6 (ENH001, Kerafast) and secondary antibody were diluted in 5% BSA in 0.1% PBST and the standard IF protocol was followed. This protocol was modified from the classical heat-induced antigen retrieval method for paraformaldehyde-fixed tissues using Tris-EDTA buffer [213].

The error bars in all figures represent standard error of the mean (SEM) and the P value was calculated by two-way ANOVA and Tukey's multiple comparisons test. *p<0.05, **p<0.01, ***p<<0.01.

Microscopy and laser light irradiation

Prior to laser irradiation, except for GFP-XRCC1 transfected cells, live cells were treated with 0.1 mM 8-MOP in Opti-MEM medium (Gibco) in glass bottom dishes and incubated for 10 min at 37°C.

Fluorescent images were obtained and processed with an FV-500 confocal scanning laser microscopy system (Olympus). U2OS and neuronal cells were placed on a temperature-controlled

(37°C) plate. A 405-nm scan laser system (Olympus) for irradiation of cells in the epifluorescence path of the microscope system was used. One scan of the laser light at full power delivers approximately 1,600 nW. We scanned cells 100-500 times with the 405-nm laser at full power focused through a 40x objective lens, which has been shown to induce SSBs and DSBs. The fluorescence intensity at an irradiated site was initially measured with a laser power/energy monitor (Orion; Ophir Optronics, Israel). The fold increase in fluorescence intensity of each site was quantified by measuring fluorescent intensity after damage induction/background nuclear intensity using ImageJ software (**Fig 2-1)** [212, 214, 215].

The error bars in all figures represent standard error of the mean (SEM) and the P value was calculated by student's unpaired *t* test. *p<0.05, **p<0.01, ***p<<0.01.

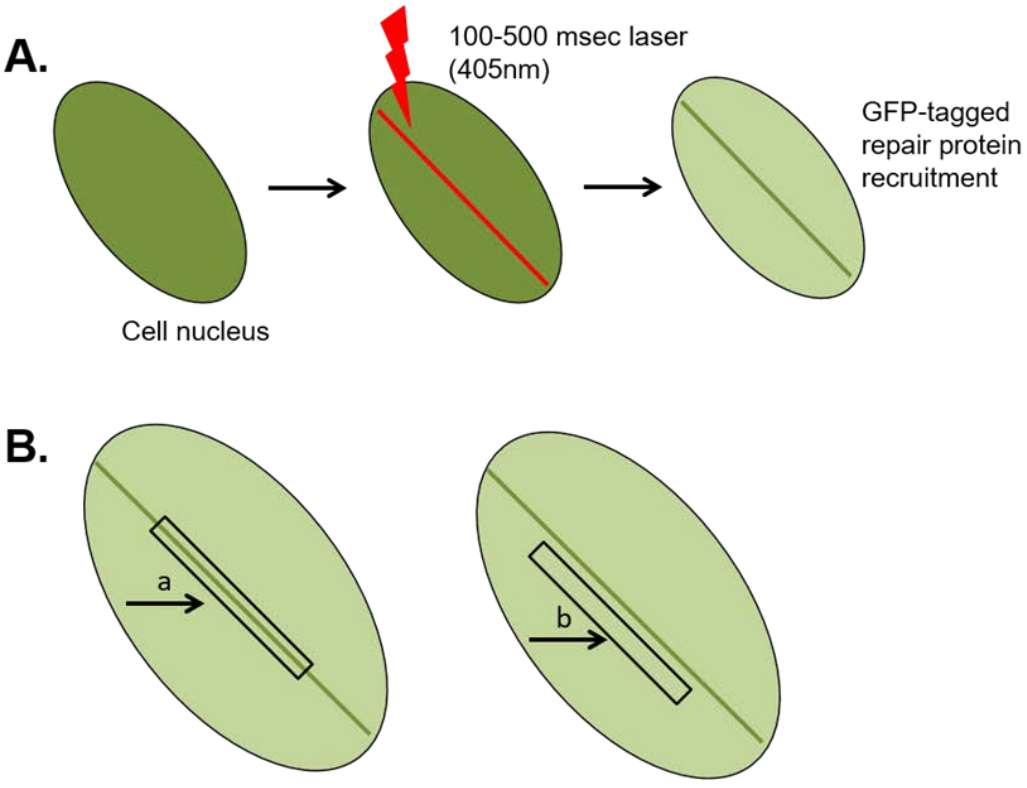

Figure 2-1 Model of laser microirradiation.

A. 405nm laser induces DNA DSB breaks in single cell nuclei allowing for real time visualization of GFP-tagged repair protein recruitment to DNA damage sites. **B.** For quantification, fluorescence intensity of (a) GFP-tagged repair protein after DNA damage induction is compared to the (b) background intensity.

Protein expression and purification

6xHis-tagged human RAD52 was expressed in *E. coli* Rosetta cells and purified as previously described [216].

Electrophoretic mobility shift assay

RAD52 protein was serial diluted to indicated concentration and mixed with 10 nM ^{32}P labeled ssDNA, ssRNA, dsDNA, dsRNA, RNA:DNA, or R-loop substrate in EMSA buffer (15 mM HEPES PH7.5, 1 mM $MgCl_2$, 2% glycerol, 0.2 ug/ul BSA, 100 mM KCl, RNaseOut 0.16 U/**μ**l). The reaction mixtures were incubated at 37°C for 10min. After addition of gel loading buffer (50% glycerol, 20 mM Tris-HCl, pH 7.4, 0.5 mM EDTA, 0.05% orange G), the reaction mixtures were resolved by 5% native polyacrylamide gel electrophoresis in 1 × TBE buffer (90 mM Tris-borate, pH 8.0, 2 mM EDTA) at 4°C. The gels were dried, and the products were visualized by Phosphorimager.

BrdU incorporation

U2OS or neurons previously transfected with GFP-XRCC1 were treated with and without 40 μM DRB and incubated at 37°C for 24 hr. Cells were then treated with laser microirradiation in sterile manner (lid not removed), then 0.01 mM BrdU was added and cells incubated at 37°C for 24 hr. Cells were rinsed with 1XPBS, fixed with 3.7% paraformaldehyde for 15 min at room temperature, rinsed three times with 1XPBS, then treated with 2.5N HCl for 30 min at 37°C. Cells were rinsed three times with PBS, permeabilized with 0.2% Triton for 5 min at room temperature, then rinsed three times with PBS. Immunofluorescent staining proceeded as above.

The error bars in all figures represent standard error of the mean (SEM) and the P value was calculated by student's unpaired *t* test. *p<0.05, **p<0.01, ***p<<0.01.

Lysates and western blot

Neurons seeded on a 24 well plate (3 wells per treatment) or 6 well plate (1 well per treatment), and U2OS cells seeded on 6 cm dishes were treated as indicated per each experiment. Cell lysates were prepared with 25-150 μL of lysis buffer per well (62.5 mM Tris pH 6.8, 5% glycerol, 2% SDS, 0.1% Nonidet P-40, 1 mM phenylmethylsulfonyl fluoride). Cells were scraped and pipetted into 1.5mL tubes, then allowed to sit on ice for 10 min. Samples were heated at 95°C and spun in a microcentrifuge at 10,000 rpm for 10 min, then the supernatant transferred to a new tube and the pellet discarded. Samples were run on 8%-12% SDS-polyacrylamide gels or 4-20% gradient gel (Mini-Protean TGX, 4561096), transferred to either PVDF or nitrocellulose membrane. For some transfers, the BioRad Trans-Blot Turbo system was used. The membranes were blocked in 5% non-fat milk with TBST for 1 hr before being incubated with primary antibody in 0.1% TBST and 5% non-fat milk overnight at 4°C. Primary antibodies used were anti-RAD52 antibody (K1512, Santa Cruz), anti-BRCA1 (D-9, sc-6954, Santa Cruz Biotechnology), and anti-γ-H2AX (ab12267, Abcam). (Samples for probing with anti- γ-H2AX were not pre-treated with benzonase nuclease.)

After primary antibody, membranes were washed with 0.1% TBST three times and incubated with secondary antibody in 0.1% TBST and 5% non-fat milk for 1 hr at room temperature. The membranes were washes three times with TBST and once with TBS before exposure using chemiluminescent HRP substrate (Millipore Catalog#: WBKLS0500). Secondary antibodies used were anti-β-Actin (A5441, Sigma Aldrich), anti-tubulin (ab6046, Abcam), and anti-GAPDH (G9545, Sigma Adrich).

Images were acquired in a BIO-RAD Universal Hood II machine or ChemiDoc Touch Imaging System (software version 2.3.0.07) and quantified with ImageLab software. All protein concentrations were normalized to loading controls before comparison to experimental controls.

The error bars in all figures represent standard error of the mean (SEM) and the P value was calculated by student's unpaired *t* test or two-way ANOVA and Tukey's multiple comparisons test. *p<0.05, **p<0.01, ***p<<0.01.

$A\beta_{1-42}$ oligomer preparation

Recombinant $A\beta_{1-42}$ oligomers were prepared from lyophilized monomers treated with HFIP (A-1163-2, rPeptide) as described [13, 217]. 0.5mg of peptide was dissolved in 22uL fresh DMSO, then further diluted in 978uL ice cold Neurobasal media or 1XPBS to make 0.5mg/mL (100uM) solution. Solution was spun at 5000rpm 5 min 4°C and supernatant removed and kept. Peptide solution was incubated at 4°C overnight to oligomerize the amyloid beta. Then the solution was spun 5000rpm 5 min 4°C and supernatant removed. Aliquots were flash frozen in dry ice and kept at -80°C. Once thawed they were not re-frozen. Control samples were made using 22uL DMSO in 978uL Neurobasal media or 1XPBS.

Protein concentration was measured using reverse phase HPLC and Pierce BCA Protein Assay Kit (Thermo Scientific). The ratio of monomers vs oligomers was determined using size exclusion chromatography on a 24 hr incubated sample. We also investigated the pelleted and supernatant fraction and observed the supernatant fraction was the toxic fraction, and DMSO did not induce the resultant effects. Additionally, we investigated $A\beta_{1-42}$ oligomers via western blot by running diluted fractions with monomeric controls on 4-20% gradient gel (Mini-Protean TGX, 4561096) (**Fig. 5-3**). After transferring the protein to nitrocellulose membrane, the membrane was boiled in a microwave for 5 min in 1XPBS, blocked with 5% non-fat milk for 1 hr, and probed with anti-6E10 antibody (BioLegend, 803004) according to western blot protocol described previously.

Transmission Electron Microscopy (TEM)

Transmission electronic microscopy was used to detect the presence of $A\beta_{1-42}$ oligomers (**Fig. 5-2B**). $A\beta_{1-42}$ sample (5 µL) was placed on a formvar grid and allowed to partly dry at room

temperature (RT). It was washed by touching it 3X to the surface of a drop of distilled water, and excess water removed by touching the grid to filter paper. Then, a small drop of 1-3% uranyl acetate in distilled deionized water was added to the grid. After 10 sec excess stain was removed by touching the edge to filter paper. The grid allowed to air dry at RT before examination using a transmission electron microscope (Jeol JEM 1400, Tokyo, Japan) imaged at 80 kV with the MegaView III Soft Imaging System (SIS).

HR and NHEJ assays

DR-GFP and Ej5-GFP stable cells were passaged onto 6-well plates and incubated in DMEM with 10% FBS until 60% confluent. Cells were transfected with pCMV-I-SceI plasmid using Lipofectamine 2000 (Life Technologies) for 48 hr and kept in the dark. 1 μM $A\beta_{1-42}$ or Aβ control media was added for 5 hr. Then cells were spun at 600 rpm and washed with 1xPBS three times. Cells were analyzed by fluorescence activated cell sorting (FACS) for HR or NHEJ repair efficiency using the Beckton Dickinson (Accuri) C6 flow cytometer and BD Accuri software.

Results were normalized to controls with untreated samples with I-SceI plasmid representing 100% repair (**Fig 5-1C**). The error bars in all figures represent standard error of the mean (SEM) and the P value was calculated by student's unpaired *t* test. *p<0.05, **p<0.01, ***p<<0.01.

Cell survival

To determine the effect of 1 μM $A\beta_{1-42}$ upon U2OS cell survival, 70% confluent U2OS cells were treated with/without 1 μM $A\beta_{1-42}$ or Aβ control media for 24 hrs. The cells were suspended and counted using the AOPI cellometer counting software (Nexcelom). 300 cells were then seeded into a 6 cm dishes in 3mL culture media and incubated at 37°C for 10 days. Colonies were fixed and stained with 0.3% crystal violet, and survival (number of colonies) was expressed

as a percentage of non-treated colonies. To determine the effect of 1 μM $A\beta_{1-42}$ upon U2OS IR sensitivity, U2OS cells were treated with/without 40 μM 5,6-Dichlorobenzimidazole 1-β-D-ribofuranoside (DRB; D1916; Sigma) for 24 hrs and/or 1 μM $A\beta_{1-42}$ or Aβ control media for 5 hrs, then seeded onto 6 cm dishes in fresh 3mL culture media. After seeding, cells were exposed to irradiation as indicated and incubated for 10 days at 37°C. Colonies were fixed and stained with 0.3% crystal violet in methanol, and then survival (number of colonies) was expressed as a percentage of non-irradiated colonies.

The error bars in all figures represent standard error of the mean (SEM) and the P value was calculated by student's unpaired *t* test. *p<0.05, **p<0.01, ***p<<0.01.

KillerRed induction

U2OS-TRE cells were cultured in 35 mm glass-bottom dishes (MatTek, P35GC-1.5-14-C) at ~60% confluence 24 h before transfection. For ROS-induced damage, cells were transfected with plasmids containing KillerRed (TA-KR/tetR-KR) or cherry controls (TA-cherry/tetR-cherry). Light-induced KillerRed activation was done by exposing cells to a 15 W Sylvania cool white fluorescent bulb for 15-20 min in a stage UVP (Uvland, CA). A transparent flask filled with cool water was placed between the light source and the dishes to avoid temperature fluctuation in the exposed dish. Dishes were then covered with foil, and cells were allowed to recover at 37°C for indicated times. For γ-H2AX staining, cells recovered for 24 h before fixation. For GFP-BRCA1 recruitment, cells recovered for 0.5-1 h before fixation.

The error bars in all figures represent standard error of the mean (SEM) and the P value was calculated by student's unpaired *t* test or two-way ANOVA and Tukey's multiple comparisons test. *p<0.05, **p<0.01, ***p<<0.01.

CRISPR-Cas9 knockout

The sgRNAs targeting RAD52 in the human genome were designed on the website http://crispr.mit.edu/ and cloned into PX330 vectors (**Table 2-1**). The sgRNAs were delivered to cells by standard transfection. After 24 hours, single cells were spread in 96-well plates or 10 cm dishes and grown for 10 days to obtain single colonies. The colonies were transferred to 24 well plates and grown for about one week before genome extraction and genotyping and western blot verification. The PCR check primers are also listed (**Table 2-1**).

Table 2-1 Sequences of sgRNA oligonucleotides

Oligo Name	Sequence
RAD52 sgRNA L1 up F	CACCGCTAGGCTGGAGTCCGACCAG
RAD52 sgRNA L1 up R	AAACCTGGTCGGACTCCAGCCTAGC
RAD52 sgRNA R1 down F	CACCGACCCACAGCAGACTTTCAGC
RAD52 sgRNA R1 down R	AAACGCTGAAAGTCTGCTGTGGGTC
RAD52 check primer F	AATTCATGTGCCTGGAAAGC
RAD52 check primer R	CCCACGTAGAACTTGCCATT

3.0 RAD52 is required for RNA-templated recombination repair in post-mitotic neurons

This chapter is modified from the following collaborative published work:

Welty, S., Teng, Y., Zhuobin, L., Weixing, Z., Sanders, L., Greenamyre, T., Rubio, M.E., Thathiah, A., Kodali, R., Wetzel, R., Levine, A., Lan, L.(2017) RAD52 is required for RNA-templated recombination repair in post-mitotic neurons. *J Biol Chem.* 293(4):1353-1362.

3.1 Introduction

The most deleterious form of DNA damage, double strand breaks (DSBs), can arise from endogenous metabolic processes or exogenous environmental factors such as radiation or chemicals [218]. Oxidative damage caused by reactive oxygen species (ROS) and consequent DSBs has been implicated in neurodegenerative disorders such as Alzheimer's disease (AD). ROS are generated endogenously by cellular metabolism and a variety of exogenous agents such as IR. In studies conducted on replicating cells, it has been found that metabolically-generated ROS can cause around 10,000 oxidative lesions per day [87].

ROS-induced damage predominantly leads to base or deoxyribose modifications that lead to single strand breaks (SSBs). DSBs can arise due to replication past ROS-induced lesions, or when SSBs occur in close proximity [125]. These lesions are repaired either via non-homologous end joining (NHEJ) or homologous recombination (HR). In NHEJ, the broken DNA ends are processed/digested and then directly ligated, potentially leading to nucleotide deletions and consequent frameshift mutations. Thus, NHEJ is considered to be error-prone [123]. HR utilizes undamaged DNA templates in order to direct error-free repair of the damaged strands. It has long

been assumed that HR can only take place during the late S/G_2 phases of the cell cycle where sister chromatids are present as templates [174]. However, recent studies in terminally differentiated cells have revealed an RNA-templated HR repair mechanism of DSBs at active transcription sites during the G_0/G_1 phase (transcription coupled homologous recombination-TC-HR). For this mechanism to occur, Cockayne syndrome B (CSB) protein is recruited to an actively transcribed damage site, followed by recruitment of RPA, RAD51, RAD51C, and RAD52; then, repair occurs utilizing the nascent RNA template produced by active transcription [177]. An RNA-templated, RAD52 directed mechanism of HR has also been reported in yeast [191]. However, it is not known if the transcription dependent HR pathway exists in neurons. Except in the hippocampus and striatum, most neurons in the adult human brain are terminally differentiated and non-dividing, and therefore are assumed to be incapable of utilizing HR for DSB repair [175, 176].

In this study, utilizing our site-specific damage induction systems, we measured the recruitment of TC-HR-associated repair protein RAD52 to sites of DNA damage with and without transcription inhibition. We found that post-mitotic neurons employ this RNA-based recombinatorial mechanism for the DNA damage response. We also discovered preferential binding of RAD52 protein to R-loops, DNA:RNA hybrid structures present during active transcription [195], as further evidence of RAD52's role in TC-HR. Given our finding of the novel TC-HR DNA repair mechanism in post-mitotic cells, we wondered if this mechanism might be affected in neurodegenerative disorders such as AD. We utilized $A\beta_{1-42}$, neurotoxic oligomers 42 amino acids in length that are heavily implicated in AD pathology as they are prone to aggregation [219]. We found that $A\beta_{1-42}$ oligomers downregulate the expression and damage response of the essential TC-HR repair protein RAD52. How this dysregulation of DNA repair may significantly contribute to the development of neurodegenerative diseases such as AD is discussed below.

3.2 Results

3.2.1 DNA repair factors are recruited to laser-induced damage in neurons

To understand how non-dividing neurons repair oxidative DNA damage, we first verified that the primary rat cortical neurons utilized for experimentation were post-mitotic. Some findings have shown a link between cell cycle activation in post-mitotic neurons and a DNA damage response leading to apoptosis [132]. Therefore, we probed DIV12 neuronal cell cultures with anti-phosphorylated histone H3 (Ser10) before and after DSB inducing gamma irradiation (**Fig. 3-1A**) [220]. Studies have shown a correlation between this phosphorylated histone H3 (Ser10) and mitotic chromosome condensation during early prophase, suggesting anti-phosphohistone H3 can be used as a mitosis-specific marker [221]. Here we observed no evidence of mitosis in the primary cortical neurons as compared to replicating U2OS cells before or 24 hr after 5Gy gamma irradiation. We utilized U2OS human osteocarcinoma cells to represent mitotic cells due to their robustness in cell culture, fast growth, and high transfection rate. This cell line has also been established in a stable cell line for use with KillerRed fusion proteins as discussed in Chapter 1.5.4.

Prior studies in our lab have shown that terminally differentiated cells utilize an RNA-templated homologous recombination mechanism for repair of DSBs in the G_0/G_1 phase of the cell cycle. This mechanism of repair can only occur with active transcription [177]. Members of our lab have also previously demonstrated by terminal deoxynucleotidyltransferase-mediated dUTP-biotin nick end labeling assay that our laser light microirradiation system induces DNA strand breaks in cells [222]. Therefore, we utilized 405 nm laser microirradiation to induce DSBs at localized sites in single cells which makes it possible to observe repair protein recruitment in non-dividing cells [214] (**Fig 3-1B)** [220]. We then investigated recruitment of GFP-tagged repair proteins specific to particular repair pathways including XRCC1 (DNA single strand break repair

[SSBR]), KU70 (NHEJ), and RAD52 (HR) (**Fig. 3-1C**) [220]. In this experiment, we were surprised to find the recruitment of TC-HR repair protein RAD52 to sites of damage in post-mitotic neurons despite the neurons' lack of a sister chromatid to utilize as a template for homologous repair.

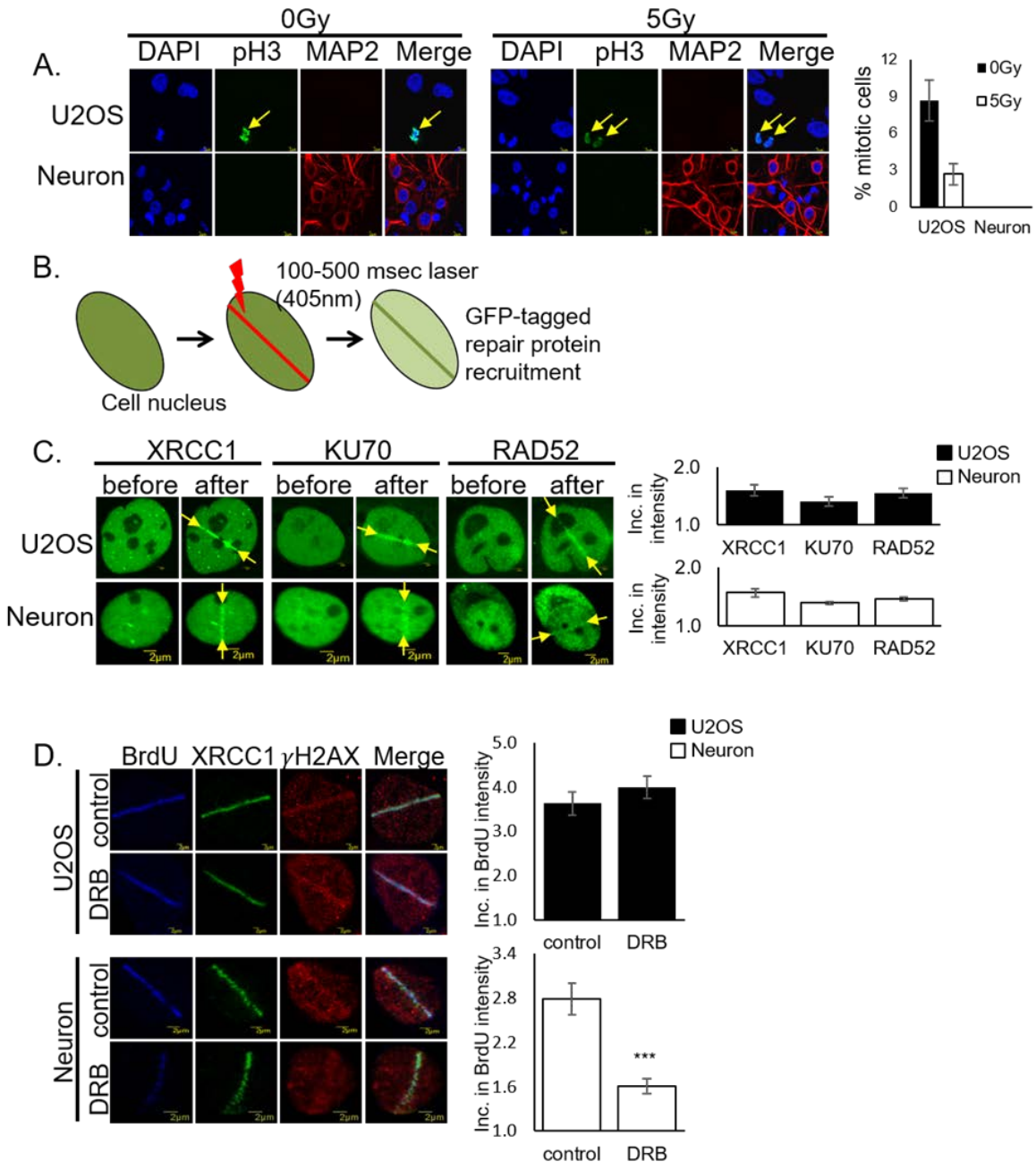

Figure 3-1 Post-mitotic neurons recruit TC-HR associated protein RAD52.

A. Rat DIV12 cortical neurons and U2OS cells were treated with and without 5Gy irradiation and probed with anti-phospho-Histone H3 (Ser10) antibody. Error bars indicate the SEM of three separate experiments (n=100), and the p values were determined by using Student's unpaired two-tailed *t* test. Cortical neurons do not show expression of phosphorylated H3 (Ser10). **B.** Schematic of 405 nm scan laser system for induction of DSBs in single cells where single cell nuclei are targeted with 100-500 msec of laser

microirradiation to visualize and quantify GFP-tagged repair protein recruitment at damage sites. **C.** Recruitment of GFP-tagged DNA repair proteins XRCC1 (SSBR), KU70 (NHEJ), and RAD52 (HR) at sites of DNA damage in U2OS and DIV12 cortical neurons before and 1 min after 100 msec-500 msec laser microirradiation. Error bars indicate the SEM of two separate experiments, and the p values were determined by using Student's unpaired two-tailed *t* test (***p<<0.01). **D.** BrdU incorporation after 100 msec laser microirradiation with and without pre-treatment with DRB (40 μM) for 24 hr in U2OS and DIV12 cortical neurons. Error bars indicate the SEM of three separate experiments, n=10, and the p values were determined by using Student's unpaired two-tailed *t* test (***p<<0.01).

3.2.2 DNA incorporation at sites of damage is affected by transcription inhibition

We next investigated whether transcription inhibition would affect the repair synthesis process of HR in post-mitotic neurons. We pre-treated the cells with the RNA polymerase II inhibitor DRB, (5,6-Dichloro-1-β-D-ribofuranosylbenzimidazole), which inhibits transcription elongation, and analyzed the incorporation of bromodeoxyuridine (BrdU), a synthetic analog of thymidine, into newly repaired DNA after laser damage. Importantly, the replication-mediated incorporation of BrdU into genomic DNA of post-mitotic neurons does not occur. Therefore, BrdU staining in neurons should indicate repair-triggered BrdU incorporation. This incorporation was significantly decreased after DRB treatment (**Fig. 3-1D**) [220], indicating that active transcription and a nascent RNA template are necessary for HR repair in post-mitotic neurons.

3.2.3 Transcription inhibition or RNase H treatment reduces the recruitment of RAD52 in neurons

RAD52 can be utilized in HR or a mutagenic repair process known as single strand annealing (SSA). SSA, which results in a deletion rearrangement between homologous repeating

sequences, is independent of active transcription [120]. Since our prior study indicated that the RAD52 dependent, RNA-templated recombination only occurs at sites of active transcription [177], we then tried to determine whether post-mitotic neurons utilize this particular recombinational mechanism for error-free repair of DSBs. To determine if active transcription is necessary for the damage response of RAD52 in post-mitotic neurons, we pretreated cells with RNA polymerase II inhibitors DRB, which inhibits transcription elongation, or α-amanitin, which inhibits transcription initiation and elongation (**Fig. 3-2A&B**) [220]. Both inhibitors block transcription, thereby preventing the production of an mRNA template for use in RNA-templated HR. We found that after inhibiting RNA polymerase II with both inhibitors, recruitment of RAD52, an essential factor for RNA-templated recombinational repair, was significantly reduced at sites of laser damage in post-mitotic neurons. This supports our findings that RNA-templated HR in post-mitotic neurons requires active transcription to take place.

To further establish that the recombination in post-mitotic neurons is associated with RNA-templated repair, we examined the effect of RNase H, an endo-ribonuclease that specifically degrades the RNA strand in an RNA-DNA hybrid structure, on the recruitment of RAD52 (**Fig. 3-2C**) [220]. After treatment with RNase H, RAD52 recruitment was significantly reduced at sites of laser damage in post-mitotic neurons. To test whether the effects of the RNase H assay were actually due to the enzyme activity or if the results were due to the conditions of the experiment, we measured recruitment of SSBR protein XRCC1 after RNase H treatment. Since XRCC1 does not rely on an RNA strand, recruitment of XRCC1 should not be affected by RNase H activity. As evidenced in **Fig. 3-2D** [220], we did not see significant reduction in XRCC1 activity after RNase H treatment. Combined, these results confirm that a nascent RNA template is necessary for HR repair to occur in post-mitotic neurons.

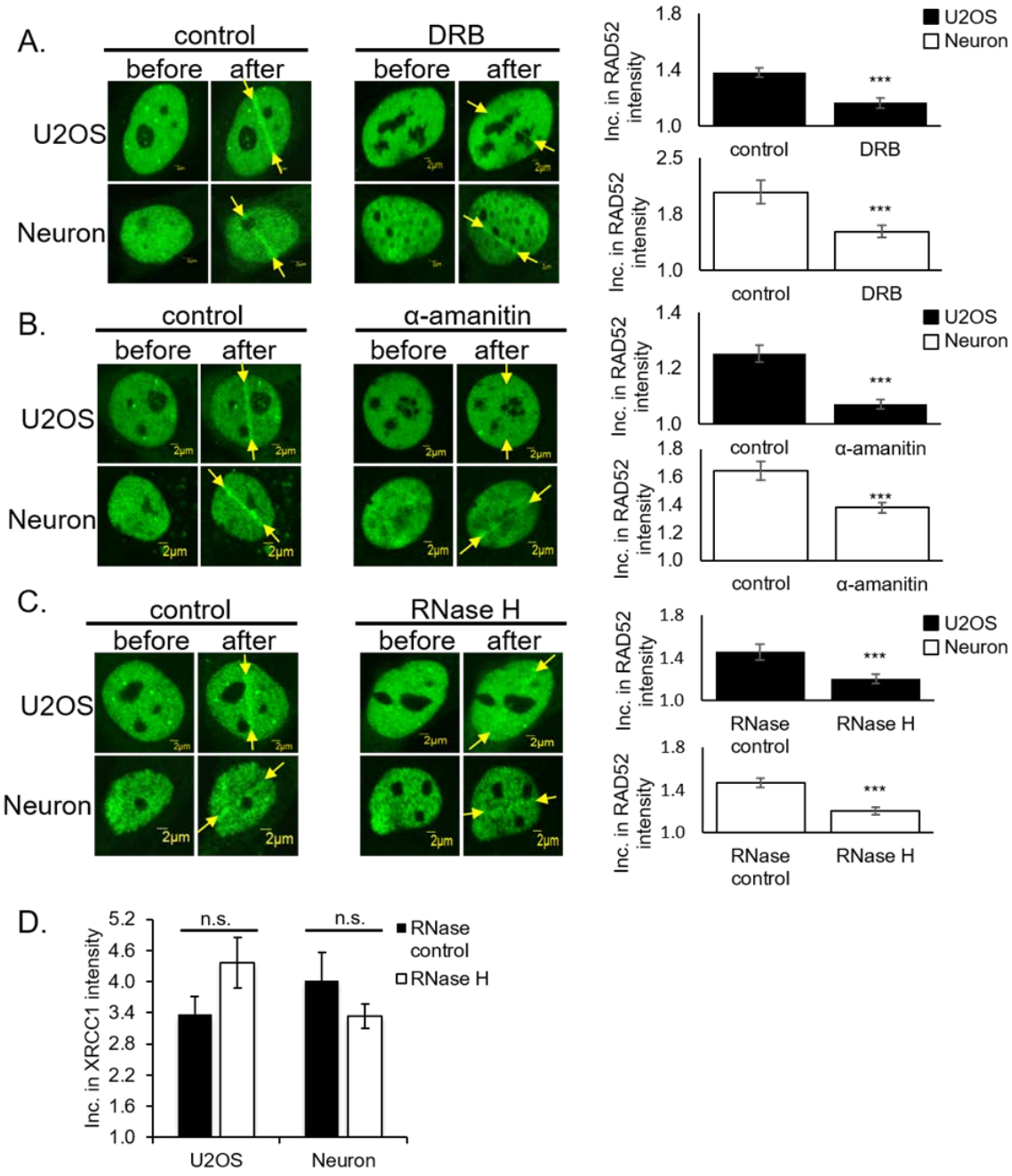

Figure 3-2 Transcription inhibition reduces template-driven repair in post-mitotic neurons.

A. Recruitment of RAD52 before and 1 min after 200-500 msec laser microirradiation treatment with and without pre-treatment with RNA polymerase II inhibitor (40 μM) DRB for 24 hr in U2OS cells and DIV12 ventral neurons. **B.** Recruitment of RAD52 before and 1 min after 200-500 msec laser microirradiation treatment with and without pre-treatment with RNA polymerase II inhibitor (100 μg/mL) α-amanitin for 0.5 hr in U2OS cells and DIV12 ventral neurons. Error bars indicate the SEM of two separate experiments,

n=10, and the p values were determined by using Student's unpaired two-tailed *t* test (***p<<0.01).**C.** Recruitment of RAD52 before and 1 min after 500 msec laser microirradiation treatment with and without pre-treatment with 15 U. RNase H for 15 min in U2OS cells and DIV12 ventral neurons. Error bars indicate the SEM of two different experiments, n=10, and the p values were determined by using Student's unpaired two-tailed *t* test (**p<0.01; ***p<<0.01). **D**. Recruitment of XRCC1 before and 1 min after 500 msec laser microirradiation treatment with and without pre-treatment with 15 U. RNase H for 15 min in U2OS cells and DIV12 cortical neurons. Error bars indicate the SEM of two different experiments, n=10, and the p values were determined by using Student's unpaired two-tailed *t* test.

3.2.4 RAD52 binds to an R-loop substrate and preferentially binds to ssRNA

RAD52 protein has been demonstrated to bind DNA structures with DSBs [223, 224]. Since previous studies from others and our study both indicate that RAD52 is involved in RNA-templated recombination repair, we tested the affinity of RAD52 for RNA related substrates by electrophoretic mobility shift assay (EMSA). Results show that purified human RAD52 protein efficiently binds both single-stranded (ss) DNA and RNA (**Fig. 3-3A&3-3B**) [220], though its binding affinity to ssRNA is higher than that of ssDNA. Binding affinities of RAD52 to double-stranded (ds) DNA and RNA (**Fig. 3-3C&3-3D**) [220] are significantly reduced compared to ss substrates (**Fig. 3-3G**) [220]. Interestingly, RAD52 has slightly higher affinity to RNA:DNA hybrid duplex than dsDNA and dsRNA (**Fig. 3-3E**) [220]. Furthermore, RAD52 has a higher binding affinity to R-loop substrates (**Fig. 3-3F**) [220], the damage-prone structures at transcriptionally active sites in the genome [195], than hybrid structures. These *in vitro* results are consistent with the possibility that RAD52 may bind ssRNA and the co-transcriptional R-loop upon transcriptional stress in post-mitotic neurons.

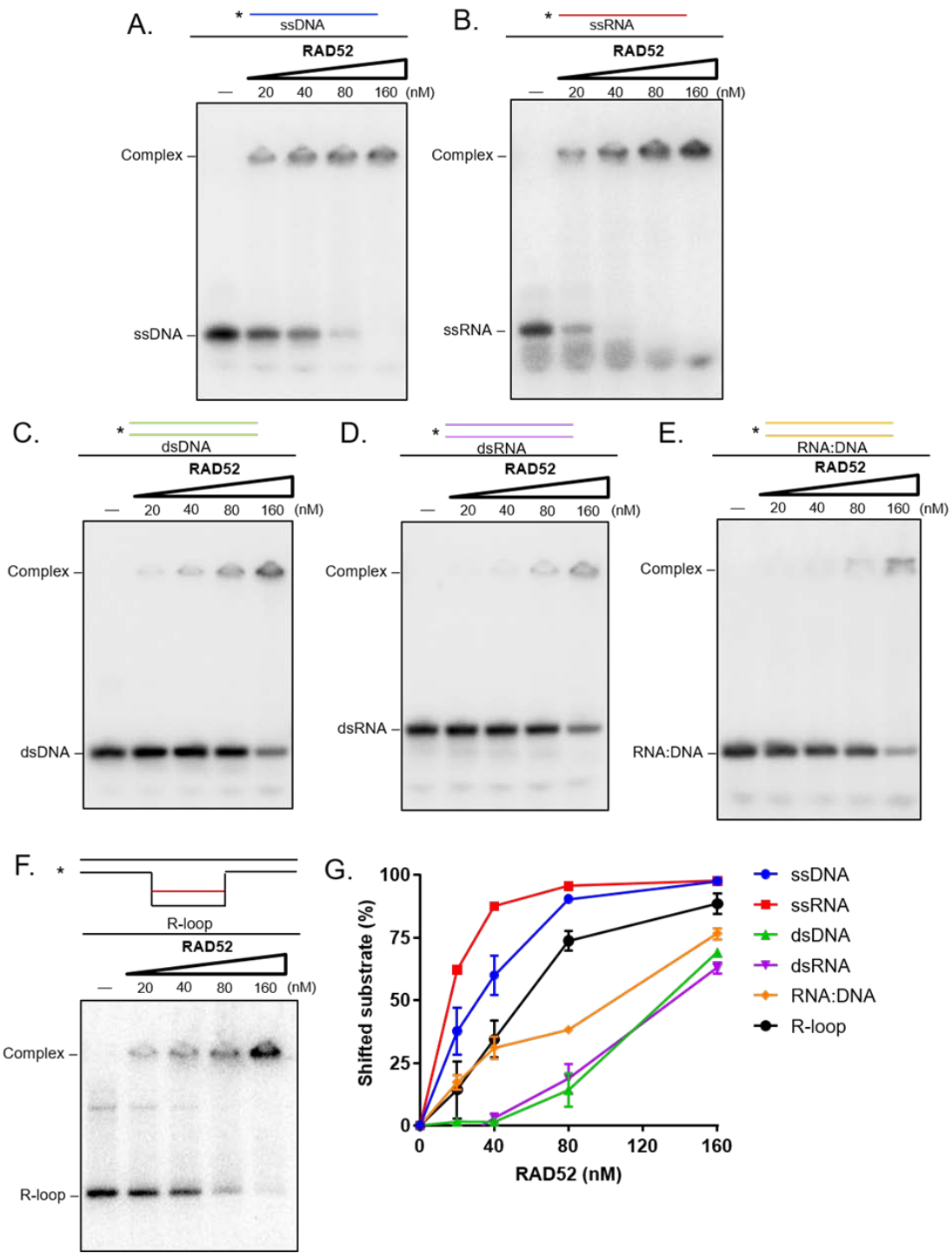

Figure 3-3 RAD52 preferentially binds ssRNA and R-loop substrate.

Electrophoretic mobility shift assay (EMSA) to test binding of RAD52 protein to: A. ssDNA, B. ssRNA, C. dsDNA, D. dsRNA, E. RNA:DNA hybrid, and F. R-loop substrate (10 nM). G. Representative graph of A-F. RAD52 preferentially binds ssRNA and R-loop.

3.2.5 Discussion

In this study, we first discovered that recruitment of HR factor RAD52 to sites of DNA damage is dependent upon the presence of a nascent mRNA template for HR, indicating the existence of a novel RNA-templated recombinational repair pathway in post-mitotic neurons. We also discovered that RAD52 preferentially binds ssRNA and has direct affinity for R-loops, reinforcing the involvement of RAD52 in TC-HR repair of double strand breaks. Utilization of this less error-prone pathway is essential for non-dividing neurons to maintain their genomic integrity when faced with environmental pressures such as metabolically-induced oxidative damage and other endogenous and exogenous stressors.

Considering the fact that terminally differentiated, post-mitotic neurons must survive a human lifetime, utilizing an error-prone pathway such as NHEJ would subject the cells to potentially lethal genomic errors. In a study on cell-cycle arrested cells, it was found that NHEJ activity was responsible for approximately half of all replication-independent frameshift mutations, primarily due to deletions. Mutant yeast cells deficient for HR (RAD54-deletion) did not exhibit an increase in the number of of replication-independent mutations in the cell-cycle arrested cells, but RAD52-deletion mutants did [225]. This study confirms both the mutagenic nature of NHEJ, and the possibility of a RAD-52 dependent pathway such as TC-HR that counteracts the frameshift-producing NHEJ pathway.

Although post-mitotic neurons do not face the acquisition of mutations after replicating DNA past DNA lesions as commonly occurs in mitotic cells, DNA DSBs still pose massive risks to essential genes when not repaired. Failure to completely repair DNA may result in cellular senescence or apoptosis as a means for the cell to cope with an excess of damage and avoid malignant transformation [226, 227]. However, unrepaired cells may also accumulate mutations that affect genes involved in regulating apoptosis, cell division, and DNA repair. If proliferating stem and neural progenitor cells incur mutations due to unrepaired DNA during development,

disease may later develop as a result of disrupted essential genes passed down through cell division or if tumor suppressing or oncogenes are no longer properly regulated [228]. In post-mitotic neurons, mutations may contribute to neuronal dysfunction and apoptosis, as seen in the pathology of AD where the cerebral cortex and hippocampus suffer extensive neuronal loss [229]. Many neurodegenerative pathologies have also been linked to genetic deficiencies in DNA repair genes. For example, in ataxia-telangiectasia (A-T), a mutation in the P 13 kinase A-T mutated (ATM) protein, which is activated by DNA DSBs and is responsible for phosphorylating numerous downstream targets involved in DNA repair, cell cycle arrest, and apoptosis, causes individuals to experience higher rates of cancer and undergo neurodegeneration before the age of five [230-232]. New research has suggested that the neuronal loss observed in AD may also result from partial loss of ATM function as AD pathology progresses [233].

Study of repair mechanisms in post-mitotic neurons is essential if we are to understand the complex nature of neurodegenerative diseases. While certain genetic aberrations may constitute a significant role in contributing to physiological aspects of AD such as the APOEε4 allele and its association with increased AD risk, other contributing factors remain unknown [234]. These factors may include deficiencies in DNA repair directly related to environmental exposures or internal processes such as the production of ROS during cellular metabolism or neuronal activity.

4.0 BRCA1 plays an important role in TC-HR

4.1 Introduction

BRCA1 is known to participate in numerous cellular processes including canonical HR. It has been shown to coexist with RAD51 and BARD1 in a complex named the BRCA1-BRCA2 Containing Complex (BRCC) which has E3 ubiquitin ligase activities responsible for regulating DNA damage response factors [235]. Although its precise mechanism in canonical HR is still debated, cells deficient in BRCA1 are more sensitive to IR and contain numerous chromosomal aberrations, possibly due to unrepaired DNA damage [236, 237]. BRCA1 also has been found to play a role in transcription coupled repair (TCR). Here, BRCA1 accumulates at actively transcribed UV damage sites dependent upon Cockayne syndrome B protein (CSB). It polyubiquitinates CSB for degradation [238, 239]. The main types of DNA damage induced by UV irradiation are the formation of cyclobutane pyrimidine dimers (CPD) and (6-4) photoproduct adducts which can be repaired via nucleotide excision repair (NER) through either TCR or global genome repair (GGR). BRCA1 is primarily found in the cytoplasm during the majority of the cell cycle, but can localize to the nucleus following DNA damage during S phase [240]. How this affects post-mitotic neurons and BRCA1's damage response has not been previously investigated. Importantly, however, the TC-HR pathway for DSB repair is dependent upon the recruitment of CSB and RAD52. Because the role of BRCA1 in TC-HR is entirely unknown, we sought to elucidate the role of BRCA1 in TC-HR.

4.2 Results

4.2.1 Recuitment of BRCA1 to transcriptionally active sites of DNA damage dependent on active transcription

We utilized the DNA damage at active transcription sites (DART) system, illustrated in **Fig. 1-5**, to study molecular responses to light-induced DNA damage at single genomic loci with controllable transcription [184, 185]. In this system, U2OS TRE cells are exposed to white light for 15 min, and the transiently transfected tet-repressor (tetR)- or tet-transcription activator (TA)-tagged KR proteins (tetR-KR or TA-KR) induce similar amounts of ROS-induced DSBs at transcriptionally inactive or active sites, respectively in real time. Recruitment of repair proteins to these sites of damage can then be measured by examining relative fluorescence intensity using fluorescent tagged proteins or immunofluorescent staining techniques. We first examined the recruitment of BRCA1 protein to both TA-KR and tetR-KR sites and control TA-cherry and tetR-cherry sites after light activation (**Fig. 4-1A**). BRCA1 was recruited to sites of both active transcription and inactive transcription after damage induction, and was not recruited to control TA-cherry or tetR-cherry sites. To determine that BRCA1 recruitment to TA-KR damage sites is dependent upon active transcription and not DNA damage alone, we utilized the RNA polymerase II inhibitors DRB (5,6-Dichloro-1-β-D-ribofuranosylbenzimidazole) and α-amanitin to examine BRCA1 recruitment to sites of active and inactive transcription after transcription inhibition (**Fig. 4-1C**). We found a significant reduction in BRCA1 recruitment at TA-KR sites after both treatments, but only saw a reduction in BRCA1 recruitment at tetR-KR sites after DRB treatment. These results with α-amanitin treatment indicate that BRCA1 is preferentially recruited to DNA damage sites where active transcription is taking place. Experimentally, DRB treatment is 24 hrs and α-amanitin is 0.5 hrs. Hypothetically the longer DRB treatment could inhibit production of

BRCA1 protein, thus affecting its recruitment regardless of transcription activity at the damage site. In order to determine if the reduction in BRCA1 recruitment to tetR-KR sites was due to overall BRCA1 protein reduction due to DRB treatment, we performed a western blot to investigate BRCA1 protein level discrepancies between the two treatments. Western blot analysis of GFP-tagged BRCA1 in U2OS cells after the same treatments shows a significant reduction in BRCA1 protein after DRB treatment, but not a reduction in BRCA1 protein after α-amanitin treatment (**Fig. 4-1B**). These results indicate that the observed reduction in BRCA1 recruitment at TA-KR damage sites is not due to a reduction in protein alone, but is due to the inhibition of active transcription. Due to the confounding effect of DRB upon overall protein reduction over a 24hr time period, we chose to utilize α-amanitin as the sole transcription inhibitor for all future experiments.

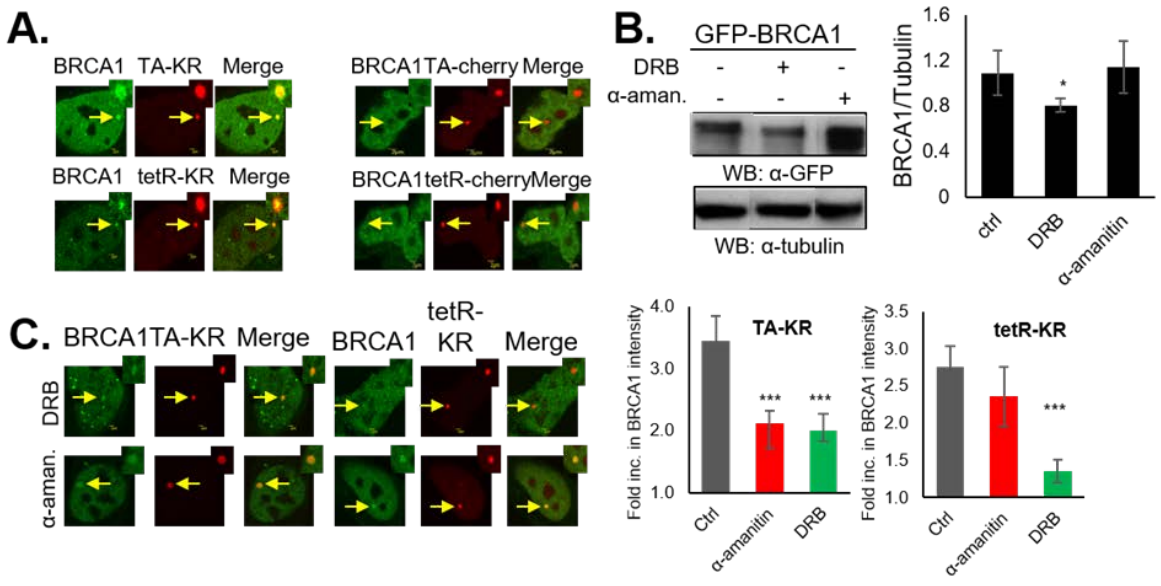

Figure 4-1 BRCA1 recruitment to TA-KR damage sites dependent upon active transcription.

A. GFP-BRCA1 and TA-KR/tetR-KR transfected U2OS-TRE cells were illuminated with 15 W fluorescent white light for 15 min for damage induction. **B**. Western blot of GFP-BRCA1 in U2OS cells with and without DRB (40 μM) for 24 hr or α-amanitin (100 μg/mL) for 0.5 hr. Error bars indicate the SEM of three separate experiments, n=10, and the p values were determined by using Student's unpaired two-tailed *t* test (*p<0.05). **C**. GFP-BRCA1 and TA-KR/tetR-KR transfected U2OS-TRE cells were pretreated with DRB (40 μM) for 24 hr or α-amanitin (100 μg/mL) for 0.5 hr. Error bars indicate the SEM of three separate experiments, n=10, and the p values were determined by using Student's unpaired two-tailed *t* test (***p<<0.01). (Of note, other treatments were included on these western blots, but were not relevant to this study; thus the cropped images.)

Previous studies have shown that BRCA1's C- and N-terminus are required for BRCA1's DSB DNA repair response [241]. In order to elucidate BRCA1's role in TC-HR, we utilized an N-terminal mutant, C61G, which contains a mutation in the highly conserved RING finger domain and has been associated with numerous breast and ovarian cancers [242, 243]. This mutation abolishes BRCA1's association with BARD1 protein and inhibits its E3 ubiquitin ligase activity [241]. Although the BRCA1/BARD1 E3 ligase activity is poorly understood, BRCA1 and BARD1

are required to recruit RAD51 and BRCA2, repair proteins involved in canonical HR [244]. We found that recruitment of C61G to light induced TA-KR sites was not significantly enriched over tetR-KR sites (**Fig. 4-2A**). C61G also did not demonstrate significantly reduced recruitment to TA-KR or tetR-KR sites compared to full length BRCA1 (**Fig 4-2B**).

Treatment with the polymerase II inhibitor α-amanitin, however, significantly reduced the recruitment of C61G to TA-KR sites (**Fig. 4-2A**). Compared to full length BRCA1, C61G also demonstrated significantly reduced recruitment to actively transcribed TA-KR damage sites (**Fig 4-2B**). These results indicate that BRCA1's recruitment at actively transcribed damage sites is dependent on its E3 ubiquitin ligase activity and BARD1 binding.

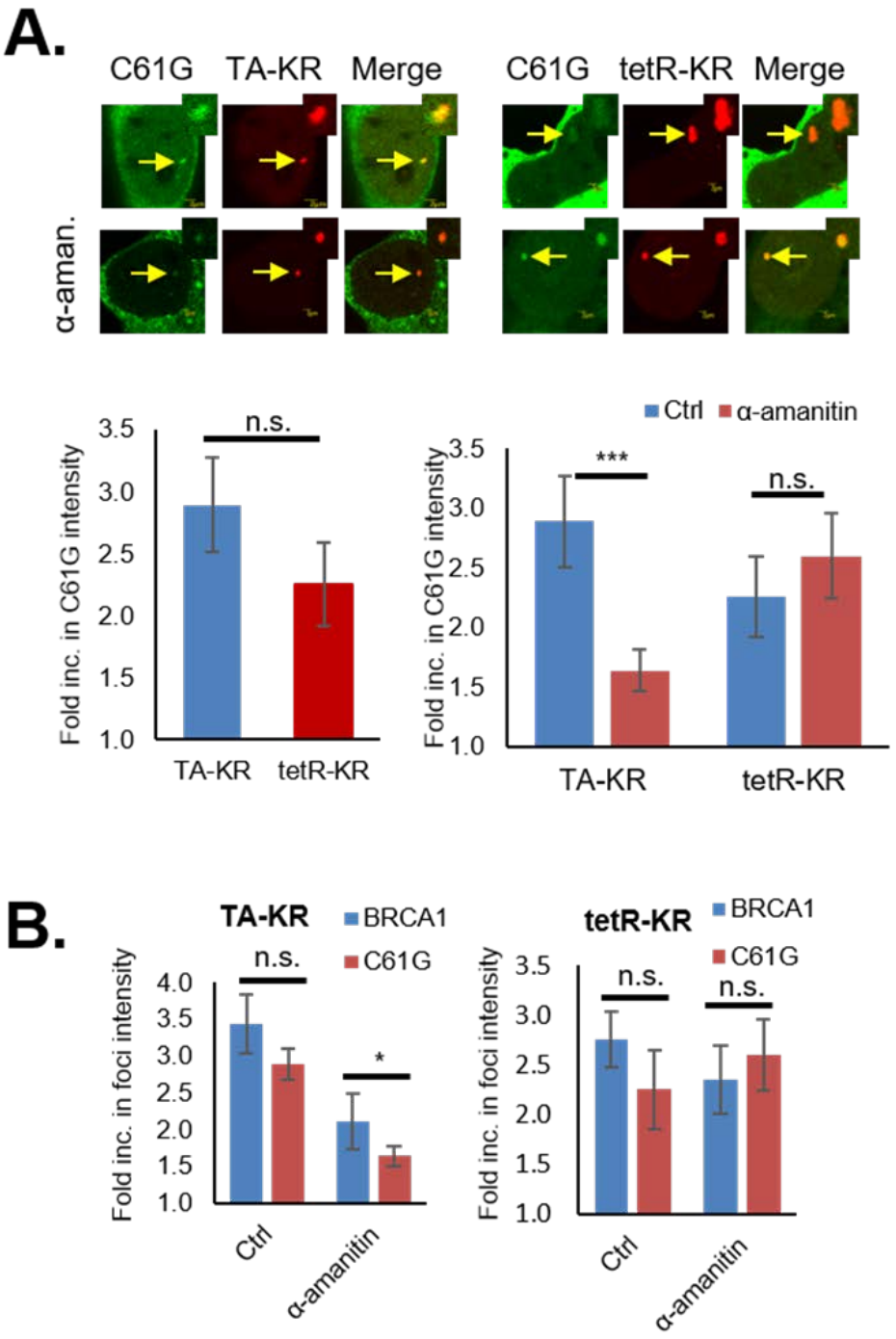

Figure 4-2 C61G recruitment dependent upon BARD binding site.

A. GFP-BRCA1 C61G mutant and TA-KR or tetR-KR transfected U2OS-TRE cells were pretreated with α-amanitin (100 μg/mL) for 0.5 hr. and illuminated with 15 W fluorescent white light for 15 min for damage

induction. **B.** GFP-BRCA1 C61G mutant or full length GFP-BRCA1 and TA-KR or tetR-KR transfected U2OS-TRE cells were pretreated with α-amanitin (100 μg/mL) for 0.5 hr. Error bars indicate the SEM of three separate experiments, n=10, and the p values were determined by using Student's unpaired two-tailed *t* test (***p<<0.01, *p<0.05).

4.2.2 BRCA1 recruitment at damage sites with active transcription independent of RAD52

In humans, BRCA1 is a key protein that promotes DSB repair by HR over NHEJ. Although the precise mechanisms of pathway choice in DSB repair are still poorly understood, a crucial step lies in the 53BP1-dependent barrier that prevents DNA resection. Studies have shown that BRCA1 relieves this barrier by promoting 53BP1 phosphorylation [245].

In yeast, RAD52 is a ring-shaped oligomer that helps load RAD51 onto RPA coated ssDNA to promote single-strand annealing [246, 247]. It also acts in strand capture during the invasion step of HR [151, 248]. RAD52 is conserved between yeast and humans, primarily in the N-terminal region [249]. However, RAD52's precise role in HR in human cells is poorly understood. A recent study has shown that RAD52 binds to the RPA-ssDNA pre-synaptic complex in canonical HR in humans and is displaced after the addition of RAD51 [216]. Previous research in the Lan lab using the DART system showed that the C-terminus of RAD52, not its DNA-binding N-terminal domain, is required for its DNA damage response to actively transcribed regions in TC-HR. RAD52 also directly binds Cockayne syndrome B (CSB) protein, the precursory protein required for TC-HR factor recruitment [177]. As we discovered in Chapter 3, RAD52 recruitment to DNA damage sites is reduced by transcription inhibition in post-mitotic neurons in the G_0/G_1 phase of the cell cycle. Purified RAD52 protein also preferentially binds ssDNA and R-loops, further implicating RAD52 early in the TC-HR pathway.

In canonical HR, BRCA1 binds BARD1 to firm a RING heterodimer. This heterodimer then interacts with BRCA2 which binds RAD51 to promote strand invasion [250, 251]. Since we

discovered BRCA1's active transcription dependent DNA damage recruitment is dependent upon its BARD1 binding activity much like in canonical HR, we wanted to investigate further to determine where BRCA1 functions in TC-HR in relation to RAD52. We hypothesized that BRCA1 functions upstream of RAD52 due to its BARD1 binding activity.

To determine if BRCA1 functions dependently or independently of RAD52 in TC-HR, we utilized a stable U2OS TRE RAD52 knockout cell line developed by members of the Lan lab using CRISPR Cas9 (**Fig. 4-3A)**. To make this knockout, sgRNA pairs were targeted to delete exon 4 in RAD52 which causes a frameshift and premature stop of RAD52 protein. Since exon 4 also contains an alternative start codon, targeting exon 4 eliminates all the isoforms of RAD52. Using the DART system, we found that after light induction, there was no significant difference in recruitment of transiently transfected GFP-tagged BRCA1 to inactively transcribed DNA damage sites (tetR-KR) over actively transcribed damage sites (TA-KR) in the RAD52 KO (**Fig. 4-3B)**. No significant difference in GFP-BRCA1 recruitment was seen even when compared to wt controls at TA-KR sites or tetR-KR sites (**Fig 4-3C**). This demonstrates that without RAD52, cells will still recruit BRCA1 at sites of damage with active transcription. When treated with RNA polymerase II inhibitor α-amanitin, however, recruitment to TA-KR sites was more significantly reduced than recruitment of BRCA1 to tetR-KR sites (**Fig. 4-3B)**. This only further demonstrates the role of BRCA1 in the active transcription dependent TC-HR pathway. Together these results indicate that BRCA1 recruitment at DNA damage sites with active transcription is independent of RAD52.

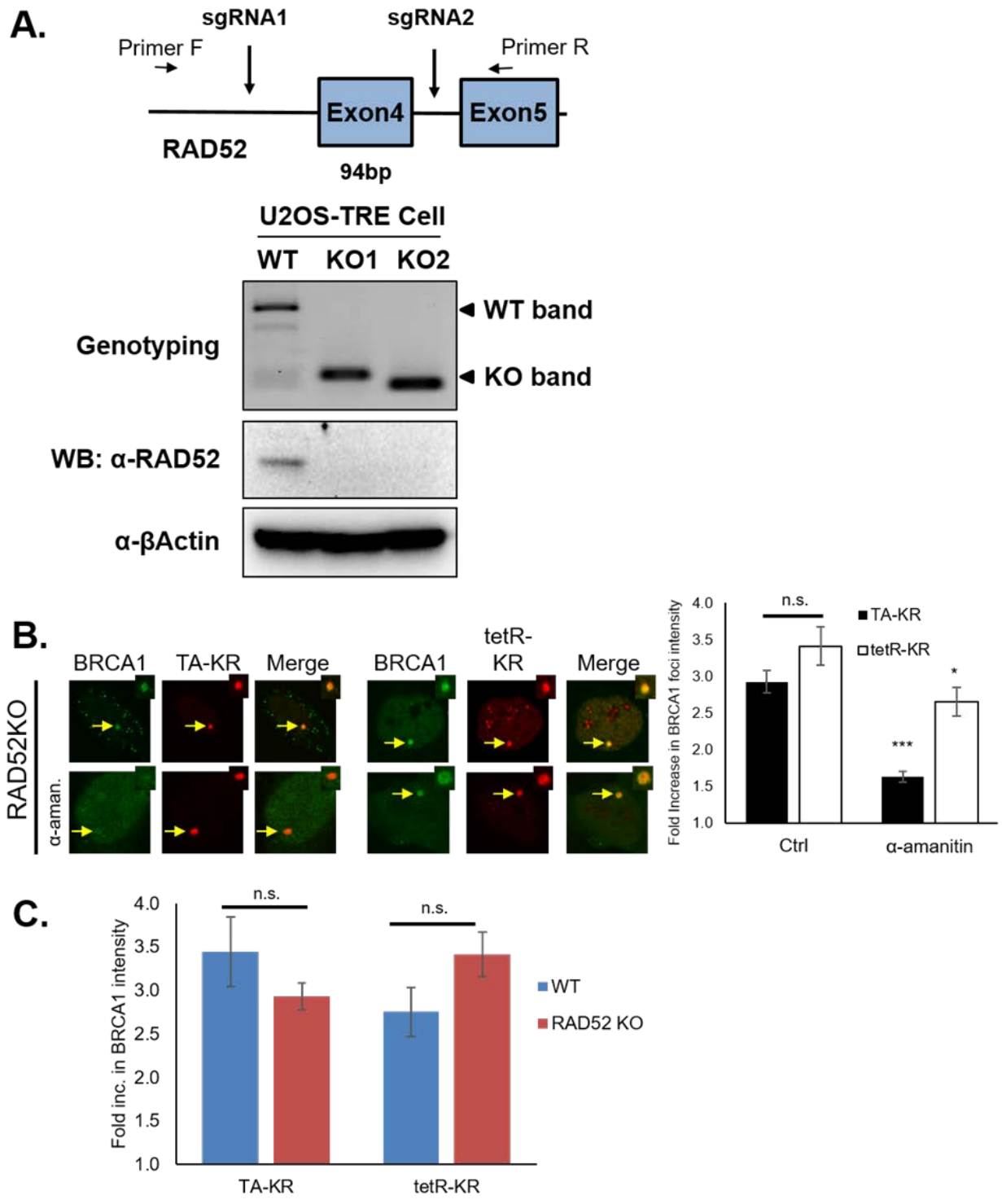

Figure 4-3 BRCA1 recruitment at actively transcribed sites independent of RAD52.

A. Schematic of RAD52 KO in U2OS-TRE cell line and western blot knockout verification. **B.** GFP-BRCA1 and TA-KR/tetR-KR transfected U2OS-TRE cells were pretreated with and without α-amanitin (100 μg/mL)

for 0.5 hr and illuminated with 15 W fluorescent white light for 15 min for damage induction. Error bars indicate the SEM of three separate experiments, n=10, and the p values were determined by using Student's unpaired two-tailed *t* test (***p<<0.01,*p<0.05). **C.** GFP-BRCA1 and TA-KR/tetR-KR transfected U2OS-TRE cells and RAD52 KO U2OS-TRE cells were illuminated with 15 W fluorescent white light for 15 min for damage induction. Error bars indicate the SEM of three separate experiments, n=10, and the p values were determined by using Student's unpaired two-tailed *t* test.

4.2.3 Discussion

We have found that BRCA1 is preferentially recruited to actively transcribed DNA damage, and that this activity is independent of BRCA1's BARD1 binding and its E3 ligase activity. Additionally, we discovered that BRCA1 recruitment to actively transcribed damage sites is independent of RAD52 in the TC-HR pathway.

Further experiments are necessary in order to define BRCA1's role in TC-HR. Many of these have already proven to be difficult due to the toxicity of BRCA1 overexpression after 24hrs. We have found that in cancer cell lines and post-mitotic neurons, GFP-BRCA1 overexpression induces cell death after more than 24hrs, resulting in observable transfection efficiencies of less than 50% after such time. Thus, some experiments have been reduced to shorter treatment times after transient transfections. Future studies would necessitate the use of stable cell lines or knockouts.

In order to further elucidate RAD52 and BRCA1's roles in TC-HR vs canonical HR, siRNA for BRCA1 and RAD52 should be used in U2OS-TRE cells to investigate γ-H2AX retention at TA-KR sites after KillerRed induction at 0h, 1h, 4h, 24h, and 48h timepoints of recovery. Greater intensity of the γ-H2AX foci at TA-KR sites at later timepoints than controls will indicate unrepaired DSBs after the knockdown of RAD52, BRCA1, and RAD52/BRCA1 together. The inability to repair DSBs with either or both repair protein knockdowns will indicate which proteins are essential for

DSB repair at actively transcribed sites of DNA damage. A survival assay can also be conducted with the same knockdowns and increasing doses of gamma irradiation ranging from 1Gy, 3Gy, and 5Gy. The knockdown with fewer surviving colonies of U2OS cells after 7-10 days will indicate which repair protein(s) is/are necessary for repair fidelity. Western blots will verify all knockdowns.

What needs to be considered in these experiments is that both RAD52 and BRCA1 function in other DNA repair pathways besides DSB repair as mentioned in Chapter Three. The siRNA knockdowns may therefore affect these pathways as well. BRCA1 knockdowns may also affect processes other than DNA repair, such as apoptosis, confounding survival assays. Previous studies have found that ectopic expression of BRCA1 led to cell cycle arrest at the G_2/M stage of the cell cycle in MCF-7 cells or apoptosis in U2OS cells [252-254]. Indeed, experiments involving transient transfection of GFP-BRCA1 and its consequent overexpression for longer than 48 hr time periods have led to decreased transfection efficiencies (<10%) in both U2OS cells and neurons. This implies that the overexpression of BRCA1 can lead to toxicity. Its knockdown should be monitored for similar effects using assays to measure apoptosis and proper controls. Also, since BRCA1 is not only localized to the nucleus, nuclear fractionation prior to western blotting may help in isolating DNA repair associated BRCA1 for specific investigations into its repair properties.

Recruitment of repair factors to DNA damage sites is essential for their roles in the DNA damage response. Further studies are indeed necessary to elucidate both BRCA1 and RAD52 repair activity in the TC-HR pathway such as comet assays and γ-H2AX retention to measure DSB repair after damage. In regards to performing repair function, however, demonstrating recruitment at DNA damage sites is significant in order to show the initiation of the repair process. For example, other investigations have been conducted into major repair pathways such as MMR using laser microirradiation and HeLa cells to demonstrate that the recruitment of key MMR repair proteins MSH2, MSH3, and MSH6 occurs at UVDE-induced SSBs in a poly(ADP-ribose)-dependent manner [255]. This study is significant because MMR is used to repair base

mismatches and mismatched loops typically formed during DNA replication. Unless a lesion contains a mismatch, MMR associated factors do not directly bind to DNA damage sites such as DNA strand breaks or UV-induced damage. The experiments conducted in this study indicate that certain MMR repair factors are, indeed, recruited to SSB damage sites prior to repair via MMR.

BRCA1 is a complex and important protein, but further defining its role in TC-HR will help to better understand how Aβ negatively affects the DNA damage response. The following section of this dissertation introduces this next concept.

5.0 $A\beta_{1-42}$ oligomers affect the DNA damage response of BRCA1 and RAD52

This chapter is expanded from the following collaborative published work:

Welty, S., Teng, Y., Zhuobin, L., Weixing, Z., Sanders, L., Greenamyre, T., Rubio, M.E., Thathiah, A., Kodali, R., Wetzel, R., Levine, A., Lan, L. (2017) RAD52 is required for RNA-templated recombination repair in post-mitotic neurons. *J Biol Chem.* 293(4):1353-1362.

5.1 Introduction

Aβ is produced by proteolytic cleavage of the transmembrane protein APP, which is expressed in numerous tissue types. Low concentrations (pM) of Aβ have been confirmed via microdialysis in the interstitial fluid of normal brains, but higher concentrations in the nM-μM range lead to neurotoxicity and neuronal death [48, 49]. It was normally assumed that blood circulating Aβ originates from Aβ produced within brain regions that then crosses the blood-brain barrier [256, 257].

Aβ can also be produced in peripheral tissues and secreted into the blood. Platelets can produce Aβ in a similar manner to neurons, and it's also been shown that skin fibroblasts, skeletal muscles, and cerebrovascular smooth muscle cells can also produce Aβ [258-262]. In a recent study using a model of parabiosis, or surgically conjoined mice which share circulating blood, it was shown that this peripherally generated Aβ circulating in the bloodstream can contribute to AD pathology. This model used a transgenic AD mouse conjoined with a wild type littermate and found evidence of human Aβ plaques, hyperphosphorylated tau tangles, and AD-related pathologies such as neurodegeneration and impaired hippocampal long term potentiation in the

wild type mouse after 12 months of parabiosis [263]. Importantly, these studies show that Aβ metabolism in both the brain and periphery can contribute to the development of late stage AD pathology.

Measurement of this circulating Aβ is often used to help diagnose AD and is believed to be a more progressive method to keep track of patients showing signs of cognitive decline in the early stages of the disease. Traditional methods include measuring $A\beta_{1-40}$ and $A\beta_{1-42}$ levels from the cerebral spinal fluid (CSF), or visualizing amyloid or tau pathologies in the brain via positron emission tomography (PET) [264]. Testing blood plasma for $A\beta_{1-40}$ and $A\beta_{1-42}$ is currently possible with sensitive measurements such as mass spectrometry, but is not commonly used for patients due to the lower levels of Aβ found in the blood [265]. What needs to be considered, however, is that measurements of circulating Aβ levels in the CSF and plasma may be confounded due to their origin.

Cellular responses to DNA damaging agents are not all the same depending upon stages of the cell cycle, cell type, regional specificity in the mammalian body, and also age. Cell cycle dependent responses to DSBs have been discussed in Chapter Two regarding canonical HR, TC-HR, and NHEJ. In addition, there is research showing cell type, age specific, and regional/tissue differences in DNA damage responses to DSBs. For example, studies have shown that differentiated mouse embryonic fibroblasts predominantly utilize error-prone NHEJ to repair DSBs. Undifferentiated mouse embryonic stem cells (ES), which would give rise to all cell types and globally affect the organism, preferentially use the more error-free canonical HR in order to increase their repair fidelity even when NHEJ repair proteins are artificially overexpressed [266]. Regarding regional specificity, lung basal stem cells were shown to use NHEJ to repair DSBs more efficiently than alveolar progenitor cells [267]. Epidermal stem cells are highly proficient in NER to repair UV induced DNA lesions, and individuals with deletions in XPA/XPC repair proteins are susceptible to squamous cell carcinoma [268].

With these studies in mind, the research in this chapter was undertaken in order to investigate the effects of extracellular toxic $A\beta_{1-42}$ oligomers on DNA DSB repair processes in mitotic and post-mitotic *in vivo* cellular models. My hypothesis was that $A\beta_{1-42}$ would downregulate the recruitment of TC-HR associated proteins, thus leading to the inhibition of repair. This section demonstrates that $A\beta_{1-42}$ negatively affects DSB repair activity dependent upon active transcription, reduces the TC-HR associated RAD52 protein and HR/TC-HR associated repair protein BRCA1 recruitment to DNA damage sites, reduces RAD52 protein levels, increases R-loop formation, and decreases DSB repair efficiency.

5.2 Results

5.2.1 $A\beta_{1-42}$ sensitizes cells to IR in the absence of active transcription

The accumulation of $A\beta_{1-42}$ in AD is correlated with DNA damage induced by oxidative stress. As mentioned in Chapter 4, a recent study has shown that high concentrations of $A\beta_{1-42}$ (1 μM) in mitotic mouse hippocampal neuron cultures and in brain samples from AD patients were correlated with reduced levels of BRCA1 and increased levels of DSB marker γ-H2AX [13]. BRCA1's role in DSB repair and other cellular processes has been discussed in Chapter 2. However, it is not known whether $A\beta_{1-42}$ affects the major DSB repair pathways: the error-prone NHEJ pathway and the less error-prone HR pathway.

We investigated the effects of $A\beta_{1-42}$ on overall HR and NHEJ in dividing U2OS cells using the HR (DR-GFP) and NHEJ (Ej5-GFP) reporter assays [269, 270] (**Fig. 5-1A&B**). For the HR reporter assay, the DR-GFP cell line utilizes an I-*Sce*I recognition site inserted into a GFP coding sequence to create a nonfunctional GFP transgene. A wild type GFP fragment has been inserted downstream of the transgene. After transfection of an I-*Sce*I expressing plasmid, a DSB is created

at the I-*Sce*I cleavage site. If successful HR occurs, fully functional GFP is restored which can be detected by fluorescence activated cell sorting (FACS). For the NHEJ assay, the Ej5-GFP cell line utilizes a GFP coding sequence interrupted by a puromycine gene which is flanked by I-*Sce*I recognition sites. After transfection of the I-*Sce*I expressing plasmid, a DSB is induced at both sites, and if NHEJ occurs, a fully functional GFP is restored which can be detectable by FACS. For these experiments, both assays were treated with 1 μM $A\beta_{1-42}$ to determine its effect on each pathway.

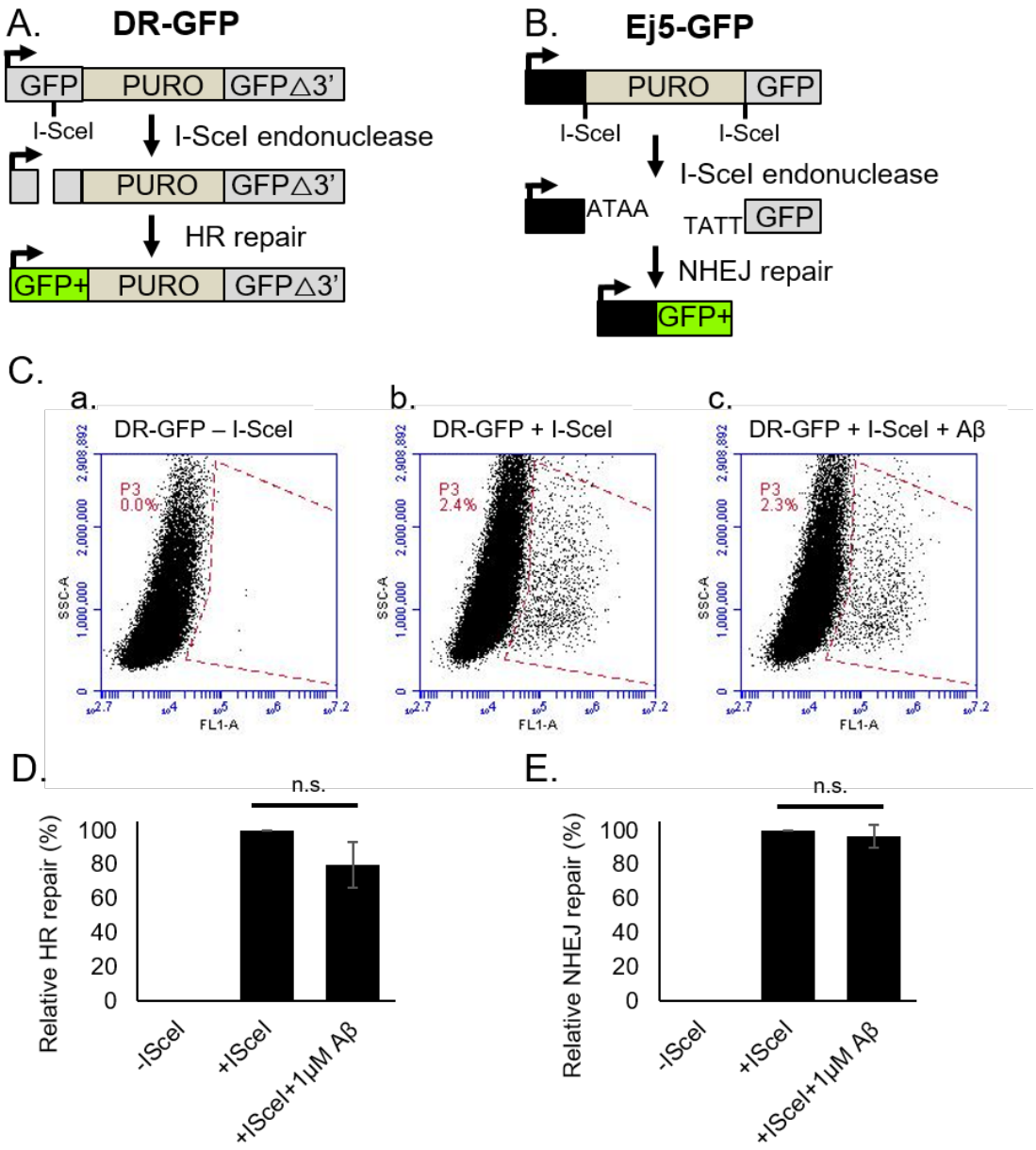

Figure 5-1 HR and NHEJ reporter assays.

A. Schematic of the DR-GFP reporter used to measure HR efficiency in U2OS cells. **B.** Schematic of the Ej5-GFP reporter used to measure NHEJ efficiency in U2OS cells. **C.** Representative FACS sample data of the DR-GFP reporter cells without I-SceI endonuclease (a.), with I-SceI endonuclease (b.), and I-SceI endonuclease and 5 hr 1 μM Aβ treatment. **D.** DR-GFP reporter cells were pretreated with 1μM Aβ for 5 hr and expression of GFP was measured by flow cytometry. Error bars indicate the SEM of three separate experiments and the p values were determined by using Student's unpaired two-tailed *t* test. **E.** Ej5-GFP

reporter cells were pretreated with 1μM Aβ for 5 hr and expression of GFP was measured by flow cytometry. Error bars indicate the SEM of three separate experiments and the p values were determined by using Student's unpaired two-tailed *t* test. Adapted from [220] with permission from the publisher.

Prior to use, $A\beta_{1\text{-}42}$ samples were investigated via western blot and Transmission electron microscopy (TEM) to verify that they contained oligomers (**Fig. 5-2A&B, 5-3**) [220].

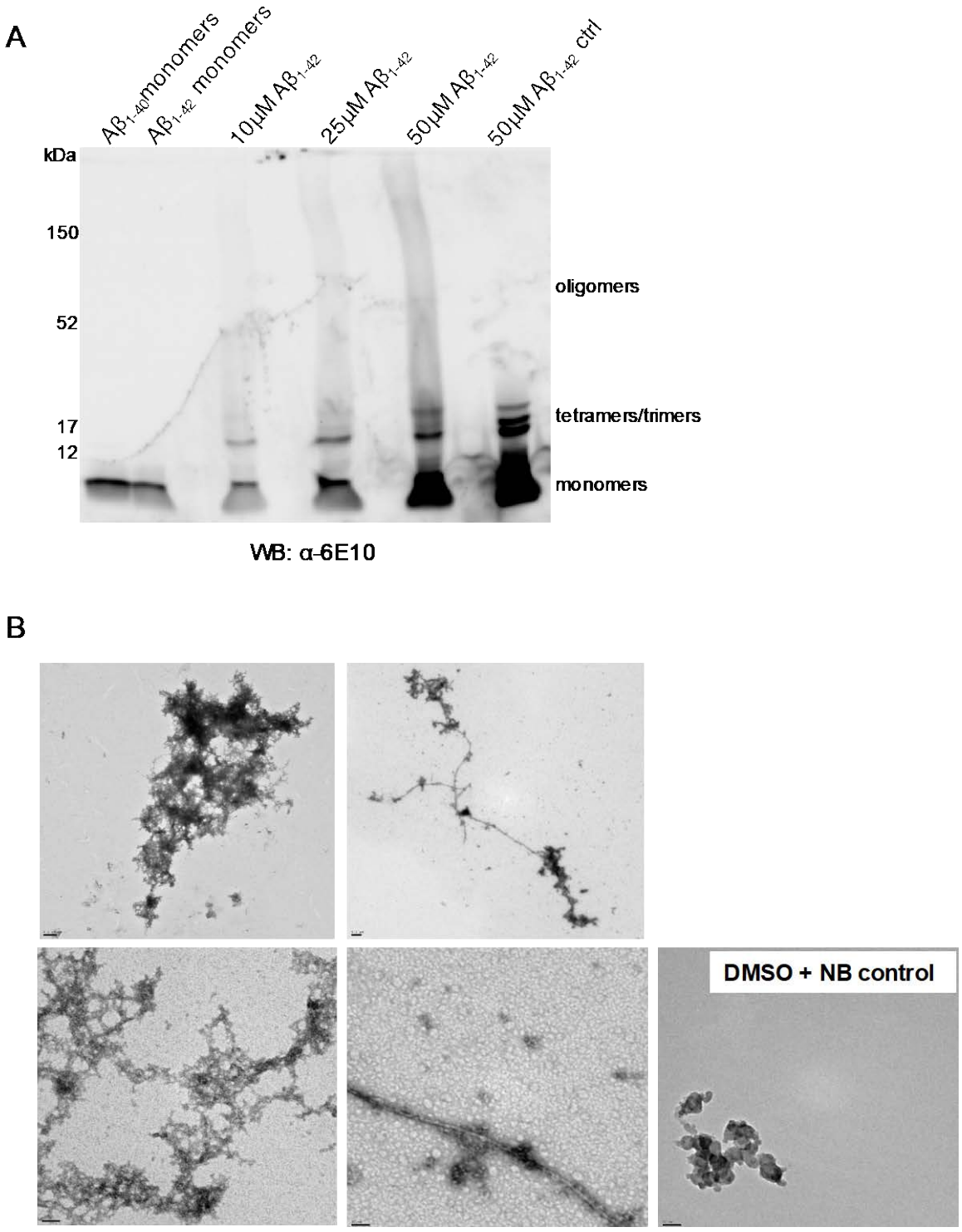

Figure 5-2 $A\beta_{1-42}$ solution contains low molecular weight oligomers.

A. Western blot of $A\beta_{1-40}$ & $A\beta_{1-42}$ monomeric controls, titrated $A\beta_{1-42}$ oligomeric solution incubated at 37℃ for 24 hrs, and $A\beta_{1-42}$ oligomeric solution control not incubated at 37℃, all probed with anti-6E10 antibody.

B. Characterization of $A\beta_{1-42}$ aggregates at 50 μM with transmission electron microscopy (TEM). The length of the segments are 0.2μm in the upper panels. The length of the segments are 50 nm in the lower panels. The lower panels represent higher magnification images.

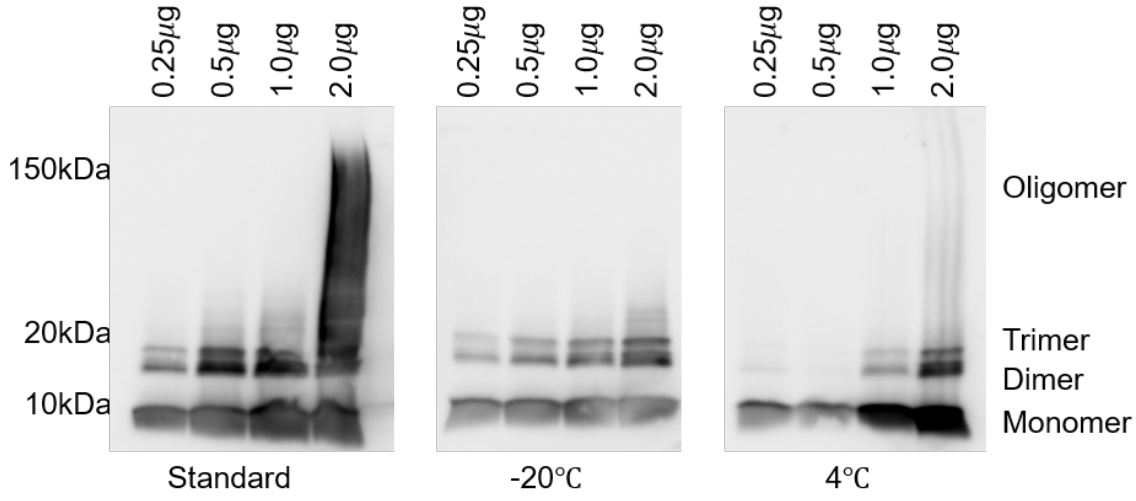

Figure 5-3 1 μM Aβ1-42 solution frozen at -20C contains oligomers.

Comparative Western blots of increasing concentrations of $A\beta_{1-42}$ standard aliquot previously stored in DMSO at -80C, 1 μM $A\beta_{1-42}$ stored at -20C, and 1 μM $A\beta_{1-42}$ stored at 4C., all probed with anti-6E10 antibody.

We found that $A\beta_{1-42}$ did not significantly affect HR or NHEJ in dividing cells (**Fig. 5-1D&E**). This is most likely due to the ability of the dividing cells to utilize canonical HR in addition to TC-HR for DSB repair.

In order to determine whether $A\beta_{1-42}$ would affect the TC-HR pathway, we utilized the RNA polymerase II inhibitor DRB to disrupt transcription in U2OS cells and measured clonogenic survival against ionizing radiation (IR). 1 μM $A\beta_{1-42}$ alone negatively affects overall U2OS survival (**Fig. 5-4A**), and as shown in **Fig. 5-4B**, DRB treatment alone renders cells more sensitive to IR. However, the addition of 1 μM $A\beta_{1-42}$ to DRB treatment did not further increase cells' sensitivity to IR (**Fig. 5-4C**). This indicates that the activity of $A\beta_{1-42}$ upon cell survival is dependent upon active

transcription, leading us to question its involvement in the downregulation of the more specific TC-HR pathway.

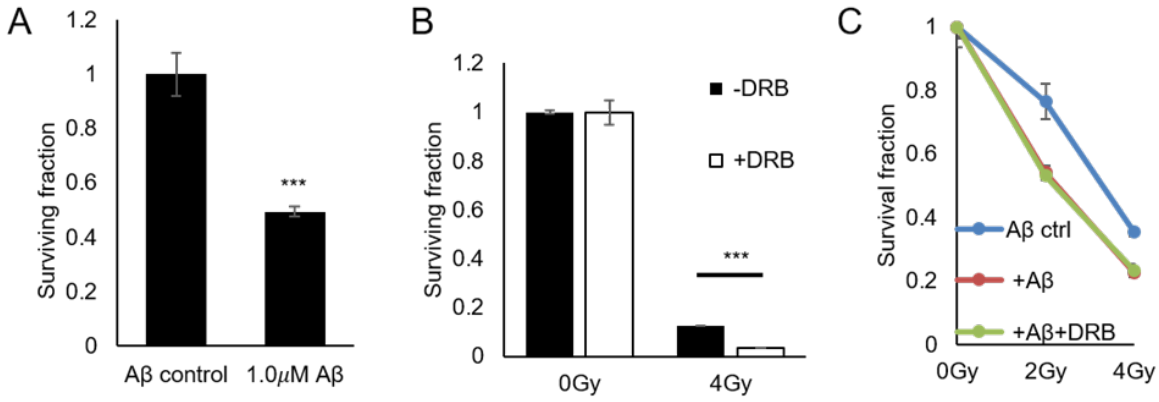

Figure 5-4 1 μM Aβ sensitizes dividing cells to IR.

A. U2OS cells were pre-treated with 1 μM Aβ for 24 hr. Colony forming assay was performed, and the surviving fraction is shown. Error bars indicate the SEM of three separate experiments, and the p values were determined by using Student's unpaired two-tailed *t* test (***p<<0.01). **B.** U2OS cells were pre-treated for 24 hr with or without DRB (40 μM), then irradiated with IR at the indicated dose. Colony forming assay was performed and the surviving fraction is shown. Error bars indicate the SEM of three separate experiments, and the p values were determined by using Student's unpaired two-tailed *t* test (***p<<0.01). **C.** U2OS cells were pre-treated for 24hrs with or without DRB (40 μM), then treated with or without 1 μM Aβ for 5 hr and irradiated with IR at the indicated dose. Colony forming assay was performed, and the surviving fraction is shown. Error bars indicate the SEM of three separate experiments, and the p values were determined by using Student's unpaired two-tailed *t* test. Adapted from [220] with permission from the publisher.

5.2.2 High concentrations of $A\beta_{1-42}$ downregulate the damage response of RAD52 and BRCA1 in post-mitotic neurons

After determining that post-mitotic neurons utilize TC-HR, we wondered if $A\beta_{1-42}$ might compromise the repair efficiency of specific proteins involved in TC-HR in non-dividing neurons. The Mucke group had previously discovered that $A\beta_{1-42}$ reduced protein concentrations of BRCA1 in hippocampal neurons [13]. These mitotic neurons are known to exhibit neurogenesis in adult humans and would primarily utilize canonical HR to repair DSBs [13]. Genome-wide microarrays have also found an increase in AD pathology correlating with the downregulation of RAD52 expression in cortical and hippocampal brain regions of AD model mice [271]. To test whether $A\beta_{1-42}$ oligomers would exhibit the same repressive effects upon the post-mitotic neurons, we treated primary rat cortical neuron cell cultures with 1 μM $A\beta_{1-42}$ and investigated the DDR response and protein amounts of TC-HR associated proteins BRCA1 and RAD52 (**Fig. 5-5&5-6)**.

Here we found that BRCA1 recruitment to laser damage sites was significantly reduced in the presence of high concentrations (1 μM) of $A\beta_{1-42}$, but not lower concentrations (1 nM) (**Fig. 5-5B**). Interestingly, BRCA1 protein expression was not significantly reduced in cortical neuron cultures after increasing concentrations of $A\beta_{1-42}$ or 5 hr and 24 hr treatment with 1 μM $A\beta_{1-42}$ (**Fig. 5-5A**).

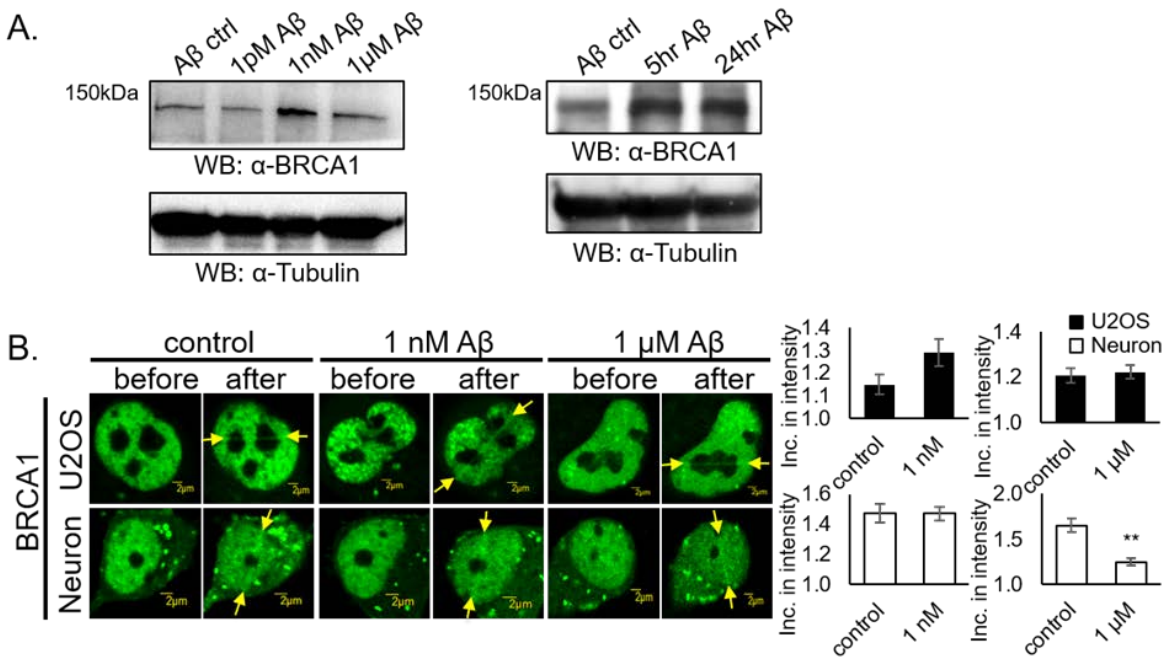

Figure 5-5 1 μM Aβ reduces BRCA1 recruitment to damage sites.

A. Western blot of endogenous BRCA1 of DIV12 primary rat cortical neurons with and without increasing concentrations of Aβ oligomers for 5 hr, and with and without 5 hr and 24 hr 1μM Aβ treatment. **B.** Recruitment of BRCA1 before and 1 min after 500 msec laser microirradiation treatment with and without 1 nMand 1 μM Aβ for 5 hr in DIV12 cortical neurons. Error bars indicate the SEM of two separate experiments, n=10, and the p values were determined by using Student's unpaired two-tailed *t* test (**p<0.01).

Western blot analysis showed that 1 μM $A\beta_{1-42}$ reduced overall RAD52 protein levels in post-mitotic neurons (**Fig. 5-6A**), but γ-H2AX expression was not significantly increased compared to untreated controls (**Fig. 5-6C**). After 24 hr of treatment, 1 μM $A\beta_{1-42}$ significantly reduced RAD52 recruitment to damage sites in both post-mitotic neurons and U2OS cancer cells (**Fig. 5-6B**). This demonstrates inhibition of RAD52 repair protein dynamics by 1 μM $A\beta_{1-42}$. The effects of 1 μM $A\beta_{1-42}$ on γ-H2AX will be further explored in sections **5.2.4** and **5.2.5**.

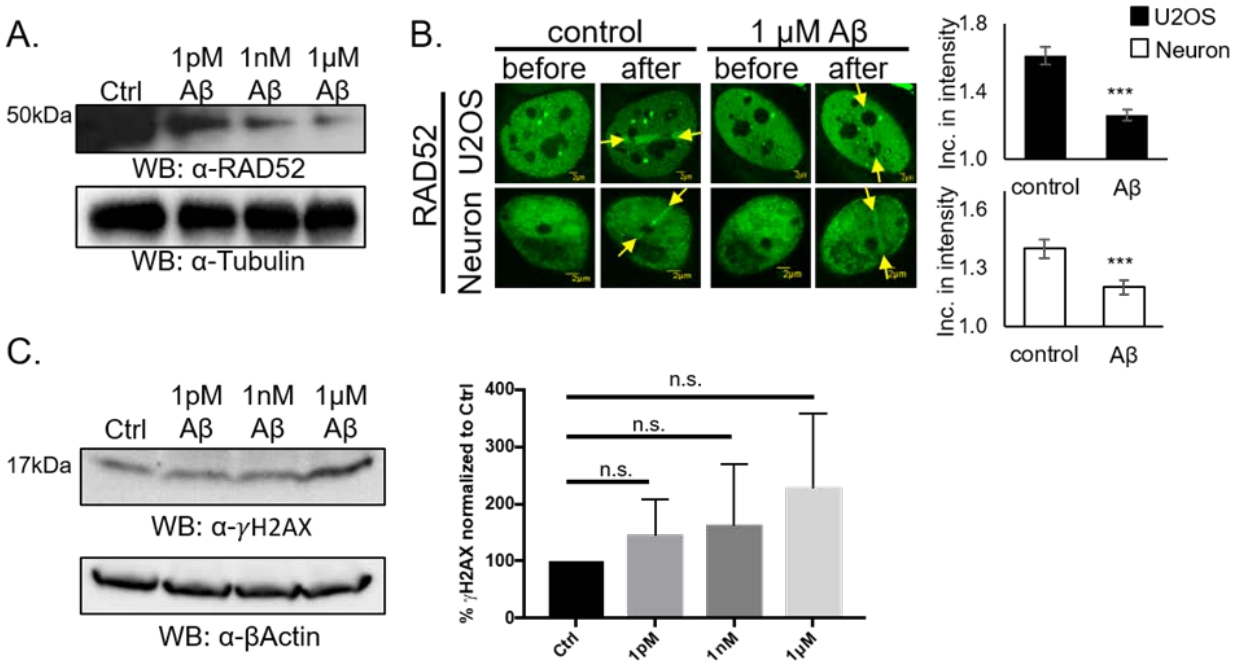

Figure 5-6 1 μM Aβ reduces RAD52 protein and recruitment to damage sites.

A. Western blot of RAD52 in DIV12 cortical neurons with and without 1 pM, 1 nM, 1 μM Aβ treatment for 5 hr. **B.** Recruitment of RAD52 before and 1 min after 500 msec laser microirradiation treatment with and without 1 μM Aβ for 24 hr in U2OS and DIV12 cortical neurons. Error bars indicate the SEM of two separate experiments, n=10, and the p values were determined by using Student's unpaired two-tailed *t* test (***p<<0.01). **C.** Western blot of endogenous γ-H2AX in DIV12 rat cortical neurons with and without 1 pM, 1 nM, 1 μM Aβ treatment for 5 hr. Error bars indicate the SEM of three separate experiments and the p values were determined by using unpaired two-tailed Student's *t* test. Adapted from [220] with permission from the publisher.

To verify the specificity of $A\beta_{1\text{-}42}$ oligomers, we also observed recruitment of GFP-tagged repair proteins specific to other repair pathways including XRCC1 (DNA single strand break repair [SSBR]) and KU70 (NHEJ) after treating primary rat cortical neuron cell cultures with 1 μM $A\beta_{1\text{-}42}$ (**Fig 5-7.**). We found that $A\beta_{1\text{-}42}$ did not reduce XRCC1 or Ku70 recruitment to damage sites after 5 hr treatments or 24 hr treatments.

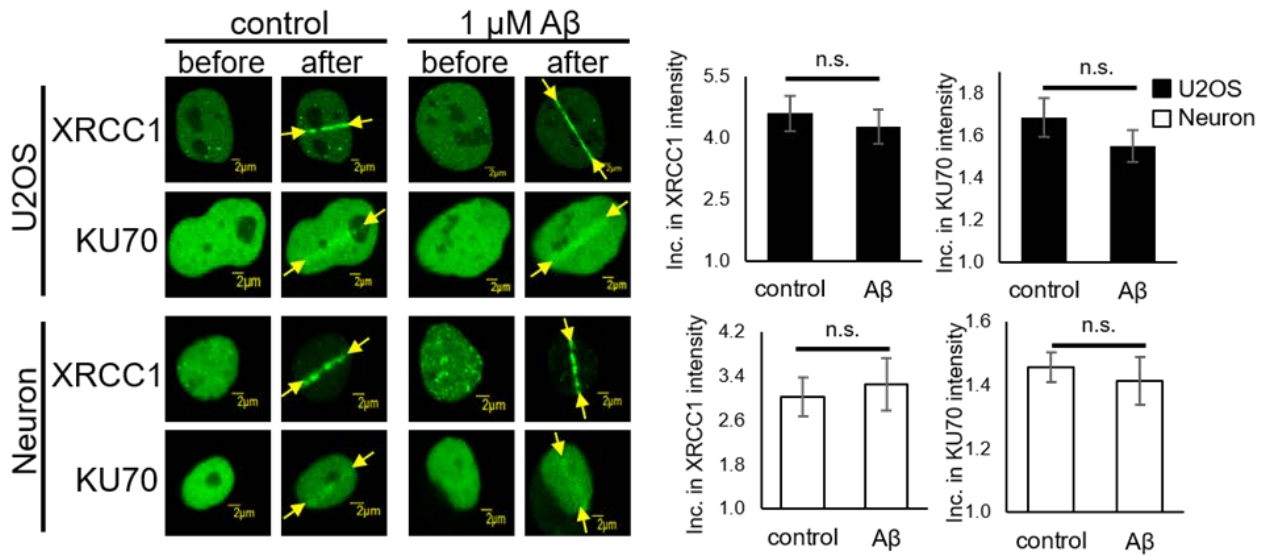

Figure 5-7 1 μM Aβ does not reduce XRCC1 and Ku70 recruitment to damage sites.

Recruitment of XRCC1 and KU70 before and 1 min after 100 msec and 500 msec laser microirradiation treatment with and without 1 μM Aβ for 5 hr in U2OS and DIV12 cortical neurons. Error bars indicate the SEM of two separate experiments, n=10, and the p values were determined by using Student's unpaired two-tailed *t* test.

The $A\beta_{1\text{-}42}$ preparations used in this project are a mixture of oligomeric and monomeric intermediates, so it is difficult to ascertain which precise species of $A\beta_{1\text{-}42}$ is responsible for the downregulatory properties demonstrated [272]. The prepared $A\beta_{1\text{-}42}$ solution consists of approximately a 50:50 ratio of monomers and oligomers as confirmed by size exclusion chromatography. In solution, these monomers and oligomers can aggregate and will pellet when centrifuged. In order to determine what fraction of the $A\beta_{1\text{-}42}$ solution exerted its toxic effect upon BRCA1 recruitment, we first performed a dose response curve to determine optimal concentration conditions (**Fig. 5-8A**). At 0.5 μM and 1.0 μM, $A\beta_{1\text{-}42}$ reduced BRCA1 recruitment to sites of laser damage similarly in post-mitotic neurons. Next, we treated cells with the pelleted and supernatant fractions of the $A\beta_{1\text{-}42}$ solution and found that the supernatant fraction containing monomers and

oligomers of $A\beta_{1-42}$, but not the aggregated forms of $A\beta_{1-42}$, was responsible for BRCA1 recruitment reduction in neurons (**Fig. 5-8B**).

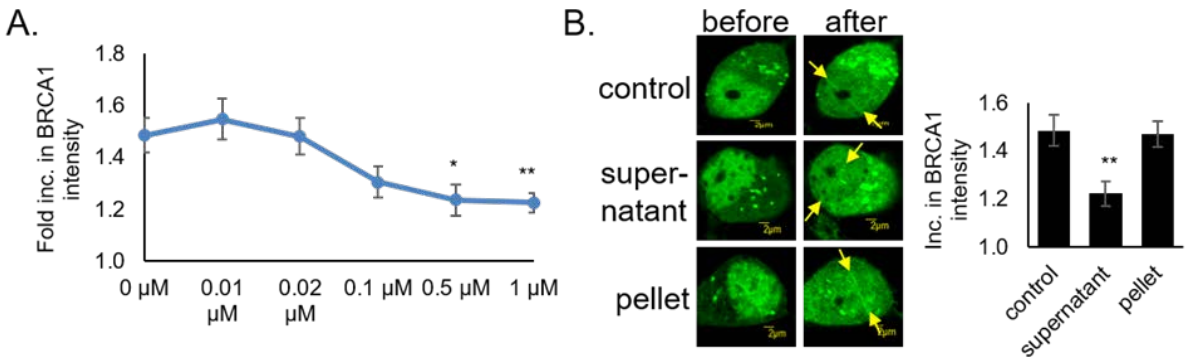

Figure 5-8 Soluble fraction of 1 μM Aβ affects repair protein recruitment.

A. Dose response curve measuring BRCA1 recruitment 1 min after 500 msec laser microirradiation treatment with indicated Aβ concentrations for 5 hr in DIV12 cortical neurons. Error bars indicate the SEM of two separate experiments, n=10, and the p values were determined by using Student's unpaired two-tailed *t* test (*p<0.05; **p<0.01). BRCA1 recruitment to damage sites was significantly reduced in post-mitotic neurons after 0.5 μM and 1 μM Aβ treatment. **B.** Recruitment of BRCA1 before and 1 min after 500 msec laser microirradiation treatment with and without 1 μM Aβ supernatant or resuspended pellet for 5 hr in DIV12 cortical neurons. Error bars indicate the SEM of two separate experiments, n=10, and the p values were determined by using Student's unpaired two-tailed *t* test (**p<0.01).

5.2.3 Increased $A\beta_{1-42}$ concentration leads to R-loop formation

Unpublished studies in the Lan lab have indicated that increased oxidative stress induces global R-loops, damage prone structures at active transcription sites. Through use of the DART system these studies have shown that R-loops are inducible at active transcription sites. $A\beta_{1-42}$ oligomers have been associated with ROS production through numerous mechanisms previously

mentioned such as the Fenton reaction, copper binding, and its methionine residue as discussed in Chapter One. Therefore, we hypothesized that overproduction of $A\beta_{1-42}$ oligomers and the consequent ROS lead to increased R-loops. This in turn leaves more surface area of DNA exposed to breakage, thus compromising overall genomic stability.

To verify this hypothesis, we treated wild type U2OS TRE cells with high concentrations of $A\beta_{1-42}$ (1μM) and investigated R-loop formation using anti-S9.6 antibody staining (**Fig. 5-9A&5-9B)**. Anti-S9.6 antibody is a mouse monoclonal antibody generated against a ϕX714 bacteriophage-derived synthetic DNA-RNA antigen which can recognize DNA-RNA hybrids. It has been verified for use to recognize the DNA-RNA hybrid formed during active transcription and is commonly used to detect R-loops [194]. We found that treatment with $A\beta_{1-42}$ significantly increased the frequency of R-loops at actively transcribed DNA damage sites compared to controls (**Fig. 5-9B)**. This demonstrates that high concentrations of $A\beta_{1-42}$ exacerbate the ROS induced R-loop formation of activated KillerRed.

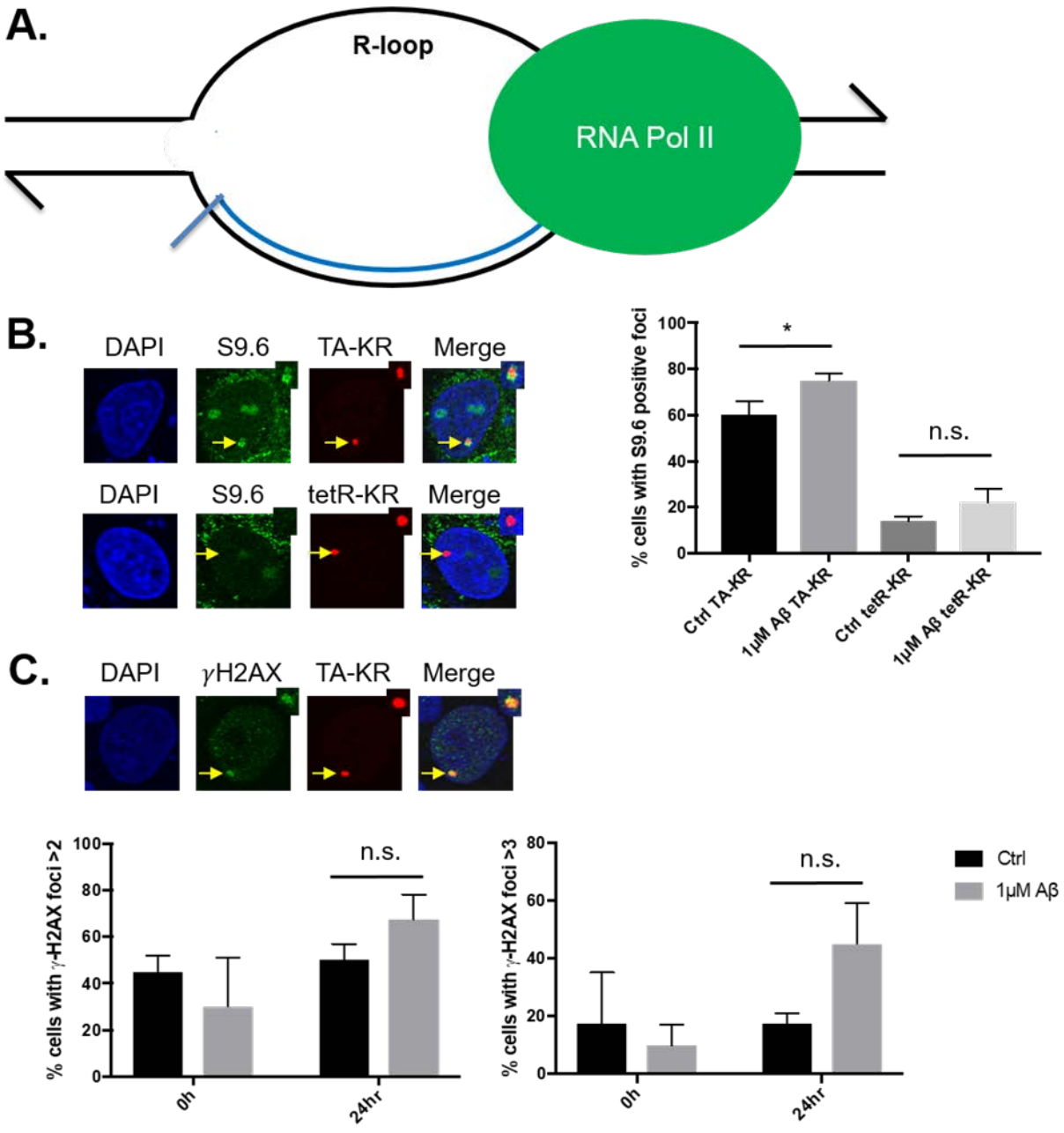

Figure 5-9 1 μM Aβ increases R-loops.

A. Diagram of R-loop formation during active transcription. **B.** TA-KR and tetR-KR transfected U2OS-TRE cells were pre-treated with 1 μM Aβ for 24hrs and cells were illuminated with 15 W fluorescent white light for 15 min for damage induction. R-loop formation was determined by co-localization of anti-S9.6 antibody to damage sites. Error bars indicate the SEM of two separate experiments, n=10, and the p values were determined by using Student's unpaired two-tailed *t* test (*p<0.05). **C.** TA-KR transfected U2OS-TRE cells

were pre-treated with 1 μM Aβ for 24 hr. Cells were illuminated with 15 W fluorescent white light for 15 min for damage induction, allowed to recover for 4hr or 24hr, then stained with anti-γ-H2AX antibody. Error bars indicate the SEM of two separate experiments, n=10, and the p values were determined by using two-way ANOVA and Tukey's multiple comparisons test.

5.2.4 Increased $A\beta_{1-42}$ delays γ-H2AX expression

Within a few minutes of DSB formation, H2AX, a variant of the histone H2A, is rapidly phosphorylated in the vicinity of the break by the ATM or DNA-PK kinases [273]. This phosphorylated form, termed γ-H2AX, is essential for cell cycle checkpoint activation and the recruitment of downstream DSB repair factors, although some studies show it is not required for the initial break recognition step [274-277]. It has been hypothesized that γ-H2AX is involved in chromatin remodeling in order to allow for repair factors to access the damaged DNA. These findings have been confirmed by studies that show $H2AX^{-/-}$ cells exhibiting radiosensitivity and genomic instability and also double p53 and H2AX KO mice rapidly developing tumors [278, 279]. γ-H2AX has, therefore, been used extensively as a marker for DSBs in both immunofluorescent staining assays and western blots [280]. In radiobiology, the ratio of DSBs correlates to γ-H2AX foci in a 1:1 ratio, although its use as an indicator for DSB repair has been debated [273, 280]. One study that compared wild-type and Ku80 deficient mice argued that at low levels of IR damage (e.g.-2Gy), γ-H2AX expression and foci retention could be used to indicate DSB repair. Higher levels of DNA DSB inducing damage (e.g.-10Gy) produced conflicting results [281]. Other studies such as those produced by the Lan lab examining γ-H2AX foci retention after damage as an indication of efficient repair have shown consistent results. Typically, γ-H2AX retention is

strongest at approximately 2-4hrs after damage induction and is significantly reduced after 24-48hrs, indicating a completion of repair [177, 282].

In order to determine if $A\beta_{1-42}$ inhibits overall DSB repair efficiency, we treated U2OS cells with 1μM concentrations of $A\beta_{1-42}$ for 24hrs and investigated γ-H2AX expression and retention after recovery from 3Gy gamma irradiation treatment (**Fig. 5-10A-D&5-11&5-12)**. Western blot analysis indicates a delay in γ-H2AX protein production in the early recovery stages of 1hr and 4hr with the most significant reduction at the 4hr timepoint (**Fig. 5-10A-D)**. (Of note, these results represent soluble γ-H2AX. Chromatin-associated γ-H2AX at repair sites may not have been completely released in lysis buffer due to lack of benzonase treatment.) There was no significant difference in γ-H2AX expression between non-irradiated control and non-irradiated samples treated with 1μM concentrations of $A\beta_{1-42}$ for 24hrs (**Fig. 5-11**). However, analysis of γ-H2AX foci retention, an indicator of DSB resolution, shows no difference in the number of cells with reduced γ-H2AX foci after 24hrs and 48hrs (**Fig 5-12**). Specifically, cells treated with 1μM concentrations of $A\beta_{1-42}$ for 24hrs and irradiated with 3Gy of gamma irradiation showed no retention of γ-H2AX foci after 24hrs or 48 hrs as compared to untreated controls. Together, these data indicate that $A\beta_{1-42}$ interferes with early stages of DSB repair, but not overall DSB repair.

We also investigated γ-H2AX retention at sites of active transcription in U2OS-TRE cells after treating cells with 1μM concentrations of $A\beta_{1-42}$ for 24hrs (**Fig 5-9C**). Analysis of γ-H2AX foci retention showed no significant differences between treated samples and controls at 0 hr, 4 hr, and 24 hr timepoints. This further indicates that $A\beta_{1-42}$ does not interfere with DSB resolution at actively transcribed sites of DNA damage.

Survival assays have demonstrated that 1μM concentrations of $A\beta_{1-42}$ for 24hrs significantly reduce cell survival (**Fig. 5-4A)**, even in mitotic cell populations that are capable of utilizing canonical HR and NHEJ for DSB repair. This supports our findings that $A\beta_{1-42}$ reduces the localization of early acting DSB repair proteins RAD52 and BRCA1 at DNA damage sites.

Such inhibition may lead to failure to repair and resultant cell death, contributing to the neurodegenerative pathology of AD. However, more studies are necessary because the reduction of γ-H2AX itself does not necessarily correlate directly with cell death.

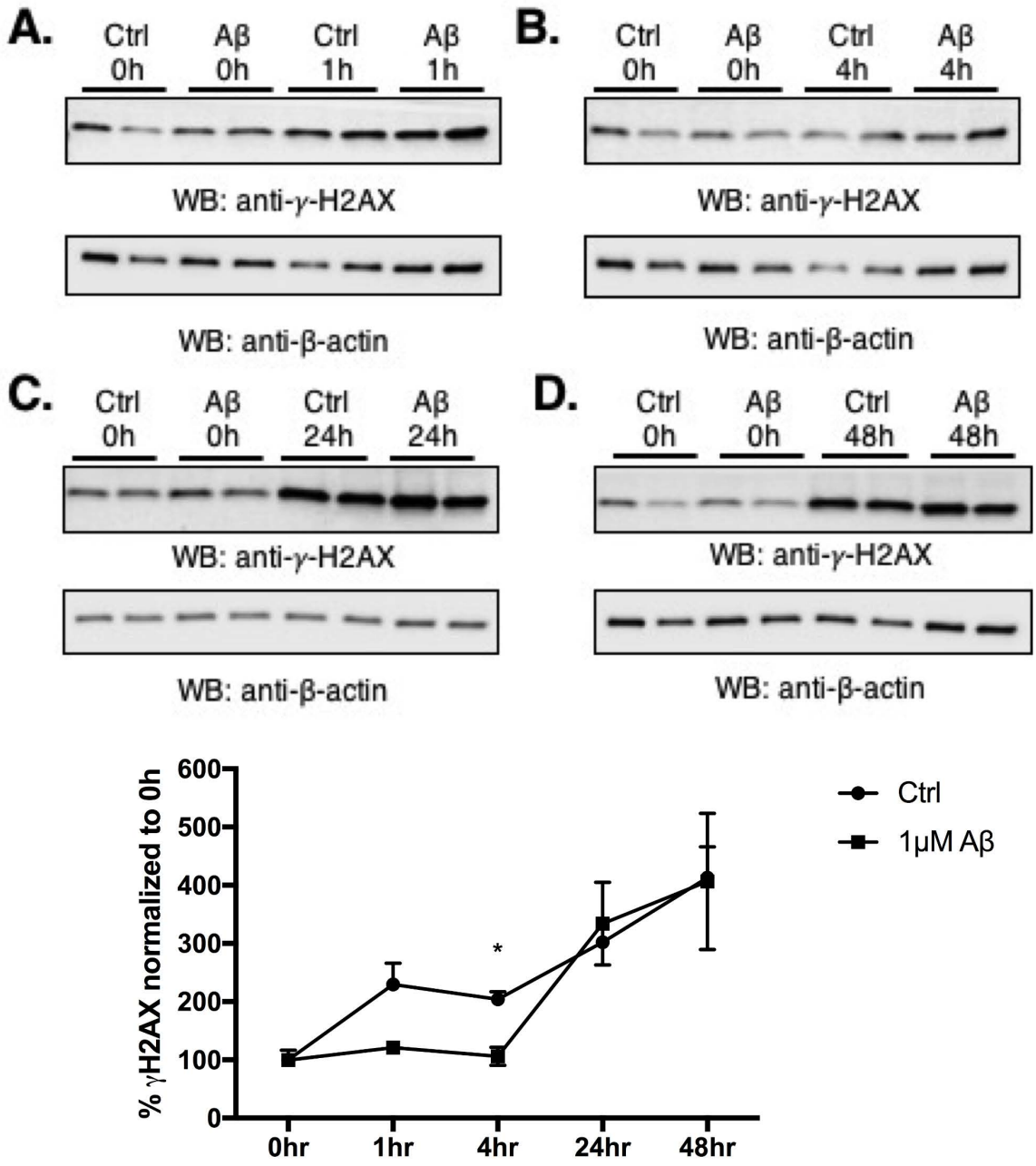

Figure 5-10 1μM $A\beta_{1-42}$ delays γ-H2AX expression after IR in mitotic cells.

U2OS cells were pre-treated with and without 1 μM Aβ for 24 hrs. Cells were then treated with 3Gy of gamma irradiation and allowed to recover for **A.** 1 hr, **B.** 4 hrs, **C.** 24 hrs, or **D.** 48 hrs at 37C, then probed via western blot with antibodies for anti-γ-H2AX. Error bars indicate the SEM of two separate experiments, and the p values were determined by using two-way ANOVA and Tukey's multiple comparisons test (*$p<0.05$).

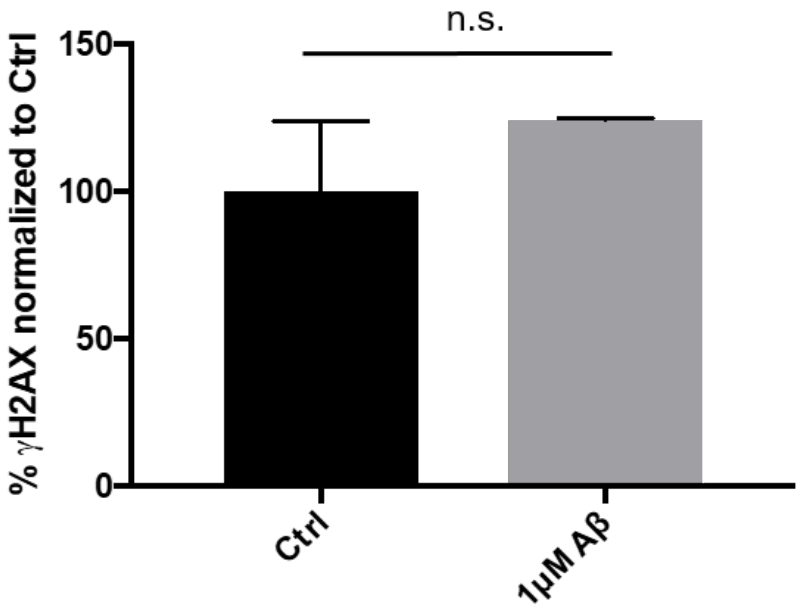

Figure 5-11 $A\beta_{1-42}$ does not alter γ-H2AX expression in U2OS cells without DNA damage.

Western blot of endogenous γ-H2AX before and after 24hrs of $A\beta_{1-42}$ treatment. Error bars indicate the SEM of two separate experiments, and the p values were determined by using Student's unpaired *t*-test.

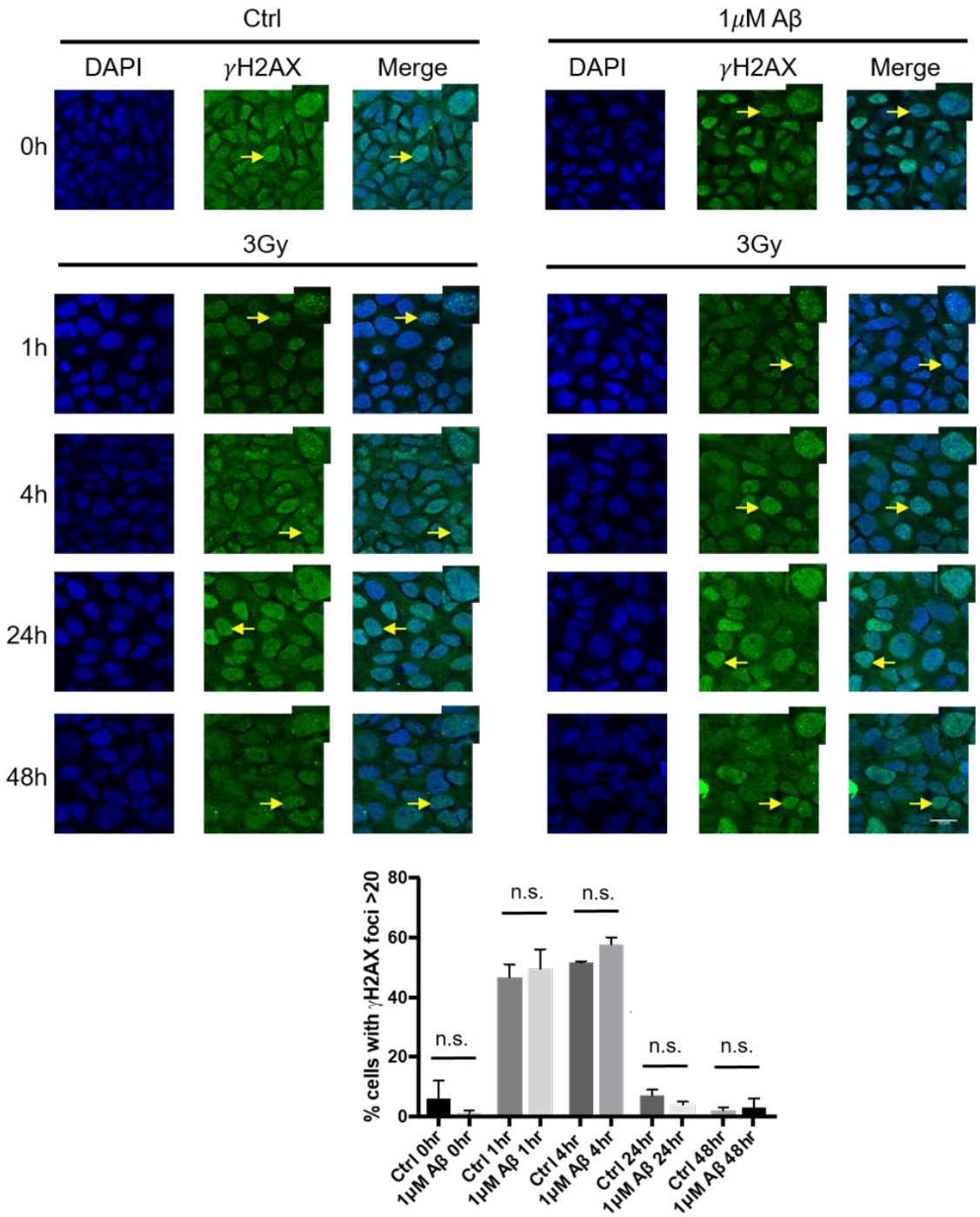

Figure 5-12 1μM $A\beta_{1-42}$ does not lead to retention of γ-H2AX foci after IR in mitotic cells.

U2OS cells were pre-treated with and without 1 μM Aβ for 24 hrs. Cells were then treated with 3Gy of gamma irradiation and allowed to recover for 1 hr, 4 hrs, 24 hrs, or 48 hrs at 37C, then stained with antibodies for anti-γ-H2AX. Error bars indicate the SEM of two separate experiments, n=100, and the p values were determined by using two-way ANOVA and Tukey's multiple comparisons test.

5.2.5 Discussion

This section has shown that $A\beta_{1-42}$ negatively affects HR in a transcriptionally dependent manner, inhibits RAD52 and BRCA1 recruitment to DNA damage sites, reduces RAD52 repair protein in post-mitotic neurons, increases R-loop formation, and inhibits γ-H2AX expression early following DNA damage. These experiments also indicate $A\beta_{1-42}$ differentially affects repair proteins depending upon the protein itself and the model system utilized. For example, in regards to RAD52, in primary rat cortical neurons, endogenous RAD52 protein is reduced and its recruitment is downregulated after $A\beta_{1-42}$ treatment (**Fig 5-6A)**. In human U2OS cells, however, as evidenced in **Fig 5-13** endogenous RAD52 protein is not reduced following $A\beta_{1-42}$ treatment.

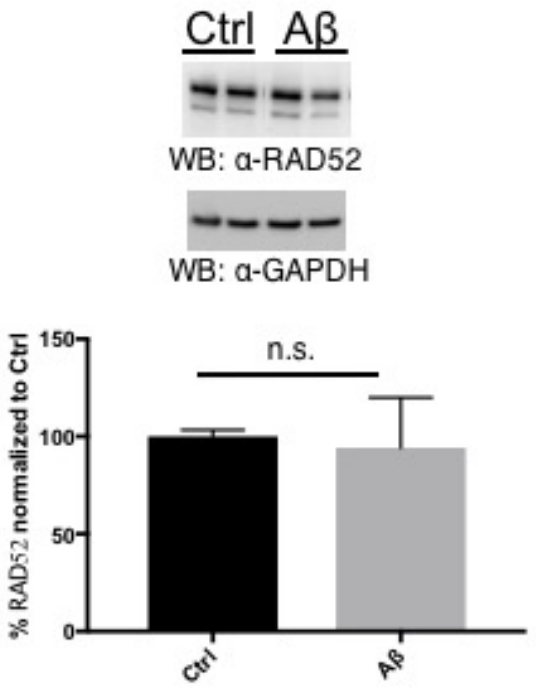

Figure 5-13 1 **μM $A\beta_{1-42}$ does not affect RAD52 protein level in U2OS cells.**

U2OS cells were pre-treated with and without 1 μM Aβ for 24 hrs. Cells were then then probed via western blot with antibodies for anti-RAD52. Error bars indicate the SEM of two separate experiments, and the p values were determined by using unpaired Student's t test. (Of note, other treatments were included on these blots, but were not relevant to this study; thus the cropped images.)

RAD52 DNA damage response recruitment is negatively affected in both cell lines after $A\beta_{1-42}$ treatment, however (**Fig 5-6B)**. This points to dysregulation of RAD52 protein, and perhaps its oxidation by $A\beta_{1-42}$. One method to verify this is to investigate RAD52 protein after $A\beta_{1-42}$ treatment for oxidation, such as evidenced by carbonyl groups as described in Chapter 2. A simple method is to quantify overall change in carbonyl content using a colorimetric assay. These assays utilize 2,4-Dinitrophenylhydrazine (DNPH) to react with protein carbonyls. The derivatization of the carbonyl results in a modified protein that can be measured at 375nm [283, 284]. To measure oxidized protein products in low concentrations (μg) like RAD52, an antibody-based ELISA assay should be used. This type of assay quantifies the DNP-bound protein immunologically using an anti-DNP antibody [111, 285]. Immunoblotting techniques using western blot to determine the species of oxidized protein do not produce accurate determinations of carbonyl concentrations, but can be used to compare relative increase/decrease in amounts as compared to untreated samples when all appropriate controls are used [283].

Another experiment that will need to be conducted following the investigation of γ-H2AX retention at DNA damage sites with active transcription as well as western blots illuminating expression of γ-H2AX after treatment with $A\beta_{1-42}$ is a comet assay. This assay utilizes lysed cells and agarose gel to measure DSBs. The DNA forms supercoiled loops and migrates through the gel by electrophoresis, and once imaged by fluorescence microscopy, presents as “comets” with the intensity of the comet tail relative to the head representing the number of DNA strand breaks [286]. Hypothetically, $A\beta_{1-42}$ treatment should induce more DSBs, and after time, more DSBs should remain, correlating with an increased expression of γ-H2AX.

$A\beta_{1-42}$ may not inhibit successful DSB repair, but if it delays the initial response due to downregulation of essential DSB repair proteins and early repair factors this could lead to cell death or use of an alternate pathway like NHEJ which could lead to error prone repair. Experiments using primary rat cortical neurons showed a trend towards an increase in γ-H2AX

protein after $A\beta_{1-42}$ treatment, though it was not statistically significant (**Fig 5-6C)**. Western blots of U2OS cells also showed no increase in γ-H2AX protein after 24hrs of $A\beta_{1-42}$ treatment (**Fig 5-11).** The differences in γ-H2AX expression may be due to model organism type (rat vs human), cell type (neuron vs carcinoma), and region specificity (cortical vs bone). It is therefore necessary to conduct more experiments with a consistent cell line (preferentially post-mitotic neuronal cultures) to investigate how $A\beta_{1-42}$ affects DSB repair and if $A\beta_{1-42}$ forces these cells to preferentially utilize NHEJ or other repair pathways over TC-HR. It is impossible to fully block cells from using TC-HR because this pathway is not completely defined. However, cells may be guided to preferentially use NHEJ over HR by using siRNA such as for BRCA1 & BRCA2 or RAD52.

Recent studies using molecular dynamics simulations have also shown that oxidized residues can induce conformational changes in Aβ, promoting less aggregation [287]. This would imply that oxidative damage to Aβ could reduce its toxicity and may have mitigated its effect upon U2OS cells in the experiments involving IR (**Fig. 5-10&5-12)**. If this is the case, then proper controls must be utilized in future studies, such as samples treated with $A\beta_{1-42}$ only and no IR.

A cyclohexamide (CHX) chase assay can be performed to investigate the effects of $A\beta_{1-42}$ upon RAD52 protein stability. CHX inhibits the translocation step in protein synthesis, preventing more protein from being made. After treatment with CHX, proteins are degraded over time by regulatory processes such as RNA decay and proteolysis. This allows for visualization of protein levels via western blotting techniques in order to determine the protein half-life and stability [288-292]. Hypothetically, if $A\beta_{1-42}$ is leading to an increase in RAD52 protein turnover (e.g.- RAD52 is being degraded more rapidly), with CHX treatment in addition to $A\beta_{1-42}$ treatment, RAD52 protein levels will be more significantly reduced more quickly than in untreated cells. More experiments also need to be conducted following the CHX chase assay such as qPCR and proteasome inhibition. The qPCR following $A\beta_{1-42}$ treatment will demonstrate whether transcription is affected or mRNA levels are disrupted by $A\beta_{1-42}$. Proteasomal inhibition in conjunction with the

CHX chase assay will show if RAD52 is degraded via the ubiquitin proteasomal pathway, and if $A\beta_{1-42}$ affects the proteasome or ubiquitination of RAD52 in some manner.

Although much work is still to be done, these findings which demonstrate how $A\beta_{1-42}$ negatively affects the initial DNA damage response in post-mitotic cells and contributes to AD pathology are an important first step in understanding early contributing factors to the development of AD disease.

6.0 Final Discussion & Future Directions

The experiments outlined in this thesis have all culminated in evidence of post-mitotic neurons utilizing a novel pathway of DSB repair, TC-HR, in order to maintain lifelong genomic integrity when faced with the excessive stress induced by endogenous and exogenous sources of ROS. Specifically, this thesis has shown that BRCA1 plays a role in the TC-HR pathway dependent upon its BARD1 binding site and independent of RAD52 recruitment. This thesis has also shown that $A\beta_{1-42}$ significantly affects the early stages of the DDR by inhibiting γ-H2AX and RAD52 expression and RAD52 and BRCA1 protein recruitment to DNA damage sites. It has also shown that $A\beta_{1-42}$ induces R-loop formation at DNA damage sites with active transcription, exposing DNA to further damage. These results provide new insights into the mechanisms with which post-mitotic neurons maintain their genome and demonstrate how dysregulation of TC-HR by $A\beta_{1-42}$ in early stages of AD can lead to downregulation of DNA repair.

Our hypothetical model proposes a negative feedback loop of $A\beta_{1-42}$ on genomic stability (**Fig. 6-1**). Excessive oxidative damage and consequent DNA DSBs induce γ-secretase to mediate the expression of β-secretase (BACE1), cleaving the transmembrane amyloid precursor protein (APP) into $A\beta_{1-42}$ monomers which later form soluble oligomers. Re-uptake of $A\beta_{1-42}$ for its aforementioned antioxidant properties leads to further intracellular ROS production and the consequent downregulation of recombinational repair proteins as we have outlined in this study. This deficit in high fidelity repair leads to genomic instability, which potentially promotes neuronal impairment and eventual apoptosis, both processes implicated in the neurodegenerative pathology of AD [293].

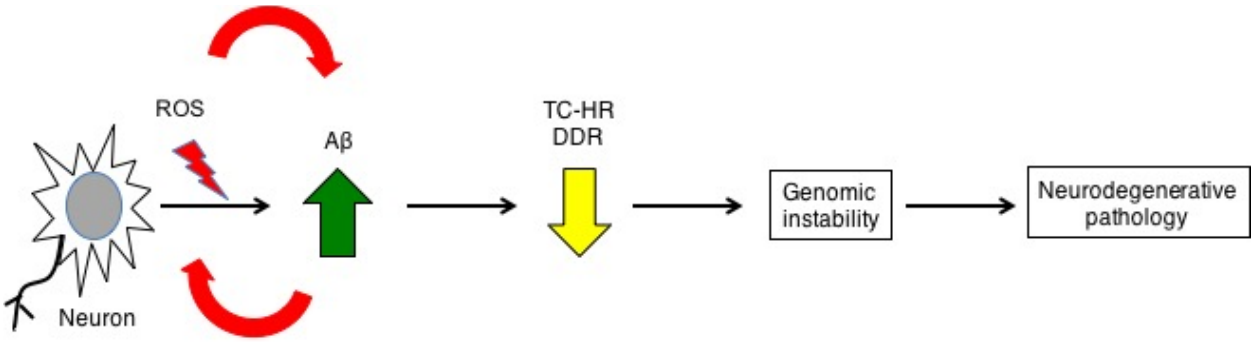

Figure 6-1 Model for $A\beta_{1-42}$ effect upon high fidelity DNA damage repair in post-mitotic neurons.

Oxidative damage to DNA leads to the induction of beta and gamma secretases, which cleave pro-amyloid (APP) to $A\beta_{1-42}$. The hypothetical model shows how oxidative damage leads to APP cleavage, consequent intracellular damage, and repair protein inhibition. This cycle leads to a downregulation in high fidelity recombinational repair and genomic instability, and may further contribute to neurodegenerative pathology.

Currently we understand very little of how $A\beta_{1-42}$ acts upon DNA repair proteins. As outlined in previous chapters, this mechanism is in need of much further investigation. What follows are some specific questions that this thesis has generated and several experimental approaches to address them.

6.1 What is the specific role of BRCA1 in the TC-HR pathway?

The findings mentioned in Chapter 4 that BRCA1 is implicated in TC-HR dependent upon its BARD1 binding and independent of RAD52 recruitment raises numerous questions about the role of BRCA1 in this pathway. For instance, whether BRCA1 still forms a complex with PALB2 and BRCA2 in order to promote RAD51 filament formation in TC-HR is unknown [140]. Also, BRCA1 poly-ubiquitinates CSB in the TCR pathway, but whether BRCA1 interacts with CSB in TC-HR has yet to be determined [238, 239]. Ubiquitination is the process where the 76-amino-

acid polypeptide ubiquitin is covalently attached to other proteins singly (mono-ubiquitination) or in the form of polyubiquitin chains (poly-ubiquination) by the actions of ubiquitin E1, E2, and E3 ligase proteins [294]. Some of these modifications target the proteins for proteasome-based degradation while others serve as docking platforms for DDR-based protein assembly. BRCA1 could be involved in the poly-ubiquitination of CSB via its E3 ligase activity. This E3 ligase activity, as mentioned earlier, is dependent upon BARD1 binding, and in canonical HR involves BRCA2 and RAD51 as well [244, 245]. CSB is essential for TC-HR and is poly-ubiquitinated at the resolution of DNA DSB repair [177]. Hypothetically, a loss of BRCA1 E3 ligase function targeted to CSB could have significantly negative impact upon DNA repair in post-mitotic neurons dependent upon the TC-HR pathway for DSB repair outside of the error-prone NHEJ pathway. This would be seen in retention of CSB at the site of damage and the failure of transcription to resume.

Considering the involvement of BRCA1 in numerous pathways aside from canonical HR and TC-HR such as apoptosis and cell cycle checkpoints, initial investigations would have to focus upon the E3 ligase activity of BRCA1 on CSB in TC-HR. Co-IP experiments must be conducted in order to determine if the two proteins interact in the TC-HR pathway after DNA damage. Since HR commonly occurs in the S phase of the cell cycle and TCR occurs with UV damage, cells can be arrested in the G_0/G_1 phase of the cell cycle to drive them into either TC-HR or NHEJ for DSB repair. These experiments can be conducted with human cells such as HeLa arrested in G_0/G_1 using double thymidine block following Lan lab protocols, or with primary rat cortical post-mitotic neurons such as those used in prior experiments [177]. Confirmation of cell cycle arrest and cell cycle phase will be done via FACS. If BRCA1 and CSB interact in G_0/G_1 arrested cells as determined by Co-IP, western blots with anti-ubiquitin antibodies can be utilized to determine if the CSB protein associated with BRCA1 is ubiquitinated, and recovery timecourses after DNA damage (IR) spanning 0h, 1h, 4h, 8h, 12h, and 24h can be conducted to determine if this ubiquitination increases over time.

To determine the binding region with which CSB interacts with BRCA1, GFP-tagged CSB fragments will be utilized in Co-IPs experiments with HA-tagged full length BRCA1. For the Co-IPs, GFP-tagged CSB fragments will be transiently transfected along with HA-tagged BRCA1 plasmids, and Co-IPs run with western blots after DNA damage (IR) to determine which CSB fragments and therefore which region(s) of CSB binds to BRCA1. Anti-ubiquitin antibodies will be used to measure the differences in CSB ubiquitination as well. CSB fragments used will be regions of amino acids 1-336, 337-590 (acidic domain), 510-960, 961-1399, 1400-1493, and full length. Survival assays using CSB knockout cell lines engineered with CRISPR as recently demonstrated in currently unpublished experiments in the Lan lab will be used. These CSB KO cell lines transiently transfected with the CSB fragments will be conducted to determine how inhibiting CSB ubiquitination affects overall cell survival.

Similar experiments will be conducted to determine the binding region with which BRCA1 interacts with CSB. GFP-tagged BRCA1 fragments will be used in Co-IP experiments with HA-tagged full length CSB, both transiently transfected. Cells will be damaged with IR and western blots run to determine which region(s) of BRCA1 binds to CSB. GFP-tagged BRCA1 fragments utilized will be the following mutants and regions of amino acids: Δ305-770 (NLS deletion), Δ775-1292, Δ1-302 (N-terminal deletion), Δ1527-1863 (C-terminal deletion), 303-1526 (N- & C-terminal deletion), 1-304 (N-terminus only), 1528-1863 (C-terminus only) (**Fig. 6-2**) [241].

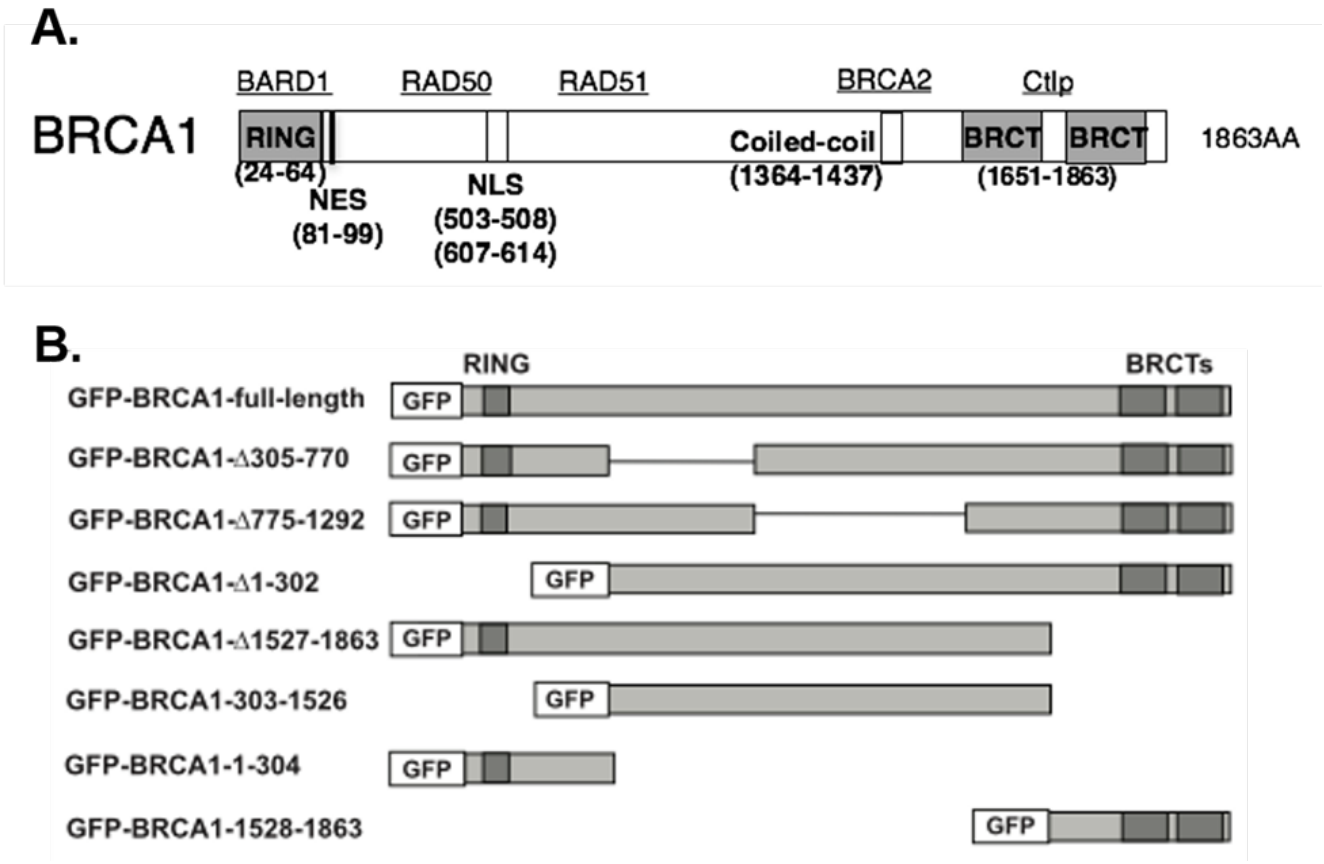

Figure 6-2 BRCA1 and GFP-BRCA1 mutants.

A. Important BRCA1 binding regions and domains. RING, Ring domain; NES, nuclear export sequence; NLS, nuclear localization sequence; BRCT, BRCA1 C-terminal domain. **B.** Diagram of GFP-tagged BRCA1 mutants and truncations.

These experiments will determine if BRCA1 is involved in the regulation of CSB in TC-HR, and if dysregulation of BRCA1 negatively affects the TC-HR pathway and overall cell survival. If the hypothesis is true that BRCA1 helps regulate CSB in TC-HR, then this will become a significant starting point to discovering a more precise role of BRCA1 in TC-HR.

6.2 Define the mechanism of $A\beta_{1-42}$ on repair proteins using a more physiologically relevant model system

A significant discovery in this thesis was that high concentrations of $A\beta_{1-42}$ reduced protein concentrations of RAD52 in post-mitotic primary rat cortical neuronal cultures, but not mitotic U2OS osteocarcinoma cell cultures (**Fig.5-6A&5-13).** High concentrations of $A\beta_{1-42}$ also only affected recruitment of specific DNA repair protein to damage sites. Notably, RAD52 and BRCA1 recruitment to DNA damage sites were reduced after treatment with $A\beta_{1-42}$, while Ku70 and XRCC1 recruitment remained unaffected (**Fig. 5-5B&5-6B&5-7)**. Essential considerations for differences in these results include 1. Potential selective $A\beta_{1-42}$ binding to proteins to affect their activity, 2. differences in model systems (rat vs human cells), 3. variability in cell types (neurons vs cancer cells, etc.), and 4. mitotic stages and differential use of repair pathways as discussed in Chapter 1.5.

If $A\beta_{1-42}$ directly binds repair proteins and alters their conformation, this could prevent them from being able to respond to DNA damage and bind to other partners, or it could lead them to be degraded by the proteasome due to their misfolding. The selectivity of $A\beta_{1-42}$ and its effect upon repair proteins could be due to the need of particular binding regions or charges on the repair protein itself. If certain repair proteins lack these, they may not interact with $A\beta_{1-42}$ at all. Those that do interact directly with $A\beta_{1-42}$ could accumulate aggregates of $A\beta_{1-42}$ and continue to misfold. This self-propagation of $A\beta_{1-42}$ aggregates has been documented in numerous studies and has been termed the “prion-like effect” [295-297]. However, it has not been explored in regards to the effect of $A\beta_{1-42}$ upon repair proteins. Such a phenomenon should be considered in this circumstance. It can be initially explored using AD mouse models and immunohistochemistry to investigate $A\beta_{1-42}$ aggregates and their co-localization with repair proteins.

The difference in RAD52 expression may also hypothetically be influenced by the mitotic U2OS cell preferential use of NHEJ to repair DSBs, and their ability to utilize canonical HR, which

is independent of RAD52 (as discussed in Chapter 1). Post-mitotic neurons, however, cannot utilize canonical HR, and so must rely predominantly on NHEJ for DSB repair. However, as outlined in Chapter 1.5.4 and in my research in Chapter 3, post-mitotic neurons can also utilize TC-HR for DSB repair, which has been associated with repair protein RAD52. As prior studies have implicated an important role for RAD52 in the TC-HR pathway, it would be reasonable to speculate that the reduction in RAD52 protein levels after $A\beta_{1-42}$ treatment is dependent upon the ability to utilize particular DSBR pathways. However, a better model system must be developed in order to rule out further complicating variables that could be influencing repair pathway choice such as cell type (neurons vs cancer cells), repair protein availability (rat vs human), and robustness of particular cell lines (U2OS vs. rat primary cortical neurons).

Another significant discovery in this research was that high concentrations of $A\beta_{1-42}$ do not lead to γ-H2AX foci retention with or without DNA damage. Contradictory to studies conducted by the Mucke group, we also found that the same high concentration of 1μM $A\beta_{1-42}$ does not lead to increased γ-H2AX expression in primary rat cortical neurons or in U2OS osteocarcinoma cells (**Fig. 5-6C)** [13]. The Mucke group utilized mouse cell cultures and AD brain samples from the hippocampal region which undergoes neurogenesis and therefore is comprised of mitotic cells. In adult humans, the generation of new neurons from a neuronal stem cell pool does not occur throughout the entire brain. This process of neurogenesis is thought to be restricted solely to the hippocampal region, namely the dentate gyrus, where glia-like precursor cells that express neuronal stem cell markers give rise to progenitor cells which develop into the neuronal granule cells found in the hippocampal region [298]. Adult neurogenesis consists of four main stages: precursor cell stage, early survivor cell stage, post-mitotic maturation stage, late survival stage. Within these stages, six distinct milestones can be identified: the radial glia-like precursor cell, three progenitor stages of adult neurogenesis with high proliferation activity, post-mitotic maturation phase, and the final granule cell (**Fig 6-3**) [299-304]. The precursor stage involves the

expansion of the cell pool with the early survival stage marking the exit from the cell cycle. The post-mitotic maturation stage involves the growth of axons and dendrites and synaptogenesis with the survival phase covering final adjustments and fine-tuning. The entirety of adult neurogenesis in the hippocampus takes ~7 weeks [299]. One of the larger and highly debated questions is how similar adult neurogenesis in the dentate gyrus is to embryonic or early post-natal neurogenesis. The data is not consistent when referring to functionality of neurons in adults compared to those produced in the neonatal period (e.g.- comparing action potentials and neurotransmitters such as glutamate), speed of maturation of the neurons, and quality and quantity of stimuli and memory contents that pass the dentate gyrus [298, 305, 306].

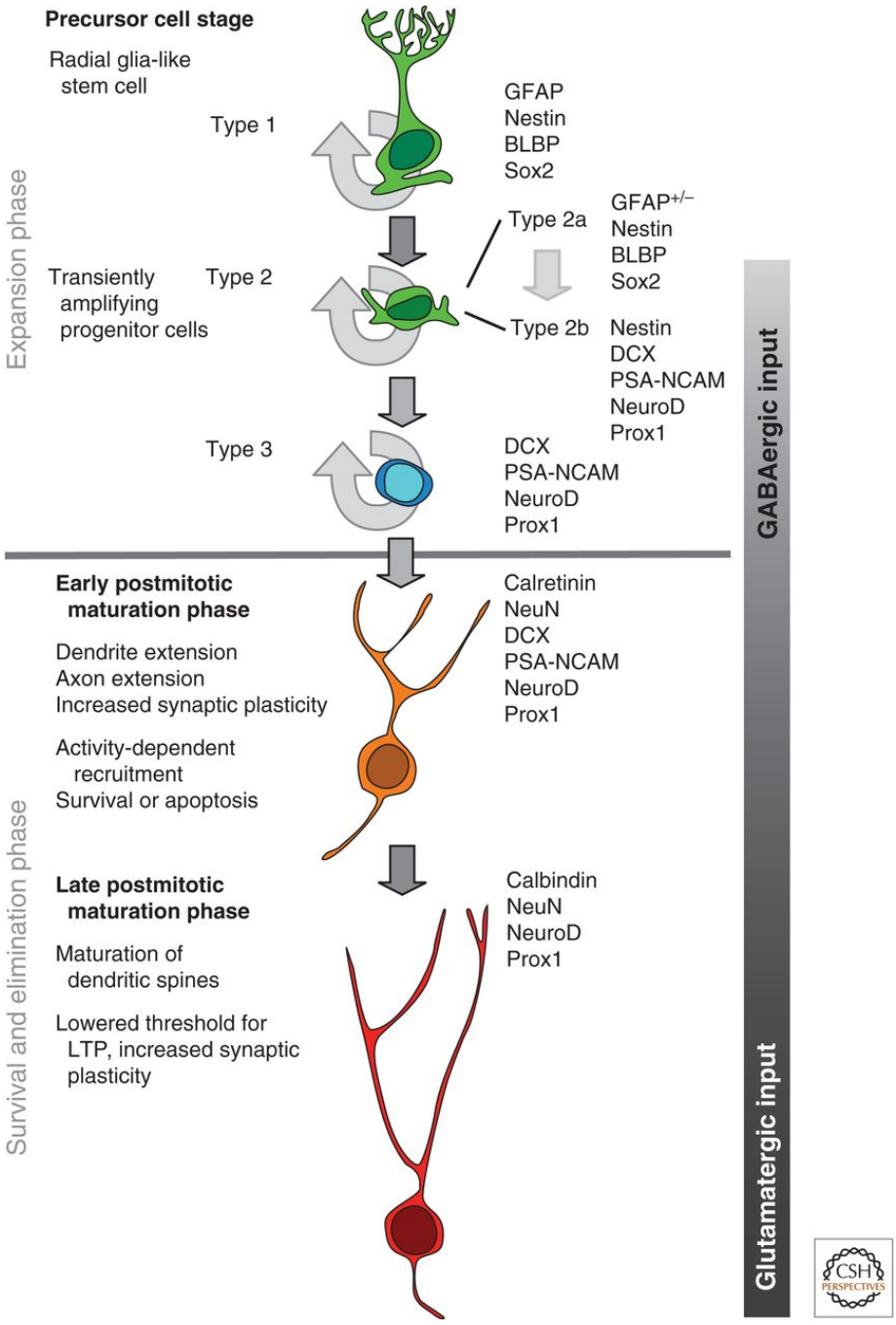

Figure 6-3 Developmental stages in the course of adult hippocampal neurogenesis.

Precursor phase: A radial glial-like precursor stem cell progresses into progenitor cells. Early postmitotic maturation phase: growth of axons, dendrites, and synaptogenesis. Late postmitotic maturation phase: final maturation of dendritic spines, fine-tuning. GFAP, Glial fibrillary acidic protein; BLBP, brain lipid-binding protein; DCX, doublecortin; PSA-NCAM, polysialilated neural-cell-adhesion molecule; LTP, long term potentiation. Adapted from [298] with permission from the publisher.

Also relevant is the plasticity of DNA damage repair during neuronal differentiation compared to mature neurons. Numerous studies have been conducted that demonstrate differentiating neurons downregulate DNA repair compared to post-mitotic neurons [307]. For example, neurospheres were used in one study to investigate BER-associated glycosylase OGG1 activity in neural stem cells compared to differentiating and adult neural cells in mice [308]. Researchers found that OGG1 activity was higher in neurospheres derived from newborn mice and decreased in those derived from adults and upon differentiation. Post-mitotic cells such as neurons have also been found to undergo an extra step prior to apoptosis. They require not only the release of cytochrome c from the mitochondria, but the additional step of releasing the X-linked inhibitor of apoptosis protein (XIAP) which regulates caspases by directly binding them and inhibiting their activity. In post-mitotic neurons, studies have found that selective nerve growth factor deprivation can relieve XIAP activity through selectively degrading it. DNA damage can also overcome XIAP activity through p53-mediated induction of apoptotic peptidase activating factor 1 (Apaf-1) [309]. Prior studies have even shown that mouse stem cells lack a G_1 checkpoint and consequently have shortened G_1 and G_2 cell cycle phases. As a result they spend over 70% of the cell cycle in S phase, implying these cells would utilize canonical HR over NHEJ for DSB repair [310, 311]. This would also imply that in the hippocampal region, namely the dentate gyrus, dividing stem cells in the precursor stage would favor HR over the typical NHEJ due to cell cycle regulation. More research into neuronal cell specificity and which DNA repair pathways are more upregulated or downregulated is essential if we are to understand how $A\beta_{1\text{-}42}$ differentially affects each neuronal type and why.

What will be most beneficial for the future is to establish a more physiologically relevant model for the investigation of selective neuronal vulnerability in DSB repair in AD. One such model is the immortalized hNPC cell line ReNcell VM (ReN). These are human neural progenitor cells which, when deprived of specific growth factors, differentiate into neurons astrocytes, and glial

cells. When engineered to express human APP with FAD associated mutations and cultured in a 3D Matrigel environment, they deposit amyloid plaques [312]. Preliminary experiments have been conducted in the Thathiah lab utilizing neurosphere cultures of ReN cells passaged onto 2D and 3D Matrigel cultures. Once differentiated over 16 days, these cell cultures were found to consist primarily of neurons (<80%) and astrocytes.

6.2.1 What DNA repair proteins are differentially expressed in neuronal progenitors, differentiated neurons, and AD patient brains?

Experiments using progenitor and differentiated ReN cell cultures will include investigations into the nuclear proteome after DNA damage using nuclear fractionation and mass spectrometry analysis. Different damaging reagents will be utilized in order to determine what significant DNA repair pathways are upregulated and downregulated dependent upon damage type (e.g.-global DNA damage using hydrogen peroxide and gamma irradiation vs DNA specific damage using phleomycin). Further investigations will also be conducted with extracellular applications of $A\beta_{1-42}$ to determine how $A\beta_{1-42}$ alters specific DNA repair pathways in progenitor vs differentiated neurons. These experiments will help isolate DNA repair proteins according to their repair function, specifically BRCA1, by investigating nuclear localized proteins only.

In regards to regional specificity and its relevance in the pathology of AD, this model system can be utilized for these investigations as well. We will determine how to further differentiate these ReN cells into specific neuronal types such as glutamatergic or GABAergic cells (excitatory and inhibitory subtypes, respectively) and investigate their response to DNA damaging agents either as a population or individually using single cell targeting methods previously described throughout this thesis.

Pittsburgh is also home to the Neuropathy Brain Bank. This branch of the University of Pittsburgh Brain Institute provides over 1000 preserved neurodegenerative disease patient brain samples for research, including AD and healthy patient samples. We are able to use specific brain region tissue to perform nuclear isolation protocol and mass spec analysis in order to compare the proteome of regional sections of AD brain tissue versus healthy controls. Once optimized, these experiments will allow us to pinpoint specific DNA repair proteins that are upregulated and downregulated in brain regions in AD, providing us with genes we can target as knockdowns or knockouts in our model ReN system to further explore the origins of AD pathology and how $A\beta_{1-42}$ and the dysregulation of essential DNA repair proteins contribute to the development of neurodegenerative disease.

6.2.2 How does $A\beta_{1-42}$ affect DNA repair proteins in neurons?

Using the more relevant ReN progenitors will also provide the means to better investigate the effect of $A\beta_{1-42}$ on canonical HR and TC-HR in human neuronal cells rather than through use of murine models or cancer cells. Since they are immortalized, progenitors can be transfected with plasmids containing mutations and post-mitotic ReN cells can be used in the same experiments in Chapter 3 to verify their use of TC-HR when canonical HR is unavailable.

Preliminary studies have already shown that $A\beta_{1-42}$ negatively affects ReN progenitor survival after IR. Optimized survival assays using ReN progenitors can therefore provide more relevant insight into the effect of $A\beta_{1-42}$ on neuronal stem cell populations in the human brain, most of which are located in the hippocampal dentate gyrus, but according to controversial studies may also be located elsewhere [313].

The CHX chase assay will provide significant results using the differentiated and progenitor ReN cell model as these two systems can be used to compare how $A\beta_{1-42}$ affects the

degradation of TC-HR associated repair proteins RAD52 and BRCA1 as well as other significant proteins in cells dependent upon TC-HR (differentiated ReN) versus those capable of using canonical HR and TC-HR (progenitor ReN). Few studies have been able to use the same cell line for such studies, so these results will be important in profiling details of $A\beta_{1-42}$ and how it affects DNA repair.

As a measure of DNA repair efficiency, we can use single-cell sequencing after IR and $A\beta_{1-42}$ treatment to determine if $A\beta_{1-42}$ treated ReN progenitor cells have repaired DNA lesions. Failure to repair efficiently will result in regions acquiring deletions, frameshift mutations, point mutations, base mismatches, etc. Unrepaired sequences will not match control sequences when nucleotide bases are compared within known genomic regions of ReN cells [314, 315]. A drawback to this technique is that DNA damage is random and the human genome is incredibly large (over 3 billion base pairs). It could take considerable time to verify the presence of unrepaired lesions even within the span of known nucleotide sequences. An additional assay to detect unrepaired DNA is the HPRT assay. This assay uses human cell culture and relies on mutations destroying the functionality of the hypoxanthine phosphoribosyl transferase (HPRT) gene, which is located on the X chromosome. Functionality of the gene/protein is tested via positive selection using a toxic analogue where HPRT deficient mutants are the surviving viable colonies [316]. ReN neuronal progenitor cells are derived from a human male, so contain only one X chromosome [317]. This makes it easier to select for loss of function. Performing this HPRT assay in conjunction with single-cell sequencing will provide a general measure of global DNA repair efficiency after $A\beta_{1-42}$ treatment in the ReN progenitor cell line.

Another major question is whether $A\beta_{1-42}$ is inducing a positive feedback loop through production of ROS, triggering more oxidative damage. As discussed in Chapter 1.3.2, $A\beta_{1-42}$ has been implicated in the production of ROS through its activity with free metal ions. In order to determine more specifically how $A\beta_{1-42}$ is causing a positive feedback loop using the ReN cell model, the production of ROS after $A\beta_{1-42}$ treatment must first be investigated. This can be done

using both progenitors and differentiated cells in 2D and 3D cultures using a simple ROS detection kit (e.g.-Abcam's ROS/Superoxide Detection Assay Kit- ab139476) to monitor the real-time production of ROS via fluorescence microscopy after $A\beta_{1-42}$ treatment. It will be interesting to see if there is a difference in ROS production between ReN progenitors and differentiated neurons, implying that uptake of $A\beta_{1-42}$ may be different as well. Antibodies for $A\beta_{1-42}$ can be used to determine nuclear localization of $A\beta_{1-42}$ after treatment, indicating $A\beta_{1-42}$ uptake. However, endogenous $A\beta_{1-42}$ production must be considered to not confound experimental results. In that circumstance, APP KO cells can be used, or γ-secretase inhibitors to inhibit APP cleavage as described in Chapter 1.3.1. If ROS production and $A\beta_{1-42}$ production/uptake is increased in neuronal progenitors, it implies that undifferentiated neuronal cells are susceptible to damage from $A\beta_{1-42}$ and its consequent ROS, and could pass on deleterious effects of this damage to their differentiated progeny. This could contribute to the progression of AD pathology.

Ultimately this data using the human neuronal ReN cell line will be important in demonstrating how $A\beta_{1-42}$ can affect high fidelity DNA repair both in neuronal precursor cells and in differentiated cell populations. It will help to illuminate specifically how and when $A\beta_{1-42}$ starts to contribute to the generation of AD pathology through its effect upon DNA repair pathways. Studies that follow may utilize this data to develop preventative therapies to combat the growing global threat of AD.

Bibliography

1. Brunnstrom, H.R. and E.M. Englund, *Cause of death in patients with dementia disorders.* Eur J Neurol, 2009. **16**(4): p. 488-92.

2. Todd, S., S. Barr, and A.P. Passmore, *Cause of death in Alzheimer's disease: a cohort study.* QJM, 2013. **106**(8): p. 747-53.

3. Armstrong, R.A., *Factors determining disease duration in Alzheimer's disease: a postmortem study of 103 cases using the Kaplan-Meier estimator and Cox regression.* Biomed Res Int, 2014. **2014**: p. 623487.

4. Garin, D., et al., *COB231 targets amyloid plaques in post-mortem human brain tissue and in an Alzheimer mouse model.* J Neurochem, 2015. **132**(5): p. 609-18.

5. Duyckaerts, C., B. Delatour, and M.C. Potier, *Classification and basic pathology of Alzheimer disease.* Acta Neuropathol, 2009. **118**(1): p. 5-36.

6. Villemagne, V.L., et al., *Amyloid beta deposition, neurodegeneration, and cognitive decline in sporadic Alzheimer's disease: a prospective cohort study.* Lancet Neurol, 2013. **12**(4): p. 357-67.

7. Reiman, E.M., et al., *Brain imaging and fluid biomarker analysis in young adults at genetic risk for autosomal dominant Alzheimer's disease in the presenilin 1 E280A kindred: a case-control study.* Lancet Neurol, 2012. **11**(12): p. 1048-56.

8. Jack, C.R., Jr., et al., *Serial PIB and MRI in normal, mild cognitive impairment and Alzheimer's disease: implications for sequence of pathological events in Alzheimer's disease.* Brain, 2009. **132**(Pt 5): p. 1355-65.

9. Bateman, R.J., et al., *Clinical and biomarker changes in dominantly inherited Alzheimer's disease.* N Engl J Med, 2012. **367**(9): p. 795-804.

10. Hyman, B.T., et al., *National Institute on Aging-Alzheimer's Association guidelines for the neuropathologic assessment of Alzheimer's disease.* Alzheimers Dement, 2012. **8**(1): p. 1-13.

11. Wicklund, A.H. and M. Gaviria, *Closing the gap between research techniques and clinical practice in the treatment of dementia.* Surg Neurol Int, 2011. **2**: p. 168.

12. Klunk, W.E., et al., *Imaging brain amyloid in Alzheimer's disease with Pittsburgh Compound-B.* Ann Neurol, 2004. **55**(3): p. 306-19.

13. Suberbielle, E., et al., *DNA repair factor BRCA1 depletion occurs in Alzheimer brains and impairs cognitive function in mice.* Nat Commun, 2015. **6**(8897): p. 8897.

14. Butterfield, D.A., et al., *Evidence of oxidative damage in Alzheimer's disease brain: central role for amyloid beta-peptide.* Trends Mol Med, 2001. **7**(12): p. 548-54.

15. Younkin, S.G., *The role of A beta 42 in Alzheimer's disease.* J Physiol Paris, 1998. **92**(3-4): p. 289-92.

16. Hall, A.M. and E.D. Roberson, *Mouse models of Alzheimer's disease.* Brain Res Bull, 2012. **88**(1): p. 3-12.

17. Head, E., et al., *Alzheimer's Disease in Down Syndrome.* Eur J Neurodegener Dis, 2012. **1**(3): p. 353-364.

18. Loy, C.T., et al., *Genetics of dementia.* Lancet, 2014. **383**(9919): p. 828-40.

19. Farrer, L.A., et al., *Effects of age, sex, and ethnicity on the association between apolipoprotein E genotype and Alzheimer disease. A meta-analysis. APOE and Alzheimer Disease Meta Analysis Consortium.* JAMA, 1997. **278**(16): p. 1349-56.

20. Mahley, R.W. and S.C. Rall, Jr., *Apolipoprotein E: far more than a lipid transport protein.* Annu Rev Genomics Hum Genet, 2000. **1**: p. 507-37.

21. Mahley, R.W., K.H. Weisgraber, and Y. Huang, *Apolipoprotein E4: a causative factor and therapeutic target in neuropathology, including Alzheimer's disease.* Proc Natl Acad Sci U S A, 2006. **103**(15): p. 5644-51.

22. Nathan, B.P., et al., *Differential effects of apolipoproteins E3 and E4 on neuronal growth in vitro.* Science, 1994. **264**(5160): p. 850-2.

23. Nathan, B.P., et al., *The inhibitory effect of apolipoprotein E4 on neurite outgrowth is associated with microtubule depolymerization.* J Biol Chem, 1995. **270**(34): p. 19791-9.

24. Strittmatter, W.J., et al., *Isoform-specific interactions of apolipoprotein E with microtubule-associated protein tau: implications for Alzheimer disease.* Proc Natl Acad Sci U S A, 1994. **91**(23): p. 11183-6.

25. Strittmatter, W.J., et al., *Hypothesis: microtubule instability and paired helical filament formation in the Alzheimer disease brain are related to apolipoprotein E genotype.* Exp Neurol, 1994. **125**(2): p. 163-71; discussion 172-4.

26. Poirier, J., *Apolipoprotein E and Alzheimer's disease. A role in amyloid catabolism.* Ann N Y Acad Sci, 2000. **924**: p. 81-90.

27. Rockenstein, E., et al., *Early formation of mature amyloid-beta protein deposits in a mutant APP transgenic model depends on levels of Abeta(1-42).* J Neurosci Res, 2001. **66**(4): p. 573-82.

28. Tamaoka, A., et al., *Biochemical evidence for the long-tail form (A beta 1-42/43) of amyloid beta protein as a seed molecule in cerebral deposits of Alzheimer's disease.* Biochem Biophys Res Commun, 1994. **205**(1): p. 834-42.

29. Maruyama, K., et al., *Secretion of Alzheimer beta/A4 protein (1-40) and intracellular retention of beta/A4 protein (1-42) in transfected COS cells.* Biochem Biophys Res Commun, 1995. **207**(3): p. 971-7.

30. Goedert, M., et al., *Multiple isoforms of human microtubule-associated protein tau: sequences and localization in neurofibrillary tangles of Alzheimer's disease.* Neuron, 1989. **3**(4): p. 519-26.

31. Ebneth, A., et al., *Overexpression of tau protein inhibits kinesin-dependent trafficking of vesicles, mitochondria, and endoplasmic reticulum: implications for Alzheimer's disease.* J Cell Biol, 1998. **143**(3): p. 777-94.

32. Stamer, K., et al., *Tau blocks traffic of organelles, neurofilaments, and APP vesicles in neurons and enhances oxidative stress.* J Cell Biol, 2002. **156**(6): p. 1051-63.

33. Spittaels, K., et al., *Prominent axonopathy in the brain and spinal cord of transgenic mice overexpressing four-repeat human tau protein.* Am J Pathol, 1999. **155**(6): p. 2153-65.

34. Gong, C.X., et al., *Post-translational modifications of tau protein in Alzheimer's disease.* J Neural Transm (Vienna), 2005. **112**(6): p. 813-38.

35. Alonso Adel, C., et al., *Promotion of hyperphosphorylation by frontotemporal dementia tau mutations.* J Biol Chem, 2004. **279**(33): p. 34873-81.

36. Gong, C.X. and K. Iqbal, *Hyperphosphorylation of microtubule-associated protein tau: a promising therapeutic target for Alzheimer disease.* Curr Med Chem, 2008. **15**(23): p. 2321-8.

37. Alonso, A.D., et al., *Abnormal phosphorylation of tau and the mechanism of Alzheimer neurofibrillary degeneration: sequestration of microtubule-associated proteins 1 and 2 and the disassembly of microtubules by the abnormal tau.* Proc Natl Acad Sci U S A, 1997. **94**(1): p. 298-303.

38. Alonso, A.D., et al., *Interaction of tau isoforms with Alzheimer's disease abnormally hyperphosphorylated tau and in vitro phosphorylation into the disease-like protein.* J Biol Chem, 2001. **276**(41): p. 37967-73.

39. Alonso, A.C., et al., *Role of abnormally phosphorylated tau in the breakdown of microtubules in Alzheimer disease.* Proc Natl Acad Sci U S A, 1994. **91**(12): p. 5562-6.

40. Zheng, W.H., et al., *Amyloid beta peptide induces tau phosphorylation and loss of cholinergic neurons in rat primary septal cultures.* Neuroscience, 2002. **115**(1): p. 201-11.

41. Luo, Y., et al., *Physiological levels of beta-amyloid peptide promote PC12 cell proliferation.* Neurosci Lett, 1996. **217**(2-3): p. 125-8.

42. Moya, K.L., et al., *The Amyloid Precursor Protein Is Developmentally-Regulated and Correlated with Synaptogenesis.* Developmental Biology, 1994. **161**(2): p. 597-603.

43. Zhang, H., et al., *Proteolytic processing of Alzheimer's beta-amyloid precursor protein.* J Neurochem, 2012. **120 Suppl 1**(Suppl 1): p. 9-21.

44. O'Brien, R.J. and P.C. Wong, *Amyloid precursor protein processing and Alzheimer's disease.* Annu Rev Neurosci, 2011. **34**: p. 185-204.

45. Edwards, D.R., M.M. Handsley, and C.J. Pennington, *The ADAM metalloproteinases.* Mol Aspects Med, 2008. **29**(5): p. 258-89.

46. Pietri, M., et al., *PDK1 decreases TACE-mediated alpha-secretase activity and promotes disease progression in prion and Alzheimer's diseases.* Nat Med, 2013. **19**(9): p. 1124-31.

47. spies, P., *reviewing reasons for the decreased CSF abeta42 concentration in alzheimer disease.* frontiers in bioscience, 2012.

48. Cirrito, J.R., et al., *In vivo assessment of brain interstitial fluid with microdialysis reveals plaque-associated changes in amyloid-beta metabolism and half-life.* J Neurosci, 2003. **23**(26): p. 8844-53.

49. Atwood, C.S., et al., *Amyloid-beta: a chameleon walking in two worlds: a review of the trophic and toxic properties of amyloid-beta.* Brain Res Brain Res Rev, 2003. **43**(1): p. 1-16.

50. Sisodia, S.S., et al., *Evidence that beta-amyloid protein in Alzheimer's disease is not derived by normal processing.* Science, 1990. **248**(4954): p. 492-5.

51. Weidemann, A., et al., *Proteolytic processing of the Alzheimer's disease amyloid precursor protein within its cytoplasmic domain by caspase-like proteases.* J Biol Chem, 1999. **274**(9): p. 5823-9.

52. Seubert, P., et al., *Secretion of beta-amyloid precursor protein cleaved at the amino terminus of the beta-amyloid peptide.* Nature, 1993. **361**(6409): p. 260-3.

53. Yumoto, S., S. Kakimi, and A. Ishikawa, *Colocalization of Aluminum and Iron in Nuclei of Nerve Cells in Brains of Patients with Alzheimer's Disease.* J Alzheimers Dis, 2018.

54. Kanti Das, T., Wati, MR, Fatima-Shad, K, *Oxidative stress gated by Fenton and Haber Weiss reactions and its association with Alzheimer's disease.* Archives of Neuroscience, 2014. **2**(3).

55. Smith, M.A., et al., *Oxidative damage in Alzheimer's.* Nature, 1996. **382**(6587): p. 120-1.

56. Smith, M.A., et al., *Widespread peroxynitrite-mediated damage in Alzheimer's disease.* J Neurosci, 1997. **17**(8): p. 2653-7.

57. Mantyh, P.W., et al., *Aluminum, iron, and zinc ions promote aggregation of physiological concentrations of beta-amyloid peptide.* J Neurochem, 1993. **61**(3): p. 1171-4.

58. Yamamoto, A., et al., *Iron (III) induces aggregation of hyperphosphorylated tau and its reduction to iron (II) reverses the aggregation: implications in the formation of neurofibrillary tangles of Alzheimer's disease.* J Neurochem, 2002. **82**(5): p. 1137-47.

59. Deibel, M.A., W.D. Ehmann, and W.R. Markesbery, *Copper, iron, and zinc imbalances in severely degenerated brain regions in Alzheimer's disease: possible relation to oxidative stress.* J Neurol Sci, 1996. **143**(1-2): p. 137-42.

60. Miller, L.M., et al., *Synchrotron-based infrared and X-ray imaging shows focalized accumulation of Cu and Zn co-localized with beta-amyloid deposits in Alzheimer's disease.* J Struct Biol, 2006. **155**(1): p. 30-7.

61. Hureau, C. and P. Faller, *Abeta-mediated ROS production by Cu ions: structural insights, mechanisms and relevance to Alzheimer's disease.* Biochimie, 2009. **91**(10): p. 1212-7.

62. Huang, X., et al., *Cu(II) potentiation of alzheimer abeta neurotoxicity. Correlation with cell-free hydrogen peroxide production and metal reduction.* J Biol Chem, 1999. **274**(52): p. 37111-6.

63. Opazo, C., et al., *Metalloenzyme-like activity of Alzheimer's disease beta-amyloid. Cu-dependent catalytic conversion of dopamine, cholesterol, and biological reducing agents to neurotoxic H(2)O(2).* J Biol Chem, 2002. **277**(43): p. 40302-8.

64. Mold, M., et al., *Copper prevents amyloid-beta(1-42) from forming amyloid fibrils under near-physiological conditions in vitro.* Sci Rep, 2013. **3**: p. 1256.

65. Frederickson, C.J., *Neurobiology of zinc and zinc-containing neurons.* Int Rev Neurobiol, 1989. **31**: p. 145-238.

66. Frederickson, C.J., J.Y. Koh, and A.I. Bush, *The neurobiology of zinc in health and disease.* Nat Rev Neurosci, 2005. **6**(6): p. 449-62.

67. Smart, T.G., A.M. Hosie, and P.S. Miller, *Zn2+ ions: modulators of excitatory and inhibitory synaptic activity.* Neuroscientist, 2004. **10**(5): p. 432-42.

68. Weiss, J.H., et al., *AMPA receptor activation potentiates zinc neurotoxicity.* Neuron, 1993. **10**(1): p. 43-9.

69. Inoue, K., D. Branigan, and Z.G. Xiong, *Zinc-induced neurotoxicity mediated by transient receptor potential melastatin 7 channels.* J Biol Chem, 2010. **285**(10): p. 7430-9.

70. Lovell, M.A., et al., *Copper, iron and zinc in Alzheimer's disease senile plaques.* J Neurol Sci, 1998. **158**(1): p. 47-52.

71. Leskovjan, A.C., et al., *Increased brain iron coincides with early plaque formation in a mouse model of Alzheimer's disease.* Neuroimage, 2011. **55**(1): p. 32-8.

72. Roberts, B.R., et al., *The role of metallobiology and amyloid-beta peptides in Alzheimer's disease.* J Neurochem, 2012. **120 Suppl 1**: p. 149-66.

73. Huang, X., et al., *The A beta peptide of Alzheimer's disease directly produces hydrogen peroxide through metal ion reduction.* Biochemistry, 1999. **38**(24): p. 7609-16.

74. Cuajungco, M.P. and K.Y. Faget, *Zinc takes the center stage: its paradoxical role in Alzheimer's disease.* Brain Res Brain Res Rev, 2003. **41**(1): p. 44-56.

75. Selkoe, D.J. and J. Hardy, *The amyloid hypothesis of Alzheimer's disease at 25 years.* EMBO Mol Med, 2016. **8**(6): p. 595-608.

76. Zheng, H., et al., *beta-Amyloid precursor protein-deficient mice show reactive gliosis and decreased locomotor activity.* Cell, 1995. **81**(4): p. 525-31.

77. Koike, M.A., et al., *APP knockout mice experience acute mortality as the result of ischemia.* PLoS One, 2012. **7**(8): p. e42665.

78. Suberbielle, E., Sanchez, P., Kravitz, A., Wang, X., Ho, K., Ellertson, K., Devidze, N., Kreitzer, A., Mucke, L, *Physiologic brain activity causes DNA double-strand breaks in neurons, with exacerbation by amyloid-b.* Nat. Neurosci., 2013. **16**: p. 613-621.

79. Luo, Y., et al., *BACE1 (beta-secretase) knockout mice do not acquire compensatory gene expression changes or develop neural lesions over time.* Neurobiol Dis, 2003. **14**(1): p. 81-8.

80. Louvi, A. and S. Artavanis-Tsakonas, *Notch signalling in vertebrate neural development.* Nat Rev Neurosci, 2006. **7**(2): p. 93-102.

81. Lathia, J.D., M.P. Mattson, and A. Cheng, *Notch: from neural development to neurological disorders.* J Neurochem, 2008. **107**(6): p. 1471-81.

82. Shen, J., et al., *Skeletal and CNS defects in Presenilin-1-deficient mice.* Cell, 1997. **89**(4): p. 629-39.

83. Wong, P.C., et al., *Presenilin 1 is required for Notch1 and DII1 expression in the paraxial mesoderm.* Nature, 1997. **387**(6630): p. 288-92.

84. Donoviel, D.B., et al., *Mice lacking both presenilin genes exhibit early embryonic patterning defects.* Genes Dev, 1999. **13**(21): p. 2801-10.

85. Herreman, A., et al., *Presenilin 2 deficiency causes a mild pulmonary phenotype and no changes in amyloid precursor protein processing but enhances the embryonic lethal phenotype of presenilin 1 deficiency.* Proc Natl Acad Sci U S A, 1999. **96**(21): p. 11872-7.

86. Golde, T.E., et al., *gamma-Secretase inhibitors and modulators.* Biochim Biophys Acta, 2013. **1828**(12): p. 2898-907.

87. Ames, B.N., M.K. Shigenaga, and T.M. Hagen, *Oxidants, antioxidants, and the degenerative diseases of aging.* Proc Natl Acad Sci U S A, 1993. **90**(17): p. 7915-22.

88. Nguyen, D., et al., *A new vicious cycle involving glutamate excitotoxicity, oxidative stress and mitochondrial dynamics.* Cell Death Dis, 2011. **2**(12): p. e240.

89. Mecocci, P., U. MacGarvey, and M.F. Beal, *Oxidative damage to mitochondrial DNA is increased in Alzheimer's disease.* Ann Neurol, 1994. **36**(5): p. 747-51.

90. Butterfield, D.A. and J. Kanski, *Methionine residue 35 is critical for the oxidative stress and neurotoxic properties of Alzheimer's amyloid beta-peptide 1-42.* Peptides, 2002. **23**(7): p. 1299-309.

91. Pogocki, D., Ghezzo-Schoneich, E., Schoneich, C., *Conformational Flexibility Controls Proton Transfer between the Methionine Hydroxy Sulfuranyl Radical and the N-Terminal Amino Group in Thr−(X)n−Met Peptides.* J. Phys. Chem. B, 2001. **105**(6): p. 1250-1259.

92. Wisniowski, P.B., et al., *Efficient alpha-(alkylthio)alkyl-type radical formation in (*)OH-induced oxidation of alpha-(methylthio)acetamide.* J Phys Chem A, 2010. **114**(1): p. 105-16.

93. Fay, D.S., et al., *In vivo aggregation of beta-amyloid peptide variants.* J Neurochem, 1998. **71**(4): p. 1616-25.

94. Markesbery, W.R., *Oxidative stress hypothesis in Alzheimer's disease.* Free Radic Biol Med, 1997. **23**(1): p. 134-47.

95. Reeg, S. and T. Grune, *Protein Oxidation in Aging: Does It Play a Role in Aging Progression?* Antioxid Redox Signal, 2015. **23**(3): p. 239-55.

96. Nitsch, R.M., et al., *Evidence for a membrane defect in Alzheimer disease brain.* Proc Natl Acad Sci U S A, 1992. **89**(5): p. 1671-5.

97. Mark, R.J., et al., *A role for 4-hydroxynonenal, an aldehydic product of lipid peroxidation, in disruption of ion homeostasis and neuronal death induced by amyloid beta-peptide.* J Neurochem, 1997. **68**(1): p. 255-64.

98. Mark, R.J., K.S. Fuson, and P.C. May, *Characterization of 8-epiprostaglandin F2alpha as a marker of amyloid beta-peptide-induced oxidative damage.* J Neurochem, 1999. **72**(3): p. 1146-53.

99. Butterfield, D.A., et al., *beta-Amyloid peptide free radical fragments initiate synaptosomal lipoperoxidation in a sequence-specific fashion: implications to Alzheimer's disease.* Biochem Biophys Res Commun, 1994. **200**(2): p. 710-5.

100. Sayre, L.M., et al., *4-Hydroxynonenal-derived advanced lipid peroxidation end products are increased in Alzheimer's disease.* J Neurochem, 1997. **68**(5): p. 2092-7.

101. Montine, K.S., et al., *4-hydroxy-2-nonenal pyrrole adducts in human neurodegenerative disease.* J Neuropathol Exp Neurol, 1997. **56**(8): p. 866-71.

102. Davies, P. and A.J. Maloney, *Selective loss of central cholinergic neurons in Alzheimer's disease.* Lancet, 1976. **2**(8000): p. 1403.

103. Lehericy, S., et al., *Heterogeneity and selectivity of the degeneration of cholinergic neurons in the basal forebrain of patients with Alzheimer's disease.* J Comp Neurol, 1993. **330**(1): p. 15-31.

104. Wilcock, G.K., et al., *Alzheimer's disease. Correlation of cortical choline acetyltransferase activity with the severity of dementia and histological abnormalities.* J Neurol Sci, 1982. **57**(2-3): p. 407-17.

105. Jo, D.G., Arumugam, T.V., Woo, H.N., Park, J.S., Tang, S.C., Mughal, M., Hyun, D.H., Park, J.H., Choi, Y.H., Gwon, A.R., Camandola, S., Cheng, A., Cai, H., Song, W.,

Markesbery, W.R., Mattson, M.P. , *Evidence that γ-Secretase Mediates Oxidative Stress-Induced β-Secretase Expression in Alzheimer's Disease.* Neurobiology of Aging, 2010. **31**(6): p. 917-925.

106. Kimberly, W.T., et al., *The intracellular domain of the beta-amyloid precursor protein is stabilized by Fe65 and translocates to the nucleus in a notch-like manner.* J Biol Chem, 2001. **276**(43): p. 40288-92.

107. von Rotz, R.C., et al., *The APP intracellular domain forms nuclear multiprotein complexes and regulates the transcription of its own precursor.* J Cell Sci, 2004. **117**(Pt 19): p. 4435-48.

108. Butterfield, A., Stadtman, E., *Protein oxidation processes in aging.* Advances in Cell Aging and Gerontology, 1997. **2**: p. 161-191.

109. Stadtman, E.R., *Protein oxidation and aging.* Free Radic Res, 2006. **40**(12): p. 1250-8.

110. Dean, R.T., et al., *Biochemistry and pathology of radical-mediated protein oxidation.* Biochem J, 1997. **324 (Pt 1)**: p. 1-18.

111. Dalle-Donne, I., et al., *Protein carbonyl groups as biomarkers of oxidative stress.* Clin Chim Acta, 2003. **329**(1-2): p. 23-38.

112. Butterfield, D.A., et al., *Amyloid beta-peptide-associated free radical oxidative stress, neurotoxicity, and Alzheimer's disease.* Methods Enzymol, 1999. **309**: p. 746-68.

113. Pocernich, C.B., et al., *Glutathione elevation and its protective role in acrolein-induced protein damage in synaptosomal membranes: relevance to brain lipid peroxidation in neurodegenerative disease.* Neurochem Int, 2001. **39**(2): p. 141-9.

114. Aksenova, M.V., et al., *Oxidation of cytosolic proteins and expression of creatine kinase BB in frontal lobe in different neurodegenerative disorders.* Dement Geriatr Cogn Disord, 1999. **10**(2): p. 158-65.

115. Lyras, L., et al., *An assessment of oxidative damage to proteins, lipids, and DNA in brain from patients with Alzheimer's disease.* J Neurochem, 1997. **68**(5): p. 2061-9.

116. Hensley, K., et al., *Brain regional correspondence between Alzheimer's disease histopathology and biomarkers of protein oxidation.* J Neurochem, 1995. **65**(5): p. 2146-56.

117. Aksenov, M.Y., et al., *Protein oxidation in the brain in Alzheimer's disease.* Neuroscience, 2001. **103**(2): p. 373-83.

118. David, S.S., V.L. O'Shea, and S. Kundu, *Base-excision repair of oxidative DNA damage.* Nature, 2007. **447**(7147): p. 941-50.

119. Brouwer, I., et al., *Human RAD52 Captures and Holds DNA Strands, Increases DNA Flexibility, and Prevents Melting of Duplex DNA: Implications for DNA Recombination.* Cell Rep, 2017. **18**(12): p. 2845-2853.

120. Bhargava, R., D.O. Onyango, and J.M. Stark, *Regulation of Single-Strand Annealing and its Role in Genome Maintenance.* Trends Genet, 2016. **32**(9): p. 566-75.

121. Sugiyama, T., J.H. New, and S.C. Kowalczykowski, *DNA annealing by RAD52 protein is stimulated by specific interaction with the complex of replication protein A and single-stranded DNA.* Proc Natl Acad Sci U S A, 1998. **95**(11): p. 6049-54.

122. McVey, M. and S.E. Lee, *MMEJ repair of double-strand breaks (director's cut): deleted sequences and alternative endings.* Trends Genet, 2008. **24**(11): p. 529-38.

123. Lieber, M.R., *The mechanism of double-strand DNA break repair by the nonhomologous DNA end-joining pathway.* Annu Rev Biochem, 2010. **79**: p. 181-211.

124. Jeppesen, D.K., V.A. Bohr, and T. Stevnsner, *DNA repair deficiency in neurodegeneration.* Prog Neurobiol, 2011. **94**(2): p. 166-200.

125. Lindahl, T., *Instability and decay of the primary structure of DNA.* Nature, 1993. **362**(6422): p. 709-15.

126. Borges, H.L., R. Linden, and J.Y. Wang, *DNA damage-induced cell death: lessons from the central nervous system.* Cell Res, 2008. **18**(1): p. 17-26.

127. Lee, Y. and P.J. McKinnon, *Responding to DNA double strand breaks in the nervous system.* Neuroscience, 2007. **145**(4): p. 1365-74.

128. Ferrer, I., *The effect of cycloheximide on natural and X-ray-induced cell death in the developing cerebral cortex.* Brain Res, 1992. **588**(2): p. 351-7.

129. Mizumatsu, S., et al., *Extreme sensitivity of adult neurogenesis to low doses of X-irradiation.* Cancer Res, 2003. **63**(14): p. 4021-7.

130. Fike, J.R., R. Rola, and C.L. Limoli, *Radiation response of neural precursor cells.* Neurosurg Clin N Am, 2007. **18**(1): p. 115-27, x.

131. Ferrer, I., et al., *Radiosensitive populations and recovery in X-ray-induced apoptosis in the developing cerebellum.* Acta Neuropathol, 1993. **86**(5): p. 491-500.

132. Kruman, I.I., et al., *Cell cycle activation linked to neuronal cell death initiated by DNA damage.* Neuron, 2004. **41**(4): p. 549-561.

133. Canugovi, C., et al., *The role of DNA repair in brain related disease pathology.* DNA Repair (Amst), 2013. **12**(8): p. 578-87.

134. Sharma, R.A. and G.L. Dianov, *Targeting base excision repair to improve cancer therapies.* Mol Aspects Med, 2007. **28**(3-4): p. 345-74.

135. Rass, U., I. Ahel, and S.C. West, *Defective DNA repair and neurodegenerative disease.* Cell, 2007. **130**(6): p. 991-1004.

136. Wang, J., W.R. Markesbery, and M.A. Lovell, *Increased oxidative damage in nuclear and mitochondrial DNA in mild cognitive impairment.* J Neurochem, 2006. **96**(3): p. 825-32.

137. Her, J. and S.F. Bunting, *How cells ensure correct repair of DNA double-strand breaks.* J Biol Chem, 2018. **293**(27): p. 10502-10511.

138. San Filippo, J., P. Sung, and H. Klein, *Mechanism of eukaryotic homologous recombination.* Annu Rev Biochem, 2008. **77**: p. 229-57.

139. Wold, M.S., *Replication protein A: a heterotrimeric, single-stranded DNA-binding protein required for eukaryotic DNA metabolism.* Annu Rev Biochem, 1997. **66**: p. 61-92.

140. Prakash, R., et al., *Homologous recombination and human health: the roles of BRCA1, BRCA2, and associated proteins.* Cold Spring Harb Perspect Biol, 2015. **7**(4): p. a016600.

141. Orthwein, A., et al., *A mechanism for the suppression of homologous recombination in G1 cells.* Nature, 2015. **528**(7582): p. 422-6.

142. Buisson, R., et al., *Coupling of Homologous Recombination and the Checkpoint by ATR.* Mol Cell, 2017. **65**(2): p. 336-346.

143. McKee, R.H. and C.W. Lawrence, *Genetic analysis of gamma-ray mutagenesis in yeast. III. Double-mutant strains.* Mutat Res, 1980. **70**(1): p. 37-48.

144. Symington, L.S., R. Rothstein, and M. Lisby, *Mechanisms and regulation of mitotic recombination in Saccharomyces cerevisiae.* Genetics, 2014. **198**(3): p. 795-835.

145. Feng, Z., et al., *Rad52 inactivation is synthetically lethal with BRCA2 deficiency.* Proc Natl Acad Sci U S A, 2011. **108**(2): p. 686-91.

146. Takata, M., et al., *Chromosome instability and defective recombinational repair in knockout mutants of the five Rad51 paralogs.* Mol Cell Biol, 2001. **21**(8): p. 2858-66.

147. Liu, J., et al., *Rad51 paralogues Rad55-Rad57 balance the antirecombinase Srs2 in Rad51 filament formation.* Nature, 2011. **479**(7372): p. 245-8.

148. Mazin, A.V., A.A. Alexeev, and S.C. Kowalczykowski, *A novel function of Rad54 protein. Stabilization of the Rad51 nucleoprotein filament.* J Biol Chem, 2003. **278**(16): p. 14029-36.

149. Wright, W.D. and W.D. Heyer, *Rad54 functions as a heteroduplex DNA pump modulated by its DNA substrates and Rad51 during D loop formation.* Mol Cell, 2014. **53**(3): p. 420-32.

150. Li, X., et al., *PCNA is required for initiation of recombination-associated DNA synthesis by DNA polymerase delta.* Mol Cell, 2009. **36**(4): p. 704-13.

151. Lao, J.P., et al., *Rad52 promotes postinvasion steps of meiotic double-strand-break repair.* Mol Cell, 2008. **29**(4): p. 517-24.

152. Wright, W.D., S.S. Shah, and W.D. Heyer, *Homologous recombination and the repair of DNA double-strand breaks.* J Biol Chem, 2018. **293**(27): p. 10524-10535.

153. Peng, G. and S.Y. Lin, *Exploiting the homologous recombination DNA repair network for targeted cancer therapy.* World J Clin Oncol, 2011. **2**(2): p. 73-9.

154. Beucher, A., et al., *ATM and Artemis promote homologous recombination of radiation-induced DNA double-strand breaks in G2.* EMBO J, 2009. **28**(21): p. 3413-27.

155. Mimitou, E.P. and L.S. Symington, *Ku prevents Exo1 and Sgs1-dependent resection of DNA ends in the absence of a functional MRX complex or Sae2.* EMBO J, 2010. **29**(19): p. 3358-69.

156. Chang, H.H.Y., et al., *Non-homologous DNA end joining and alternative pathways to double-strand break repair.* Nat Rev Mol Cell Biol, 2017. **18**(8): p. 495-506.

157. Botuyan, M.V., et al., *Structural basis for the methylation state-specific recognition of histone H4-K20 by 53BP1 and Crb2 in DNA repair.* Cell, 2006. **127**(7): p. 1361-73.

158. Fradet-Turcotte, A., et al., *53BP1 is a reader of the DNA-damage-induced H2A Lys 15 ubiquitin mark.* Nature, 2013. **499**(7456): p. 50-4.

159. Acs, K., et al., *The AAA-ATPase VCP/p97 promotes 53BP1 recruitment by removing L3MBTL1 from DNA double-strand breaks.* Nat Struct Mol Biol, 2011. **18**(12): p. 1345-50.

160. Mallette, F.A., et al., *RNF8- and RNF168-dependent degradation of KDM4A/JMJD2A triggers 53BP1 recruitment to DNA damage sites.* EMBO J, 2012. **31**(8): p. 1865-78.

161. Jacquet, K., et al., *The TIP60 Complex Regulates Bivalent Chromatin Recognition by 53BP1 through Direct H4K20me Binding and H2AK15 Acetylation.* Mol Cell, 2016. **62**(3): p. 409-421.

162. Tang, J., et al., *Acetylation limits 53BP1 association with damaged chromatin to promote homologous recombination.* Nat Struct Mol Biol, 2013. **20**(3): p. 317-25.

163. Pellegrino, S., et al., *Replication-Coupled Dilution of H4K20me2 Guides 53BP1 to Pre-replicative Chromatin.* Cell Rep, 2017. **19**(9): p. 1819-1831.

164. Gell, D. and S.P. Jackson, *Mapping of protein-protein interactions within the DNA-dependent protein kinase complex.* Nucleic Acids Res, 1999. **27**(17): p. 3494-502.

165. Ding, Q., et al., *Autophosphorylation of the catalytic subunit of the DNA-dependent protein kinase is required for efficient end processing during DNA double-strand break repair.* Mol Cell Biol, 2003. **23**(16): p. 5836-48.

166. West, R.B., M. Yaneva, and M.R. Lieber, *Productive and nonproductive complexes of Ku and DNA-dependent protein kinase at DNA termini.* Mol Cell Biol, 1998. **18**(10): p. 5908-20.

167. Ma, Y., et al., *The DNA-dependent protein kinase catalytic subunit phosphorylation sites in human Artemis.* J Biol Chem, 2005. **280**(40): p. 33839-46.

168. Goodarzi, A.A., et al., *DNA-PK autophosphorylation facilitates Artemis endonuclease activity.* EMBO J, 2006. **25**(16): p. 3880-9.

169. Gu, J., et al., *DNA-PKcs regulates a single-stranded DNA endonuclease activity of Artemis.* DNA Repair (Amst), 2010. **9**(4): p. 429-37.

170. Nick McElhinny, S.A., et al., *A gradient of template dependence defines distinct biological roles for family X polymerases in nonhomologous end joining.* Mol Cell, 2005. **19**(3): p. 357-66.

171. Ramadan, K., et al., *De novo DNA synthesis by human DNA polymerase lambda, DNA polymerase mu and terminal deoxyribonucleotidyl transferase.* J Mol Biol, 2004. **339**(2): p. 395-404.

172. Grawunder, U., et al., *Activity of DNA ligase IV stimulated by complex formation with XRCC4 protein in mammalian cells.* Nature, 1997. **388**(6641): p. 492-5.

173. Pannunzio, N.R., G. Watanabe, and M.R. Lieber, *Nonhomologous DNA end-joining for repair of DNA double-strand breaks.* J Biol Chem, 2018. **293**(27): p. 10512-10523.

174. Sonoda, E., et al., *Differential usage of non-homologous end-joining and homologous recombination in double strand break repair.* DNA Repair (Amst), 2006. **5**(9-10): p. 1021-9.

175. Eriksson, P.S., et al., *Neurogenesis in the adult human hippocampus.* Nat Med, 1998. **4**(11): p. 1313-7.

176. Ernst, A., et al., *Neurogenesis in the striatum of the adult human brain.* Cell, 2014. **156**(5): p. 1072-83.

177. Wei, L., et al., *DNA damage during the G0/G1 phase triggers RNA-templated, Cockayne syndrome B-dependent homologous recombination.* Proc Natl Acad Sci U S A, 2015. **112**(27): p. E3495-504.

178. Hanawalt, P.C., *Role of transcription-coupled DNA repair in susceptibility to environmental carcinogenesis.* Environ Health Perspect, 1996. **104 Suppl 3**: p. 547-51.

179. Kitsera, N., et al., *Cockayne syndrome: varied requirement of transcription-coupled nucleotide excision repair for the removal of three structurally different adducts from transcribed DNA.* PLoS One, 2014. **9**(4): p. e94405.

180. Weidenheim, K.M., D.W. Dickson, and I. Rapin, *Neuropathology of Cockayne syndrome: Evidence for impaired development, premature aging, and neurodegeneration.* Mech Ageing Dev, 2009. **130**(9): p. 619-36.

181. Tan, W.H., et al., *Cockayne syndrome: the developing phenotype.* Am J Med Genet A, 2005. **135**(2): p. 214-6.

182. Cramers, P., et al., *Impaired repair of ionizing radiation-induced DNA damage in Cockayne syndrome cells.* Radiat Res, 2011. **175**(4): p. 432-43.

183. Ropolo, M., et al., *Defective resolution of pH2AX foci and enhanced DNA breakage in ionizing radiation-treated cockayne syndrome B cells.* IUBMB Life, 2011. **63**(4): p. 272-6.

184. Lan, L., et al., *Novel method for site-specific induction of oxidative DNA damage reveals differences in recruitment of repair proteins to heterochromatin and euchromatin.* Nucleic Acids Res, 2014. **42**(4): p. 2330-45.

185. Lan, L., et al., *The ACF1 Complex Is Required for DNA Double-Strand Break Repair in Human Cells.* Molecular Cell, 2010. **40**(6): p. 976-987.

186. Bulina, M.E., et al., *A genetically encoded photosensitizer.* Nat Biotechnol, 2006. **24**(1): p. 95-9.

187. Carpentier, P., et al., *Structural basis for the phototoxicity of the fluorescent protein KillerRed.* FEBS Lett, 2009. **583**(17): p. 2839-42.

188. Marnef, A., S. Cohen, and G. Legube, *Transcription-Coupled DNA Double-Strand Break Repair: Active Genes Need Special Care.* J Mol Biol, 2017. **429**(9): p. 1277-1288.

189. Meers, C., H. Keskin, and F. Storici, *DNA repair by RNA: Templated, or not templated, that is the question.* DNA Repair (Amst), 2016. **44**: p. 17-21.

190. Ouyang, J., L. Lan, and L. Zou, *Regulation of DNA break repair by transcription and RNA.* Sci China Life Sci, 2017. **60**(10): p. 1081-1086.

191. Keskin, H., et al., *Transcript-RNA-templated DNA recombination and repair.* Nature, 2014. **515**(7527): p. 436-9.

192. Roy, D. and M.R. Lieber, *G clustering is important for the initiation of transcription-induced R-loops in vitro, whereas high G density without clustering is sufficient thereafter.* Mol Cell Biol, 2009. **29**(11): p. 3124-33.

193. Reaban, M.E., J. Lebowitz, and J.A. Griffin, *Transcription induces the formation of a stable RNA.DNA hybrid in the immunoglobulin alpha switch region.* J Biol Chem, 1994. **269**(34): p. 21850-7.

194. Ginno, P.A., et al., *R-loop formation is a distinctive characteristic of unmethylated human CpG island promoters.* Mol Cell, 2012. **45**(6): p. 814-25.

195. Skourti-Stathaki, K. and N.J. Proudfoot, *A double-edged sword: R loops as threats to genome integrity and powerful regulators of gene expression.* Genes Dev, 2014. **28**(13): p. 1384-96.

196. Aguilera, A., *The connection between transcription and genomic instability.* EMBO J, 2002. **21**(3): p. 195-201.

197. Li, X. and J.L. Manley, *Cotranscriptional processes and their influence on genome stability.* Genes Dev, 2006. **20**(14): p. 1838-47.

198. Aguilera, A. and T. Garcia-Muse, *R loops: from transcription byproducts to threats to genome stability.* Mol Cell, 2012. **46**(2): p. 115-24.

199. Bellaiche, Y., V. Mogila, and N. Perrimon, *I-SceI endonuclease, a new tool for studying DNA double-strand break repair mechanisms in Drosophila.* Genetics, 1999. **152**(3): p. 1037-44.

200. Potter, L.T., *Synthesis, storage and release of [14C]acetylcholine in isolated rat diaphragm muscles.* J Physiol, 1970. **206**(1): p. 145-66.

201. Colovic, M.B., et al., *Acetylcholinesterase inhibitors: pharmacology and toxicology.* Curr Neuropharmacol, 2013. **11**(3): p. 315-35.

202. Ferreira-Vieira, T.H., et al., *Alzheimer's disease: Targeting the Cholinergic System.* Curr Neuropharmacol, 2016. **14**(1): p. 101-15.

203. Bartus, R.T., *On neurodegenerative diseases, models, and treatment strategies: lessons learned and lessons forgotten a generation following the cholinergic hypothesis.* Exp Neurol, 2000. **163**(2): p. 495-529.

204. Muir, J.L., et al., *Attentional functions of the forebrain cholinergic systems: effects of intraventricular hemicholinium, physostigmine, basal forebrain lesions and intracortical grafts on a multiple-choice serial reaction time task.* Exp Brain Res, 1992. **89**(3): p. 611-22.

205. Rogers, J.L. and R.P. Kesner, *Cholinergic modulation of the hippocampus during encoding and retrieval of tone/shock-induced fear conditioning.* Learn Mem, 2004. **11**(1): p. 102-7.

206. Selkoe, D.J., *Alzheimer's disease is a synaptic failure.* Science, 2002. **298**(5594): p. 789-91.

207. Sze, C.I., et al., *Loss of the presynaptic vesicle protein synaptophysin in hippocampus correlates with cognitive decline in Alzheimer disease.* J Neuropathol Exp Neurol, 1997. **56**(8): p. 933-44.

208. Counts, S.E., et al., *Differential expression of synaptic proteins in the frontal and temporal cortex of elderly subjects with mild cognitive impairment.* J Neuropathol Exp Neurol, 2006. **65**(6): p. 592-601.

209. Cummings, J., et al., *Alzheimer's disease drug development pipeline: 2018.* Alzheimers Dement (N Y), 2018. **4**: p. 195-214.

210. Doody, R.S., et al., *Phase 3 trials of solanezumab and bapineuzumab for Alzheimer's disease.* N Engl J Med, 2014. **370**(15): p. 1460.

211. Sanders, L.H., et al., *Mitochondrial DNA damage: molecular marker of vulnerable nigral neurons in Parkinson's disease.* Neurobiol Dis, 2014. **70**: p. 214-23.

212. Lan, L., et al., *In situ analysis of repair processes for oxidative DNA damage in mammalian cells.* Proc Natl Acad Sci U S A, 2004. **101**(38): p. 13738-43.

213. Celik, S., *Understanding the complexity of antigen retrieval of DNA methylation for immunofluorescence-based measurement and an approach to challenge.* J Immunol Methods, 2015. **416**: p. 1-16.

214. Lan, L., et al., *Accumulation of Werner protein at DNA double-strand breaks in human cells.* Journal of Cell Science, 2005. **118**(18): p. 4153-4162.

215. Wei, L.Z., et al., *Damage response of XRCC1 at sites of DNA single strand breaks is regulated by phosphorylation and ubiquitylation after degradation of poly(ADP-ribose).* Journal of Cell Science, 2013. **126**(19): p. 4414-4423.

216. Ma, C.J., et al., *Human RAD52 interactions with replication protein A and the RAD51 presynaptic complex.* J Biol Chem, 2017. **292**(28): p. 11702-11713.

217. Cisse, M., et al., *Reversing EphB2 depletion rescues cognitive functions in Alzheimer model.* Nature, 2011. **469**(7328): p. 47-52.

218. Yun-Zhong, F., Sheng, Y., Guoyao, W. , *Free radicals, antioxidants, and nutrition.* Nutrition, 2002. **18**: p. 872-879.

219. Yankner, B.A.D., L.R.; Fisher, S.; Villa-Komaroff, L.; Oster-Granite, M.L.; Neve, R.L., *Neurotoxicity of a fragment of the amyloid precursor associated with Alzheimer's disease.* Science, 1989. **245**(4916): p. 417-420.

220. Welty, S., et al., *RAD52 is required for RNA-templated recombination repair in post-mitotic neurons.* J Biol Chem, 2018. **293**(4): p. 1353-1362.

221. Hendzel, M.J., et al., *Mitosis-specific phosphorylation of histone H3 initiates primarily within pericentromeric heterochromatin during G2 and spreads in an ordered fashion coincident with mitotic chromosome condensation.* Chromosoma, 1997. **106**(6): p. 348-360.

222. Karmakar, P., et al., *BLM is an early responder to DNA double-strand breaks.* Biochem Biophys Res Commun, 2006. **348**(1): p. 62-9.

223. Haber, J.E., *DNA repair. Gatekeepers of recombination.* Nature, 1999. **398**(6729): p. 665, 667.

224. Ristic, D., et al., *Rad52 and Ku bind to different DNA structures produced early in double-strand break repair.* Nucleic Acids Res, 2003. **31**(18): p. 5229-37.

225. Heidenreich, E.N., R.; Kneidinger, B.; Holzmann, V.; Wintersberger, U., *Non-homologous end joining as an important mutagenic process in cell cycle-arrested cells.* The EMBO Journal, 2003. **22**(9): p. 2274-2283.

226. Campisi, J., *From cells to organisms: can we learn about aging from cells in culture?* Experimental Gerontology, 2001. **36**(4-6): p. 607-618.

227. Collado, M. and M. Serrano, *Senescence in tumours: evidence from mice and humans.* Nat Rev Cancer, 2010. **10**(1): p. 51-7.

228. Lawson, A.R., et al., *RAF gene fusion breakpoints in pediatric brain tumors are characterized by significant enrichment of sequence microhomology.* Genome Res, 2011. **21**(4): p. 505-14.

229. Wenk, G.L., *Neuropathologic changes in Alzheimer's disease.* J Clin Psychiatry, 2003. **64(suppl 9)**: p. 7-10.

230. Shiloh, Y. and G. Rotman, *Ataxia-telangiectasia and the ATM gene: linking neurodegeneration, immunodeficiency, and cancer to cell cycle checkpoints.* J Clin Immunol, 1996. **16**(5): p. 254-60.

231. Barlow, C., et al., *Atm selectively regulates distinct p53-dependent cell-cycle checkpoint and apoptotic pathways.* Nat Genet, 1997. **17**(4): p. 453-6.

232. K.K., K., *Cancer risk and the ATM gene: a continuing debate.* J Natl Cancer Inst, 2000. **92**: p. 795-802.

233. Shen, X., et al., *Neurons in Vulnerable Regions of the Alzheimer's Disease Brain Display Reduced ATM Signaling.* eNeuro, 2016. **3**(1): p. ENEURO.0124–15.2016.

234. Corder, E.H., et al., *Gene dose of apolipoprotein E type 4 allele and the risk of Alzheimer's disease in late onset families.* Science, 1993. **261**(5123): p. 921-3.

235. Dong, Y., et al., *Regulation of BRCC, a holoenzyme complex containing BRCA1 and BRCA2, by a signalosome-like subunit and its role in DNA repair.* Mol Cell, 2003. **12**(5): p. 1087-99.

236. Shen, S.X., et al., *A targeted disruption of the murine Brca1 gene causes gamma-irradiation hypersensitivity and genetic instability.* Oncogene, 1998. **17**(24): p. 3115-24.

237. Xu, X., et al., *Centrosome amplification and a defective G2-M cell cycle checkpoint induce genetic instability in BRCA1 exon 11 isoform-deficient cells.* Mol Cell, 1999. **3**(3): p. 389-95.

238. Wei, L., et al., *BRCA1 contributes to transcription-coupled repair of DNA damage through polyubiquitination and degradation of Cockayne syndrome B protein.* Cancer Sci, 2011. **102**(10): p. 1840-7.

239. Le Page, F., et al., *BRCA1 and BRCA2 are necessary for the transcription-coupled repair of the oxidative 8-oxoguanine lesion in human cells.* Cancer Res, 2000. **60**(19): p. 5548-52.

240. Jin, Y., et al., *Cell cycle-dependent colocalization of BARD1 and BRCA1 proteins in discrete nuclear domains.* Proc Natl Acad Sci U S A, 1997. **94**(22): p. 12075-80.

241. Wei, L., et al., *Rapid recruitment of BRCA1 to DNA double-strand breaks is dependent on its association with Ku80.* Mol Cell Biol, 2008. **28**(24): p. 7380-93.

242. Abel, K.J., et al., *Mouse Brca1: localization, sequence analysis and identification of evolutionarily conserved domains.* Human Molecular Genetics, 1995. **4**(12): p. 2265-2273.

243. Sharan, S.K., M. Wims, and A. Bradley, *Murine Brca1: sequence and significance for human missense mutations.* Human Molecular Genetics, 1995. **4**(12): p. 2275-2278.

244. Greenberg, R.A., et al., *Multifactorial contributions to an acute DNA damage response by BRCA1/BARD1-containing complexes.* Genes Dev, 2006. **20**(1): p. 34-46.

245. Isono, M., et al., *BRCA1 Directs the Repair Pathway to Homologous Recombination by Promoting 53BP1 Dephosphorylation.* Cell Rep, 2017. **18**(2): p. 520-532.

246. Shinohara, A., et al., *Rad52 forms ring structures and co-operates with RPA in single-strand DNA annealing.* Genes Cells, 1998. **3**(3): p. 145-56.

247. New, J.H., et al., *Rad52 protein stimulates DNA strand exchange by Rad51 and replication protein A.* Nature, 1998. **391**(6665): p. 407-10.

248. McIlwraith, M.J. and S.C. West, *DNA repair synthesis facilitates RAD52-mediated second-end capture during DSB repair.* Mol Cell, 2008. **29**(4): p. 510-6.

249. Muris, D.F., et al., *Cloning of human and mouse genes homologous to RAD52, a yeast gene involved in DNA repair and recombination.* Mutat Res, 1994. **315**(3): p. 295-305.

250. Scully, R., et al., *Dynamic changes of BRCA1 subnuclear location and phosphorylation state are initiated by DNA damage.* Cell, 1997. **90**(3): p. 425-35.

251. Chen, J.J., et al., *BRCA1, BRCA2, and Rad51 operate in a common DNA damage response pathway.* Cancer Res, 1999. **59**(7 Suppl): p. 1752s-1756s.

252. MacLachlan, T.K., et al., *BRCA1 effects on the cell cycle and the DNA damage response are linked to altered gene expression.* J Biol Chem, 2000. **275**(4): p. 2777-85.

253. Harkin, D.P., et al., *Induction of GADD45 and JNK/SAPK-dependent apoptosis following inducible expression of BRCA1.* Cell, 1999. **97**(5): p. 575-86.

254. Holt, J.T., et al., *Growth retardation and tumour inhibition by BRCA1.* Nat Genet, 1996. **12**(3): p. 298-302.

255. Hong, Z., et al., *Recruitment of mismatch repair proteins to the site of DNA damage in human cells.* J Cell Sci, 2008. **121**(Pt 19): p. 3146-54.

256. Zlokovic, B.V., et al., *Brain uptake of circulating apolipoproteins J and E complexed to Alzheimer's amyloid beta.* Biochem Biophys Res Commun, 1994. **205**(2): p. 1431-7.

257. Deane, R. and B.V. Zlokovic, *Role of the blood-brain barrier in the pathogenesis of Alzheimer's disease.* Curr Alzheimer Res, 2007. **4**(2): p. 191-7.

258. Li, Q.X., et al., *Proteolytic processing of Alzheimer's disease beta A4 amyloid precursor protein in human platelets.* J Biol Chem, 1995. **270**(23): p. 14140-7.

259. Evin, G., et al., *Proteolytic processing of the Alzheimer's disease amyloid precursor protein in brain and platelets.* J Neurosci Res, 2003. **74**(3): p. 386-92.

260. Citron, M., et al., *Excessive production of amyloid beta-protein by peripheral cells of symptomatic and presymptomatic patients carrying the Swedish familial Alzheimer disease mutation.* Proc Natl Acad Sci U S A, 1994. **91**(25): p. 11993-7.

261. Kuo, Y.M., et al., *Elevated abeta42 in skeletal muscle of Alzheimer disease patients suggests peripheral alterations of AbetaPP metabolism.* Am J Pathol, 2000. **156**(3): p. 797-805.

262. Van Nostrand, W.E. and J.P. Melchor, *Disruption of pathologic amyloid beta-protein fibril assembly on the surface of cultured human cerebrovascular smooth muscle cells.* Amyloid, 2001. **8 Suppl 1**: p. 20-7.

263. Bu, X.L., et al., *Blood-derived amyloid-beta protein induces Alzheimer's disease pathologies.* Mol Psychiatry, 2017.

264. Lue, L.F., A. Guerra, and D.G. Walker, *Amyloid Beta and Tau as Alzheimer's Disease Blood Biomarkers: Promise From New Technologies.* Neurol Ther, 2017. **6**(Suppl 1): p. 25-36.

265. Grasso, G., *The use of mass spectrometry to study amyloid-beta peptides.* Mass Spectrom Rev, 2011. **30**(3): p. 347-65.

266. Tichy, E.D., et al., *Mouse embryonic stem cells, but not somatic cells, predominantly use homologous recombination to repair double-strand DNA breaks.* Stem Cells Dev, 2010. **19**(11): p. 1699-711.

267. Gadbois, D.M. and B.E. Lehnert, *Cell cycle response to DNA damage differs in bronchial epithelial cells and lung fibroblasts.* Cancer Res, 1997. **57**(15): p. 3174-9.

268. Hanawalt, P.C., *Transcription-coupled repair and human disease.* Science, 1994. **266**(5193): p. 1957-8.

269. Nakanishi, K., et al., *Homologous recombination assay for interstrand cross-link repair.* Methods Mol Biol, 2011. **745**: p. 283-91.

270. Helfricht, A., et al., *Remodeling and spacing factor 1 (RSF1) deposits centromere proteins at DNA double-strand breaks to promote non-homologous end-joining.* Cell Cycle, 2013. **12**(18): p. 3070-82.

271. Matarin, e.a., *Mouseac.* 2015.

272. Misra, P., et al., *Rapid alpha-oligomer formation mediated by the Abeta C terminus initiates an amyloid assembly pathway.* Nat Commun, 2016. **7**(12419): p. 12419.

273. Rogakou, E.P., et al., *DNA double-stranded breaks induce histone H2AX phosphorylation on serine 139.* J Biol Chem, 1998. **273**(10): p. 5858-68.

274. Bassing, C.H. and F.W. Alt, *H2AX may function as an anchor to hold broken chromosomal DNA ends in close proximity.* Cell Cycle, 2004. **3**(2): p. 149-53.

275. Celeste, A., et al., *Histone H2AX phosphorylation is dispensable for the initial recognition of DNA breaks.* Nat Cell Biol, 2003. **5**(7): p. 675-9.

276. Fernandez-Capetillo, O., et al., *H2AX: the histone guardian of the genome.* DNA Repair (Amst), 2004. **3**(8-9): p. 959-67.

277. Shroff, R., et al., *Distribution and dynamics of chromatin modification induced by a defined DNA double-strand break.* Curr Biol, 2004. **14**(19): p. 1703-11.

278. Celeste, A., et al., *Genomic instability in mice lacking histone H2AX.* Science, 2002. **296**(5569): p. 922-7.

279. Bassing, C.H., et al., *Histone H2AX: a dosage-dependent suppressor of oncogenic translocations and tumors.* Cell, 2003. **114**(3): p. 359-70.

280. Rogakou, E.P., et al., *Megabase chromatin domains involved in DNA double-strand breaks in vivo.* J Cell Biol, 1999. **146**(5): p. 905-16.

281. Bouquet, F., C. Muller, and B. Salles, *The loss of gammaH2AX signal is a marker of DNA double strand breaks repair only at low levels of DNA damage.* Cell Cycle, 2006. **5**(10): p. 1116-22.

282. Mariotti, L.G., et al., *Use of the gamma-H2AX assay to investigate DNA repair dynamics following multiple radiation exposures.* PLoS One, 2013. **8**(11): p. e79541.

283. Weber, D., M.J. Davies, and T. Grune, *Determination of protein carbonyls in plasma, cell extracts, tissue homogenates, isolated proteins: Focus on sample preparation and derivatization conditions.* Redox Biol, 2015. **5**: p. 367-80.

284. Levine, R.L., et al., *Determination of carbonyl content in oxidatively modified proteins.* Methods Enzymol, 1990. **186**: p. 464-78.

285. Buss, H., et al., *Protein carbonyl measurement by a sensitive ELISA method.* Free Radic Biol Med, 1997. **23**(3): p. 361-6.

286. Collins, A.R., *The comet assay for DNA damage and repair: principles, applications, and limitations.* Mol Biotechnol, 2004. **26**(3): p. 249-61.

287. Razzokov, J., M. Yusupov, and A. Bogaerts, *Oxidation destabilizes toxic amyloid beta peptide aggregation.* Sci Rep, 2019. **9**(1): p. 5476.

288. Tran, J.R. and J.L. Brodsky, *Assays to measure ER-associated degradation in yeast.* Methods Mol Biol, 2012. **832**: p. 505-18.

289. Obrig, T.G., et al., *The mechanism by which cycloheximide and related glutarimide antibiotics inhibit peptide synthesis on reticulocyte ribosomes.* J Biol Chem, 1971. **246**(1): p. 174-81.

290. Ennis, H.L. and M. Lubin, *Cycloheximide: Aspects of Inhibition of Protein Synthesis in Mammalian Cells.* Science, 1964. **146**(3650): p. 1474-6.

291. Kerridge, D., *The effect of actidione and other antifungal agents on nucleic acid and protein synthesis in Saccharomyces carlsbergensis.* J Gen Microbiol, 1958. **19**(3): p. 497-506.

292. Buchanan, B.W., et al., *Cycloheximide Chase Analysis of Protein Degradation in Saccharomyces cerevisiae.* J Vis Exp, 2016(110).

293. Hou, Y., et al., *Genome instability in Alzheimer disease.* Mech Ageing Dev, 2017. **161**(Pt A): p. 83-94.

294. Pickart, C.M., *Mechanisms underlying ubiquitination.* Annu Rev Biochem, 2001. **70**: p. 503-33.

295. Honda, R., *Amyloid-beta Peptide Induces Prion Protein Amyloid Formation: Evidence for Its Widespread Amyloidogenic Effect.* Angew Chem Int Ed Engl, 2018. **57**(21): p. 6086-6089.

296. Ruiz-Riquelme, A., et al., *Prion-like propagation of beta-amyloid aggregates in the absence of APP overexpression.* Acta Neuropathol Commun, 2018. **6**(1): p. 26.

297. Watts, J.C. and S.B. Prusiner, *beta-Amyloid Prions and the Pathobiology of Alzheimer's Disease.* Cold Spring Harb Perspect Med, 2018. **8**(5).

298. Kempermann, G., H. Song, and F.H. Gage, *Neurogenesis in the Adult Hippocampus.* Cold Spring Harb Perspect Biol, 2015. **7**(9): p. a018812.

299. Kempermann, G., et al., *Milestones of neuronal development in the adult hippocampus.* Trends Neurosci, 2004. **27**(8): p. 447-52.

300. Steiner, B., et al., *Type-2 cells as link between glial and neuronal lineage in adult hippocampal neurogenesis.* Glia, 2006. **54**(8): p. 805-14.

301. Brandt, M.D., et al., *Transient calretinin expression defines early postmitotic step of neuronal differentiation in adult hippocampal neurogenesis of mice.* Mol Cell Neurosci, 2003. **24**(3): p. 603-13.

302. Filippov, V., et al., *Subpopulation of nestin-expressing progenitor cells in the adult murine hippocampus shows electrophysiological and morphological characteristics of astrocytes.* Mol Cell Neurosci, 2003. **23**(3): p. 373-82.

303. Fukuda, S., et al., *Two distinct subpopulations of nestin-positive cells in adult mouse dentate gyrus.* J Neurosci, 2003. **23**(28): p. 9357-66.

304. Encinas, J.M., A. Vaahtokari, and G. Enikolopov, *Fluoxetine targets early progenitor cells in the adult brain.* Proc Natl Acad Sci U S A, 2006. **103**(21): p. 8233-8.

305. Laplagne, D.A., et al., *Functional convergence of neurons generated in the developing and adult hippocampus.* PLoS Biol, 2006. **4**(12): p. e409.

306. Overstreet-Wadiche, L.S., A.L. Bensen, and G.L. Westbrook, *Delayed development of adult-generated granule cells in dentate gyrus.* J Neurosci, 2006. **26**(8): p. 2326-34.

307. Fortini, P. and E. Dogliotti, *Mechanisms of dealing with DNA damage in terminally differentiated cells.* Mutat Res, 2010. **685**(1-2): p. 38-44.

308. Hildrestrand, G.A., et al., *The capacity to remove 8-oxoG is enhanced in newborn neural stem/progenitor cells and decreases in juvenile mice and upon cell differentiation.* DNA Repair (Amst), 2007. **6**(6): p. 723-32.

309. Vaughn, A.E. and M. Deshmukh, *Essential postmitochondrial function of p53 uncovered in DNA damage-induced apoptosis in neurons.* Cell Death Differ, 2007. **14**(5): p. 973-81.

310. Savatier, P., et al., *Analysis of the cell cycle in mouse embryonic stem cells.* Methods Mol Biol, 2002. **185**: p. 27-33.

311. Tichy, E.D. and P.J. Stambrook, *DNA repair in murine embryonic stem cells and differentiated cells.* Exp Cell Res, 2008. **314**(9): p. 1929-36.

312. Kim, Y.H., et al., *A 3D human neural cell culture system for modeling Alzheimer's disease.* Nat Protoc, 2015. **10**(7): p. 985-1006.

313. Ma, D.K., et al., *Adult neural stem cells in the mammalian central nervous system.* Cell Res, 2009. **19**(6): p. 672-82.

314. Gawad, C., W. Koh, and S.R. Quake, *Single-cell genome sequencing: current state of the science.* Nat Rev Genet, 2016. **17**(3): p. 175-88.

315. Pellegrino, M., et al., *High-throughput single-cell DNA sequencing of acute myeloid leukemia tumors with droplet microfluidics.* Genome Res, 2018. **28**(9): p. 1345-1352.

316. Johnson, G.E., *Mammalian cell HPRT gene mutation assay: test methods.* Methods Mol Biol, 2012. **817**: p. 55-67.

317. Donato, R., et al., *Differential development of neuronal physiological responsiveness in two human neural stem cell lines.* BMC Neurosci, 2007. **8**: p. 36.